P-14-05

# SR-PSU Bedrock hydrogeology

## TD12 – Water-supply wells in rock

Johan Öhman, Geosigma AB

Patrik Vidstrand, Svensk Kärnbränslehantering AB

December 2014

**Svensk Kärnbränslehantering AB**
Swedish Nuclear Fuel
and Waste Management Co

Box 250, SE-101 24 Stockholm
Phone +46 8 459 84 00

ISSN 1651-4416
SKB P-14-05
ID 1435401

# SR-PSU Bedrock hydrogeology

## TD12 – Water-supply wells in rock

Johan Öhman, Geosigma AB

Patrik Vidstrand, Svensk Kärnbränslehantering AB

December 2014

*Keywords:* Hydrogeology, Bedrock, Modelling, Temperate, Forsmark, SFR, Safety assessment

# Abstract

As a part of the license application for extending the existing repository for short-lived low and intermediate radioactive waste (SFR), the Swedish Nuclear Fuel and Waste Management Company (SKB) has undertaken a project to assess the radiological safety for the SFR repository after closure, SR-PSU (SKB 2014). The SR-PSU project employs a groundwater flow model, developed in SDM-PSU (SKB 2013), to perform hydrogeological modelling tasks that are defined in terms of so-called Task Descriptions (TDs). This report presents an assessment of groundwater-flow interactions between potential water-supply wells and the backfilled repository (i.e. the existing SFR 1 as well as its planned extension, SFR 3). The task reported here is described in Task Description TD12. In a preceding task, TD11, the combined effects of heterogeneity and conceptual uncertainty in bedrock parameterization were studied by means of a sensitivity analysis, for future stages of shoreline retreat.

To delimit the complexity of this study, all simulations employ a single model setup, which is "static" in terms of bedrock parameterisation and shoreline retreat. For this study, the Base case bedrock parameterisation from TD11 and the time slice 5000 AD are selected to form the most representative model setup. At 5000 AD, areas of arable land have recently emerged from the sea and the flow regime has reached a more or less stationary state (it is unaffected by further shoreline retreat). The output of this study, combined with the preceding TD11 modelling task, will facilitate dose assessments that can be related to radionuclide transport to water-supply wells.

The specific objectives of TD12 are to study the following:

(1) The influence of water abstraction from water-supply wells on groundwater flow through the facility (SFR 1 and SFR 3).

(2) Groundwater-flow interaction between the facility (SFR 1 and SFR 3) and water-supply wells.

The analysed well locations fall into two categories: 1) water-supply wells for settlements associated to potential arable land and 2) an area downstream from SFR where the highest concentrations of radionuclides originating from SFR can be expected. The wells are assumed to be drilled 60 m vertically into the bedrock. The assumed well depth is based on data from the SGU Well Archive, delivered to SKB in 2011 (see e.g. Werner et al. 2013). Specifically, updated well-depth statistics are calculated for 5,164 wells, located in the same area in northern Uppland previously analysed by Gentzschein et al. (2007). The wells for settlements associated to areas of arable land (Figure 1-2) are located where the bedrock is sufficiently conductive for sustaining an assumed water demand of a self-sustaining community of modern farmers, 700 L/d.

Results demonstrate that all wells associated to arable land have negligible influence on disposal-room cross flow and their groundwater-flow interactions are very small. These results are in line with expectations, as the wells have remote emplacements, relative to SFR. Pumping within the well-interaction area has a small, but noticeable effect on the flow through disposal rooms of SFR 1 and SFR 3. However, the influence never exceeds 1.4%, even for a water abstraction rate of 2,800 L/d.

Well interactions are determined by means of a particle-tracking approach. It is confirmed that either particle-tracking direction can be used in the determination of interactions, i.e. tracking upstream or downstream the flow field is interchangeable if compensated by the ratio between disposal-room cross flow and well abstraction rate.

The highest interactions in the well-interaction area occur just northeast of deformation zone ZFMNW0805A/B (Figure 4-22). One of the wells in the interaction area (well 12) has the highest overall interactions, particularly for disposal rooms of SFR 1. To some extent, details in simulation results, e.g. relative interaction strength among the different disposal rooms, are specific to the underlying bedrock-parameterisation variant, and hence care must be taken so as not to overgeneralise interpretations without consideration to uncertainty and heterogeneity originating from the bedrock parameterisation.

# Sammanfattning

Som en del av ansökan för utbyggnad av Slutförvaret för kortlivat radioaktivt avfall (SFR) har Svensk Kärnbränslehantering (SKB) genomfört ett projekt för att bedöma den radiologiska säkerheten för förvaret efter förslutning, SR-PSU (SKB 2014). I SR-PSU tillämpas den grundvattenmodell som utvecklats i SDM-PSU (SKB 2013) för att genomföra olika hydrogeologiska modelleringsuppgifter, vilka finns definierade i särskilda uppgiftsbeskrivningar (*Eng:* Task Descriptions; TDs). Denna rapport presenterar en utvärdering av interaktioner i grundvattenflöde mellan potentiella vattenförsörjningsbrunnar och det återförslutna förvaret (d.v.s. det befintliga SFR1, såväl som, dess planerade utbyggnad, SFR3). Denna studie specificeras i uppgiftsbeskrivning TD12. I den föregående uppgiften, TD11, undersöktes de kombinerade effekterna av heterogenitet och konceptuell osäkerhet i parameterisering av berggrunden med hjälp av en känslighetsanalys under framtida stadier av strandlinjeförskjutning.

För att begränsa komplexiteten i studien används en utvald modelluppställning, som är "statisk" avseende bergmassans parameterisering och strandlinjeförskjutning. Den mest representativa modelluppställningen har bedömts vara den parameterisering som benämns basfallet (*Eng:* Base case, enligt bedömning i den föregående uppgiften TD11) samt strandlinjeförskjutningen vid 5000 AD (en tidpunkt då odlingsbar mark nyligen exponerats ur havet och flödesregimen nått ett mer eller mindre stationärt tillstånd). Resultaten av denna studie kommer, i kombination med resultaten i föregående modelleringsuppgifter, användas för dosberäkningar som kan relateras till radionuklidtransport till vattenförsörjningsbrunnarna.

De specifika målen med TD12 är att undersöka:

(1) Påverkan av pumpning i brunnarna på grundvattenflödet genom förvaret (SFR1 och SFR3).

(2) Interaktioner i grundvattenflöde mellan förvaret (SFR1 och SFR3) och vattenförsörjningsbrunnar.

De brunnslägen som ingår i analysen indelas i två kategorier: 1) vattenförsörjningsbrunnar för bosättningar vid potentiellt odlingsbar mark och 2) ett område nedströms SFR där de högsta radionuklidhalterna med ursprung från SFR kan förväntas. Brunnarna antas vara vertikalt borrade till 60 m djup ned i berggrunden. Det antagna djupet baseras på data från SGUs brunnsarkiv. Mer specifikt baseras det på statistik för 5164 brunnar i som borrats inom samma område av norduppland, enligt en tidigare analys av Gentzschein et al. (2007). Brunnarna som förknippas till bosättningar vid potentiellt odlingsbar mark placeras där berggrunden är tillräckligt konduktiv för att upprätthålla det antagna behovet för en självförsörjande bosättning av moderna jordbrukare, 700 L/d.

Resultaten visar att de brunnar som är kopplade till odlingsbar mark har försumbar påverkan på flöden i förvarsutrymmen och deras interaktioner i grundvattenflöden är mycket låga. Dessa resultat överensstämmer med förväntningarna eftersom brunnarnas lägen är avlägsna relativt SFR. Vattenuttag inom interaktionsområdet har en liten men påvisbar inverkan på flödet genom förvarsutrymmena. Dock överstiger påverkan aldrig 1.4%, inte ens för vattenuttag på 2800 L/d).

Interaktioner utvärderas med hjälp av en partikelspårningsmetod, som beskrivs i Öhman et al. (2014). Det bekräftas att partikelspårningen kan utföras i båda riktningarna (d.v.s. resultaten av uppströms och nedströms spårning är utbytbara, såvida hänsyn tas till förhållandet mellan flöde i förvarsutrymme, $Q_i$, och brunnsuttaget, $Q_j$). I fysiska termer motsvarar detta flödesförhållande till utspädning i vattenuttaget från brunn.

De högsta interaktionerna inom det definierade "interaktionsområdet" förekommer precis nordöst om deformationszonen ZFMNW0805A/B (Figure 4-22). Brunn 12, avsedd som ett "värsta brunnsscenario", kan bekräftas ha de högsta interaktionerna, sammantaget, i synnerhet avseende förvarsutrymmena i SFR1. Delvis kan vissa detaljer i simuleringsresultaten kopplas till den särskilda bergbeskrivning som tillämpats i modelluppställningen (exempelvis relativa skillnader i resultat mellan förvarsutrymmena). Därför måste somliga resultat betraktas med viss försiktighet, så att inte tolkningar övergeneraliseras utan hänsyn till den variabilitet och osäkerhet som härrör bergbeskrivningen (Öhman et al. 2014).

# Contents

# 1 Introduction

## 1.1 Background of the SR-PSU project

The final repository for low and intermediate level short-lived radioactive waste (SFR) was constructed in its first stage and taken into operation in 1987. The SFR facility requires an extension due to: 1) the pending decommissioning of the closed reactors (Barsebäck, Studsvik, and Ågesta), 2) the increased amounts of operational waste caused by the extended operating time of the remaining nuclear power plants, and 3) the future decommission of the remaining nuclear power plants. The existing facility is denoted SFR 1, while the planned extension is denoted SFR 3.

As a part of the license application for SFR 3, the Swedish Nuclear Fuel and Waste Management Company (SKB) initiated a project for the planned extension of SFR (PSU) in 2008 (SKB 2008). The overall purpose of PSU is to develop a site descriptive model (SDM-PSU; SKB 2013) and to assess the radiological safety for the entire SFR-repository after closure (SR-PSU). All hydrogeological modelling tasks within SR-PSU are defined and referred to by means of so-called Task Descriptions (TDs).

The groundwater flow model, which was developed within the SDM-PSU project to describe the hydrogeological conditions at SFR, is applied in SR-PSU as a numerical tool to assess the performance of the backfilled repository. In a preceding modelling task, TD11, one model setup was identified as a representative Base case (out of 17 parameterisation variants analysed; Öhman et al. 2014). This document summarizes the model results of TD12, where the Base-case model setup is used to analyse the hydraulic interactions between the disposal rooms of SFR 1 and SFR 3 and a number of hypothetical water-supply wells.

## 1.2 Settings

SFR is located in northern Uppland within the municipality of Östhammar, about 120 km north of Stockholm (Figure 1-1). The site is located about 2 km north of the site selected for the final repository for spent nuclear fuel (SDM-Site Forsmark; Follin 2008).

The current ground surface in the Forsmark region forms a part of the sub-Cambrian peneplain in south-eastern Sweden, which represents a relatively flat topographic surface with a gentle dip towards the east. The Forsmark region is characterised by small-scale topography at low elevation. The whole area is located below the highest coastline associated with the last glaciation, and large parts of the area emerged from the Baltic Sea only during the last 2,000 years. Both the flat topography and the still ongoing shoreline displacement of about 6 mm per year strongly influence the current landscape. In the long-term perspective, sea bottoms are continuously transformed into new terrestrial areas or freshwater lakes, and lakes and wetlands are successively covered by peat.

Currently, most of the area around SFR is submerged below sea, but with the continuing shore-line displacement, the seafloor above SFR will rise above the shoreline within c 1,000 years. By 5000 AD, several areas of potentially arable land will have emerged from the sea (Figure 1-2) and the flow regime will have reached a stationary state (i.e. more or less unaffected by further shoreline retreat). This study is therefore devoted to addressing water-supply wells drilled in rock by the stage of shoreline retreat at 5000 AD.

The existing repository facility, SFR 1, consists of four rock vaults and one vertically extending silo. The four rock vaults of SFR 1 are contained within an elevation range from c –70 m to –90 m (elevation system RHB 70), whereas the silo extends from c –70 m to –140 m. The planned extension, SFR 3, consists of six rock vaults, which will extend from c –120 m to –140 m (the relative depths of disposal rooms can be inferred from Figure 2-4b).

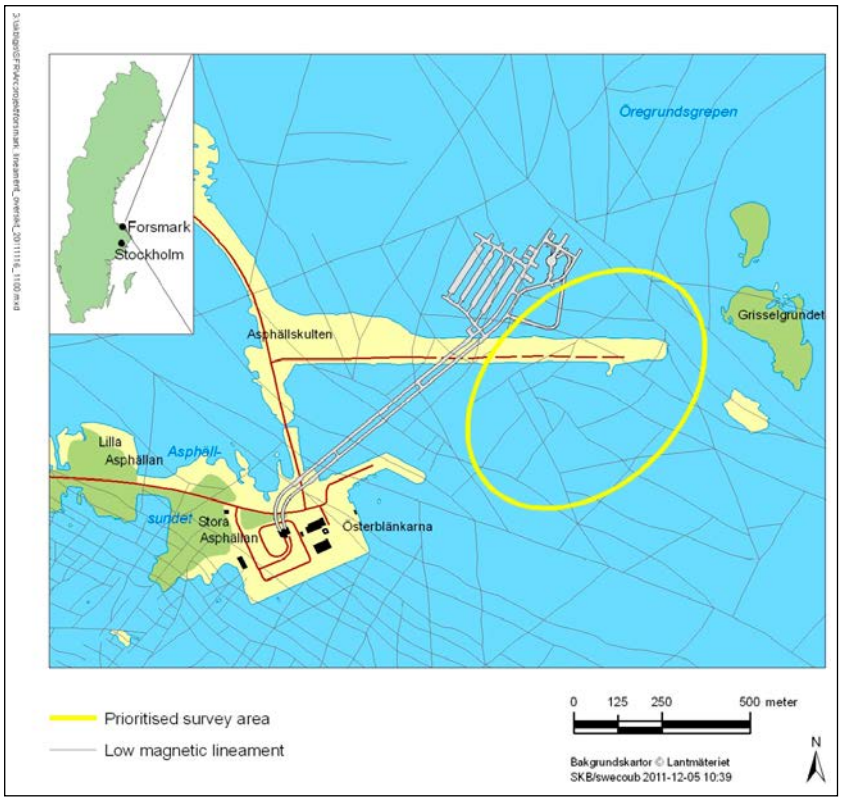


***Figure 1-1.*** *Map of the existing SFR facility (SFR 1) and the suggested area for the SFR extension (SFR 3; yellow in the map). In this report, the man-made wave breaker above the facility is referred to as the 'SFR Pier'.*

## 1.3 Objectives

The outputs of earlier hydrogeological modelling tasks, TD11 and TD08, have provided predicted performance measures under *undisturbed conditions* for the biosphere assessment (i.e. in the absence of abstraction from water-supply wells). The purpose of this study, TD12, is to assess the impact of hypothetical, future water-supply wells drilled in rock, such that the output, combined with the previous outputs from TD11, will facilitate dose assessments that can be related to radionuclide transport to wells. Earlier simulations have demonstrated that SFR is hosted in a dynamic hydrogeological setting due to the ongoing shore-line displacement (Öhman et al. 2014); the current study is limited to address the stage of shoreline retreat at 5000 AD.

More specifically, the TD12 objectives are to study:

(1) The influence that the abstraction of water from wells may have on groundwater flow through the facility (SFR 1 and SFR 3).

(2) Groundwater-flow interaction between the facility (SFR 1 and SFR 3) and water-supply wells.

The purposes of this task are twofold: 1) to provide a general understanding of the hydrogeological possibilities to use drilled wells for water supply downstream from SFR, and associated effects on groundwater flow, and 2) to provide input data for dose-assessment modelling in the biosphere assessment (Saetre et al. 2013, Werner et al. 2013). For these purposes, two types of well locations are addressed: 1) water-supply wells for settlements associated to potential arable land (Figure 1-2) and 2) the area where the highest radionuclide concentrations originating from SFR can be expected (Figure 1-3).

The modelling scope, divided into Subtasks A, B, and C, is presented in more detail in Section 1.4, along with a presentation of the selected well locations.

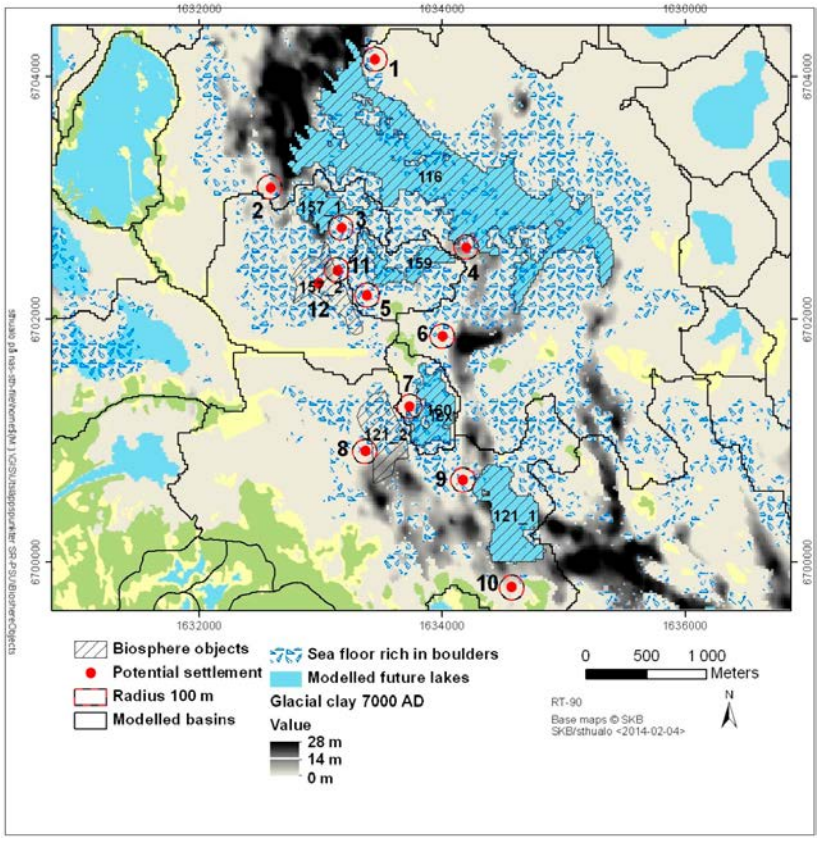


***Figure 1-2.*** *Settlements associated to potential arable land (Werner et al. 2013) and associated wells 1 to 11 (Table 1-1). Well 12 is not associated to potential arable land, but is located in the so-called well-interaction area (Figure 1-3).*

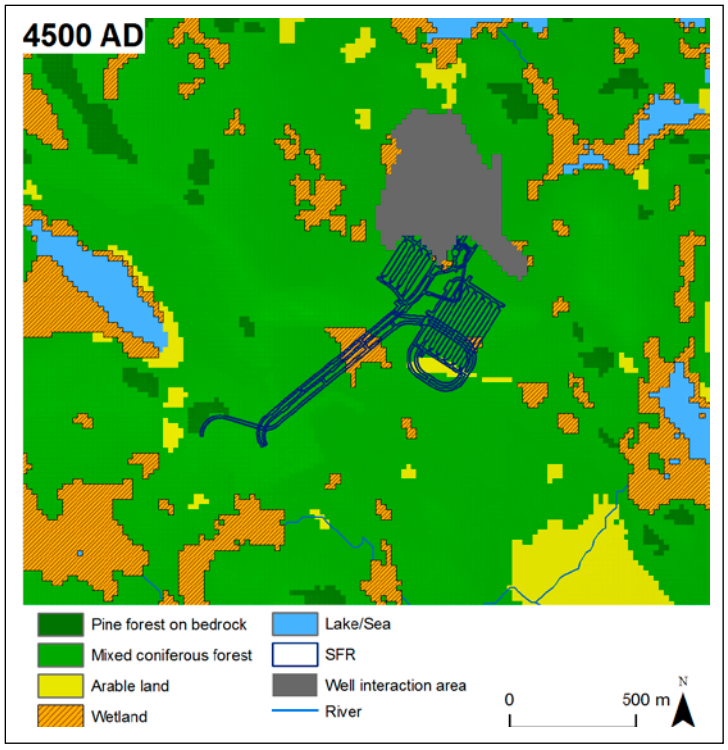


***Figure 1-3.*** *Well-interaction area, where the highest concentrations of radionuclides originating from SFR are expected, delineated based on TD11 particle-tracking results (Werner et al. 2013).*

## 1.4 Modelling scope

The flow simulations in this study employ the groundwater-flow model that was developed in SDM-PSU (SKB 2013). A sensitivity analysis was undertaken in TD11 (Öhman et al. 2014) to assess the combined effects of model uncertainty, bedrock heterogeneity, and the transient hydrogeological setting due to shoreline retreat and landscape development. Hence, these aspects are not addressed here, and instead all attention is directed towards the hypothetical water-supply wells.

The execution of the TD12 was organised to meet the objectives within the given time line of the SR-PSU project. Hence, the simulations were setup within the framework of existing numerical approaches developed in preceding modelling tasks, e.g. Öhman et al. 2014). For example, water-supply wells are given a simplistic model representation (Section 3.1) and the model top-boundary condition is based on a flow solution from previous work (i.e. here implemented with only a minimum of necessary adaptation; Section 3.3.3).

All flow simulations in TD12 employ the "Base case" model setup, which was selected as the most representative out of 17 analysed parameterisation variants (more precisely, [BASE_CASE1_DFN_R85_L1BC]; Öhman et al. 2014). Moreover, all simulations address the hydrogeological setting for the stage of shoreline retreat by 5000 AD. There are two reasons for selecting this time point: 1) potential arable land around SFR has recently been exposed and 2) the groundwater flow regime has reached a pseudo-stationary state, more or less unaffected by further shoreline retreat.

The TD12 study is divided into three steps, referred to as Subtasks A–C (see below), each focusing on specific aspects related to future wells drilled in rock.

### 1.4.1 Well definitions

In total, 20 water-supply wells are included in this study, of which all are assumed to be vertical and drilled 60 m deep into the bedrock. The assumed well depth is based on data from the SGU Well Archive, delivered to SKB in 2011 (see e.g. Werner et al. 2013). Specifically, updated well-depth statistics are calculated for 5,164 wells, located in the same area in northern Uppland previously analysed by Gentzschein et al. (2007). Details regarding their numerical representation in the computational grid and specifics concerning well casing are provided in Chapter 3. The standard production rate of wells, $Q_{well}$, is set to 700 L/d, corresponding to the estimated total water demand for a self-sustaining community of modern farmers in SR-PSU (Werner et al. 2013). As discussed below, suitable locations must be determined for certain wells, such that the water-consumption demand can be met for realistic drawdowns.

Two types of well locations are studied to meet the objectives of TD12 (Section 1.3); these have been chosen to represent two different aspects:

1) Water-supply wells to meet the demand for settlements associated to potential arable land (i.e. locations reflecting assumed future land use, and in turn, water consumption; Figure 1-2).
2) Water-supply wells in the well-interaction area downstream from SFR, i.e. the area in which wells may have the highest concentrations of radionuclides originating from SFR (Figure 1-3). The motivation for analysing these wells is that it cannot be ruled out that future drilling of water-supply wells may occur also at other locations, decoupled from any foreseeable land use for a self-sustaining community.

Correspondingly, the following water-supply well positions are therefore addressed (Table 1-1):

1) Wells 1 to 11, associated to potential arable land (Subtask A).
2) Well 12 in the interaction area (Subtasks A and B).
3) Wells 21 to 28 in the interaction area (Subtask C).

As mentioned above, wells 1 to 11 are water-supply wells associated to agricultural settlements in areas of potential arable land (Figure 1-2). In the model setup for Subtask A, these water-supply wells are to be located in the vicinity of these potential settlements (within 100 m radius, as indicated by circles in Figure 1-2). The emplacements of these settlements (provided in Table 1-1) are used as reference for identifying functional well locations, i.e. suitable locations for satisfying the assigned water demand. Well 12, which is also analysed in Subtask A, is not associated to agricultural settlements, but was included in the subtask to enable an early comparison against a well in the interaction area. Wells 21 to 28 are intended to map out the locations of maximum interaction, in order to improve the understanding of well interactions and to test if well 12 indeed is a "worst-case scenario".

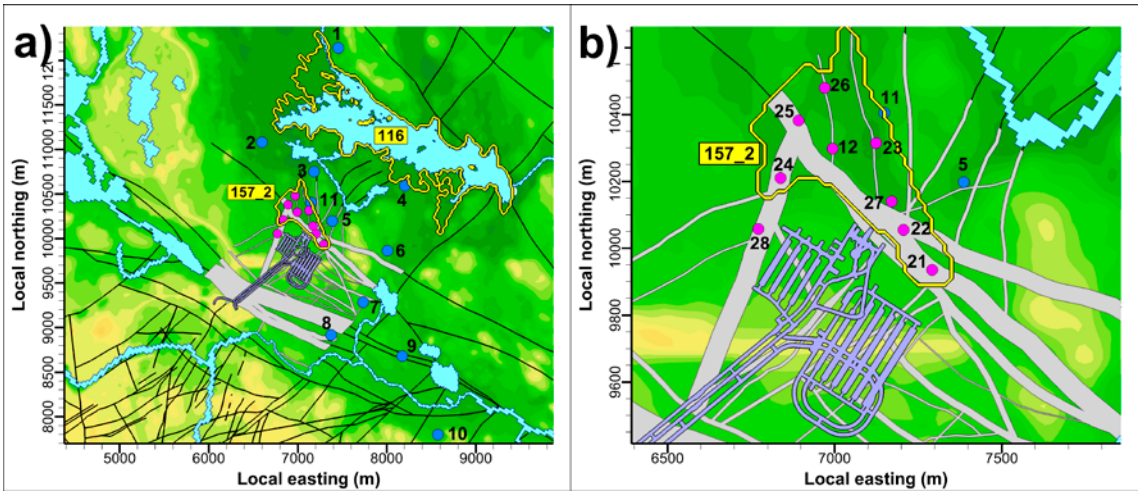


***Figure 1-4.*** *Locations of the water-supply wells to be analysed; a) wells associated to settlements in areas of potential arable land (blue dots; wells 1 to 11 in Table 1-1) and b) wells in the interaction area downstream of SFR (pink dots; wells 12 and 21 to 28 in Table 1-1). Biosphere objects 116 (also referred to as Charlie's lake) and 157_2 (identified as the main discharge area for SFR; Öhman et al. 2014) are included for spatial reference.*

**Table 1-1. Initial well locations. Provided from Werner et al. (2013).**

| Well[1)] | Initial location[2)] | | Rotated model coordinates[3)] | | Association type |
|---|---|---|---|---|---|
| | Easting (m) | Northing (m) | x' (m) | y' (m) | |
| Batch 1 | | | | | |
| 1 | 1633455 | 6704141 | 5704.89 | 12246.2 | Arable land |
| 2 | 1632597 | 6703081 | 5552.88 | 10890.97 | Arable land |
| 3 | 1633182 | 6702751 | 6223.52 | 10928 | Arable land |
| 4 | 1634204 | 6702592 | 7170.26 | 11344.48 | Arable land |
| 5 | 1633386 | 6702198 | 6693.25 | 10571.93 | Arable land |
| 6 | 1634009 | 6701862 | 7399.13 | 10624.38 | Arable land |
| 7 | 1633736 | 6701284 | 7480.42 | 9990.34 | Arable land |
| 8 | 1633373 | 6700918 | 7371.7 | 9486.45 | Arable land |
| 9 | 1634174 | 6700681 | 8174.24 | 9718.18 | Arable land |
| 10 | 1634574 | 6699798 | 8986.85 | 9189.63 | Arable land |
| 11 | 1633149 | 6702405 | 6382.07 | 10618.7 | Arable land |
| 12[4)] | 1632994 | 6702298 | 6309.1 | 10445.06 | Well-interaction area |
| Batch 2 | | | | | |
| 21 | 1633292 | 6701935 | 6755.7 | 10299.71 | Well-interaction area |
| 22 | 1633206 | 6702055 | 6618.61 | 10354.5 | Well-interaction area |
| 23 | 1633124 | 6702315 | 6409.48 | 10529.4 | Well-interaction area |
| 24 | 1632838 | 6702210 | 6225.06 | 10286.89 | Well-interaction area |
| 25 | 1632892 | 6702382 | 6177.92 | 10460.9 | Well-interaction area |
| 26 | 1632971 | 6702480 | 6191.7 | 10586.02 | Well-interaction area |
| 27 | 1633171 | 6702140 | 6543.34 | 10407.27 | Well-interaction area |
| 28 | 1632771 | 6702058 | 6250.48 | 10122.74 | Well-interaction area |

[1)] Notation used in this report.

[2)] For wells 1 to 11, the well location refers to the centre of the corresponding agricultural settlement area (i.e. it is not the final well location). For well 12, the given well location is approximate and it is relocated to a conductive zone to maximise interaction with SFR. For wells 21 to 28, the final well locations are given (they are not re-located).

[3)] Rotated model coordinates explained in Section 2.2.2.

[4)] To emphasise its association to the well-interaction area, well 12 is denoted "Well 29" in Werner et al. (2013).

### 1.4.2 Subtask A – Water-supply wells associated to arable land compared to a well in the interaction area

Subtask A addresses 11 water-supply wells associated to settlements at potential arable land (Figure 1-2) and a well in the well-interaction area (well 12; Figure 1-3), decoupled from arable land. The provided data for Subtask A are 11 areas of potential agricultural settlements and an approximate location for well 12. The provided initial well locations (Table 1-1) are based on the local bedrock properties, and specifically, the locations are not compliant to the local heterogeneity as parameterised and discretised in the particular flow model setup (i.e. the base case, as defined in TD11; Öhman et al. 2014).

In other words, the provided initial locations are not intended as functional well locations *per se*, but rather act as reference for localising appropriate well positions, according to the following principles:

- The well shall be located within 100 m distance from the centre of the assigned settlement area (marked by circles in Figure 1-2. Well 12 may be re-located 100 m from its initially assigned location).
- In SR-PSU, the total water demand for a self-sustaining community of modern farmers is assumed to be 700 L/d. This well production, $Q_{well} \geq 700$ L/d, is taken as a prerequisite for the well emplacement. The well production shall be "sustainable" in terms of a steady-state simulation.
- The depth of wells is 60 m into the bedrock, which effectively sets the theoretical maximum drawdown to, $s < 60$ m. TD12 concerns larger-scale groundwater flow patterns and is not focused on the flow pattern in or in the immediate vicinity of wells. Therefore, well dimensions are not explicitly resolved in the computational grid (Section 3.1.1), and it is judged reasonable to assume a maximum required drawdown of $s \approx 10$ m in the model cells in the bedrock that represent the well.
- It is assumed that for any given well location, the well capacity, $Q_{well}/s$ ($m^2/s$), can be directly evaluated from grid-cell properties (Section 3.2), thereby circumventing time-consuming flow simulations to assess well capacities. In turn, the required well production and the assumed maximum drawdown, $s \approx 10$ m, provide an estimate of the minimum well capacity, $Q_{well}/s \geq 8.1 \cdot 10^{-7}$ $m^2/s$. A geometrical sampling algorithm is therefore developed to determine well capacities in each potential settlement area (wells 1–11) and within 100 m from the initially assigned location of well 12. This algorithm is based on geometrical sampling of the local hydrogeological parameterisation of the bedrock (details in Section 3.2.1).

The method developed to conform the well locations to the local bedrock heterogeneity, as parameterised and discretised in the base-case model setup, is presented in Sections 3.1 and 3.2. As a second preparatory step prior to simulations, tests are carried out to find a suitable modelling sequence (recharge phase, steady-state phase) for representation of water-supply wells in DarcyTools (Section 3.3).

For each well, interactions with the SFR facility, as well as performance measures of those flow paths, are determined by means of particle tracking, as follows:

- Forward tracking of totally $10^6$ particles, uniformly released within the disposal rooms of SFR 1 (1BTF, 2BTF, 1BLA, 1BMA and Silo).
- Forward tracking of totally $10^6$ particles, uniformly released within the disposal rooms of SFR 3 (2BLA, 3BLA, 4BLA, 5BLA, 2BMA and 1BRT).
- Backward tracking of totally $10^6$ particles from the pumped well, or more precisely, all particles are released within the "pump cell" of the well, as explained in Section 3.3).

### 1.4.3 Subtask B – Impact of water abstraction rate

The simulated water-abstraction rate of 700 L/d in wells 1 to 12 (Subtask A) is found to have a very small influence on the flow across disposal rooms (Section 4.2). Consequently, Subtask B addresses the impact of variable water-abstraction rates in well 12 in the well interaction area (Figure 1-3). Well 12 is chosen for this analysis, as it was found to have the highest influence on disposal-room flow in Subtask A (0 to 0.4%; Table 4-7). It should be emphasised that well 12 is not associated to any settlement at potential arable land.

Subtask B follows the same sequence of flow and particle-tracking simulations as Subtask A. Specifically, the following pumping rates are addressed for well 12:

- $Q_{well}$ = 1,000 L/d, approximately the present-day water demand for 5 individuals (Werner et al. 2013).
- $Q_{well}$ = 1,400 L/d, i.e. twice the pumping rate in Subtask A.
- $Q_{well}$ = 2,800 L/d, i.e. four times the pumping rate in Subtask A.

### 1.4.4 Subtask C – Wells in the well-interaction area

Based on the simulation results of TD11, a well-interaction area has been defined as the area in which wells may have the highest concentrations of radionuclides originating from SFR (Figure 1-3). One well in this area (well 12) was studied in Subtasks A and B. The aim of Subtask C is to survey interactions between SFR and wells in the well-interaction area for another 8 wells (wells 21 to 28; Table 1-1; Figure 1-4). The execution of this task employs the same flow-simulation sequence as Subtasks A and B, although only forward particle-tracking is performed in the analysis of interactions and performance measures of interacting flow paths.

## 1.5 SR-PSU performance measures

The primary objective of TD12 is to assess groundwater-flow interactions between the disposal rooms of the SFR facility (SFR 1 and SFR 3) and water-supply wells. The interactions are determined by means of particle tracking, as the fraction of bedrock particle trajectories that pass through a disposal room and terminate in a pumped water-supply well. The interactions can be determined by traversing the flow field in both directions (described in detail in Section 3.4):

1) *Forward*-tracked interactions, $f_{ij}$ [–], is the fraction of particles, released uniformly in a disposal room $i$, that that reach a pumped well, $j$.
2) *Back*-tracked interactions, $f_{ji}$ [–], is the fraction of particles in a pumped well, $j$, for which upstream flow paths pass a disposal room, $i$.

The particle-tracking results should be independent on direction of execution; this is verified by employing and comparing both concepts, which is of particular interest in Subtask B. The performance measures studied in SR-PSU are summarised briefly below.

#### *Disposal-room cross flow (Q)*

The cross flow through disposal rooms, $Q$ ($m^3/s$), is an important performance measure in the SR-PSU groundwater flow modelling, as it affects the strength of the source term in radionuclide transport modelling. Cross flow refers to the flow over a predefined cross-sectional area in the computational grid. This area is defined as the interface between a subunit of interest (e.g. a well or a disposal room) and the surrounding, arbitrary grid cells. The calculation of disposal-room cross flow is explained in more detail in the preceding sensitivity analysis, where the combined effects of conceptual uncertainty and bedrock heterogeneity were addressed (Öhman et al. 2014).

The determination of disposal-room cross flow must be cautiously treated, as the flow occurs over an enclosed surface, which by definition has a zero net flow. Consequently, the "cross flow" must be determined as either in inward-directed flow, $\Sigma Q^+$, or outward-directed flow, $\Sigma Q^-$, which are identical in magnitude, $\Sigma Q^+ = |\Sigma Q^-|$. However, discretisation artefacts tend to exaggerate the magnitude in flow terms, $\Sigma Q^+$ and $|\Sigma Q^-|$, depending on the level of alignment between tunnel geometry, grid discretisation, and the direction of flow (see evaluation in TD08, SKBdoc 1395214). This error is significantly reduced by employing the rotated coordinate system to align the computational grid to tunnel geometry (Section 2.2.2) and to determine the cross flow based on the "cell-net principle" to reduce local corner-flow effects, as explained in (Öhman et al. 2014). It should be noted that the rotated coordinate system does not improve the performance of the Silo, owing to its cylindrical geometry.

Due to an inbuilt error in the DarcyTools pressure correction between cells of different sizes (briefly described in Section 2.1.1 and analysed in detail in SKBdoc 1396127) a separate algorithm must be applied for rock cavern 2BMA. Due to a particular configuration of cell size and tunnel conductivity parameterisation, the tunnel flow across 2BMA cannot be calculated for tunnel cells, but must instead be based on flow across its surrounding *bedrock cells*. This approach is found to reduce the error in flow for 2BMA to c 4% (SKBdoc 1396127).

TD12 addresses two aspects of disposal-room cross flow: 1) the potential influence of water abstraction in water-supply wells (expressed as a percentage relative to the TD11 results) and 2) the "flow ratio", $Q_i/Q_j$ [–], between $Q_i$, the flow through disposal-room $i$, and $Q_j$, the water abstraction from a well $j$. The flow ratio is the key to: 1) verify that the particle-tracking results are independent on the direction of execution, as well as, 2) relate determined particle interactions to dilution phenomena (i.e. fraction of abstracted water that originates via a disposal room of the SFR facility).

#### *Particle exit location*

Exit locations are determined by means of *forward* particle tracking, and defined as the point where the particle passes the bedrock/regolith surface (expressed in RT90 coordinates). The corresponding "recharge location" at the bedrock/regolith surface can analogously be determined by means of *backward* particle tracking. Exit and recharge locations are useful for visualisation purposes and provide a framework for interpreting the hydrogeological setting and radionuclide transport in the context of the location of wells.

#### *Flow-related transport resistance ($F_r$)*

The flow-related transport resistance in rock, $F_r$ (y/m), is an entity, integrated along flow paths, that quantifies the flow-related (hydrodynamic) aspects of the possible retention of solutes transported in a fractured medium. It is also an important performance measure in the SR-PSU groundwater flow modelling. In the SR-PSU project, information about the flow-related transport resistance governs the calculation of radionuclide transport, hydrogeochemical calculations of salt diffusion into and out from the matrix, as well as oxygen ingress. In its most intuitive form, although not necessarily most generalised, the flow-related transport resistance is proportional to the ratio of flow-wetted fracture surface area (FWS) and flow rate (Joyce et al. 2010). An alternative definition is the ratio of FWS per unit volume of flowing water multiplied by the advective travel time.

#### *Advective travel time ($t_{w,r}$)*

The travel time, $t_{w,r}$ (y), is the cumulative advective residence time for a particle along a trajectory in the rock. Kinematic porosity, as determined from upscaled transport apertures of the underlying fracture-network realization, is a critical parameter for determining the advective travel time of particle trajectories. Fracture transport aperture is assumed to be correlated to transmissivity, as suggested by Dershowitz et al. (2003), based on Äspö Task Force 6c results

$$e_t = 0.46\sqrt{T} \tag{1-1}$$

where $e_t$ is the transport aperture [m] of a fracture and $T$ is its transmissivity [$m^2/s$].

# 2 Modelling context

This chapter presents an outline for the approach taken to meet the TD12 objectives (Section 1.3). The foundation of all flow simulations in TD12 is the model setup that was defined as the "Base case" in TD11, [BASE_CASE1_DFN_R85_L1BC], and the hydrogeological setting for the stage of shoreline retreat by 5000 AD (Öhman et al. 2014). Only the most fundamental concepts of the model setup and execution are summarized in this chapter, for a more detailed outline of the modelling sequence (i.e. handling of input data, model setup, and execution procedure for simulations), the reader is referred to Öhman et al. (2014). The focus of this chapter is to describe the model adaptations that have been made to meet the TD12 objectives, i.e. introducing a model representation of the future hypothetical water-supply wells (Table 1-1).

The flow-simulation code used, DarcyTools, is the corner stone in this modelling task, and therefore its inbuilt feasibilities, limitations and user control set the framework for the numerical approach. As the flow-simulation code has a significant influence on the numerical approach, this chapter starts off with a brief presentation of DarcyTools (Section 2.1).

## 2.1 Modelling tool

All flow simulations in this study employ the computer code DarcyTools, which has been specifically developed for the analysis of a repository for spent nuclear fuel (Svensson et al. 2010, Svensson and Ferry 2010).

DarcyTools is based on the Continuum Porous-Medium (CPM) approach (Svensson et al. 2010), in which the hydraulic properties of a flowing fracture network are approximated by those of a porous medium. DarcyTools allows transferring fracture-network characteristics, as observed in borehole data, onto its computational grid by means of geometrical upscaling over grid cells. These upscaled properties are referred to as Equivalent Continuum Porous Medium (ECPM) properties. As the ECPM approach is based on an underlying stochastic DFN model, the resulting ECPM properties are also stochastic. The uncertainty related to hydraulic heterogeneity can therefore be handled by addressing multiple DFN realisations.

The appeal of the ECPM approach is its computational parsimony and an upscaled conductivity field that bears the hydraulic traits of an underlying fracture network, for example anisotropic correlation structures. Unfortunately, *geometrical* up-scaling does not always ensure *hydraulic* consistency between the complex heterogeneity of the underlying flowing fracture network and the approximated ECPM. It must therefore be emphasised that the term "equivalent" requires a fine resolution of the computational grid in order to be valid.

Another key feature in DarcyTools is its unstructured Cartesian grid system, which allows great flexibility in local grid refinement to represent detailed geometry of objects (e.g. tunnel layout). All grid geometry is handled via so-called DarcyTools objects (a code-specific file format), which have been constructed from original CAD data geometry.

### 2.1.1 Identified error related to parameter <nbgrad>

All simulations in this study are performed with code versions DarcyTools v.3.4.18 and Migal v. 4.01. During the execution of TD11 an error was identified in these code versions. Owing to the unstructured grid arrangement, DarcyTools employs a pressure-correction algorithm (controlled by the parameter <nbgrad>), which is intended to hamper artificial gradients between cells of different conductivity and size. Unfortunately, this algorithm was found to be numerically unstable for particular configurations of conductivity/cell-size contrasts.

Significant attention has been paid to circumvent this error from affecting the performance measures (described in detail in separate PM, SKBdoc 1396127). A particular configuration of grid discretisation and tunnel-conductivity parameterisation in rock cavern 2BMA (Öhman et al. 2014) is found to cause large, local artefacts in tunnel-wall flow, and in turn resulting in a one-order-of-magnitude error in its evaluation of disposal-room cross flow, Q. To minimise the effects of these artefacts, the algorithm was changed so as *not* to calculate Q from *tunnel cells*, but instead from the *bedrock cells* surrounding 2BMA (which are unaffected by the numerical error). This workaround reduces the error in 2BMA to c 4% (SKBdoc 1396127). The error is not observed for other rock caverns.

Although the occurrence of these numerical artefacts is rare, the phenomenon has been found at scattered locations in the bedrock (related to extreme conductivity contrasts, which arise from ECPM translation of the underlying stochastic fracture network). These artefacts take the form of *local flow cells*, which are not judged to have any effect on the large-scale flow solution, but may force particles into loops, and in turn, overestimate their cumulative performance measures, such as path length, travel time, $t_{w,r}$, and flow-related transport resistance in rock, $F_r$ (Section 1.5). Overall, the impact of particle looping is found to be small; the fraction of particles where the overestimation in transport properties exceeds one order of magnitude is only 0.001%. The particle-tracking algorithm was modified to prevent accumulation inside loops, which effectively eliminates the impact on transport properties (SKBdoc 1396127).

The inbuilt pressure-correction algorithm, related to the parameter <nbgrad>, is corrected in all subsequent versions of DarcyTools.

## 2.2 Modelling concepts used in SR-PSU

The modelling procedure, including specifications to input data, model setup, execution, and derivation of performance measures, has been explained in detail in TD11 (Öhman et al. 2014).The focus of this chapter is to describe the model adaptations made to meet the TD12 objectives, i.e. introducing a model representation of the future hypothetical water-supply wells (Table 1-1).

### 2.2.1 Flow domain

The flow domain defines the outer perimeter of the model volume, i.e. the vertical sides of the model (Figure 2-1). The vertical sides of the model are intended to represent no-flow boundaries in simulations (Section 3.3.3), and therefore the flow domain is defined based on topographical water divides and sub-catchments. Areas that are currently below sea are chosen with respect to 1) modelled future topographical divides in the RLDM (Brydsten and Strömgren 2013), 2) the deep seafloor trench (the so-called Gräsörännan), and 3) general expectations of the regional future hydraulic gradient. The flow domain extends vertically from +100 m to –1,100 m elevation.

### 2.2.2 Coordinate systems

All input and output data are provided in the RT90 coordinate system. Modelling and visualisation of model output employs a translated, local coordinate system (cf. Figure 2-1), with a local origin defined at the RT90 coordinate [1626000, 6692000].

DarcyTools simulations employ a rotated local coordinate system that is parallel to the rock caverns of the existing SFR1. The principles of this rotated grid are provided in Öhman et al. (2013). A coordinate in the DarcyTools grid is referred to as [x', y'], and it has been rotated counter-clockwise by the rotation angle: 32.58816946° around the pivot point [6400, 9200] in local coordinate system. However, as stated above, all model output is back-rotated to the Cartesian local coordinate system.

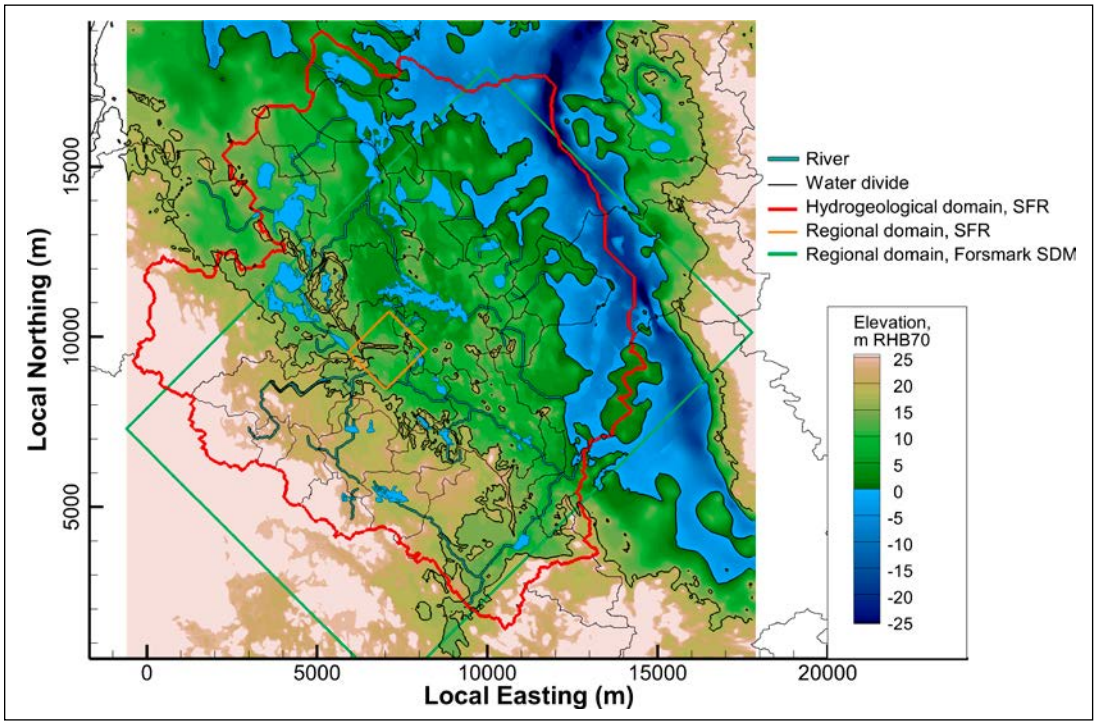


***Figure 2-1.*** *The flow domain (red line) is the outer boundary in the flow simulation. The SFR Regional domain (orange line) is the boundary for local bedrock parameterisation developed within SDM-PSU. The current shoreline, the shoreline at 5000 AD, and water divides are shown as black lines.*

### 2.2.3 Bedrock parameterisation

The applied groundwater flow model is subject to heterogeneity and model uncertainty; this has been addressed by means of a sensitivity analysis of bedrock parameterisation variants, referred to as "Bedrock cases" in TD11. This study focusses on future, hypothetical water-supply wells (Table 1-1). To reduce model complexity, a single bedrock parameterisation, the Base case, is employed in all flow simulations of this study (Figure 2-2). This implies that:

1) Simulation results in TD12 are performed for a single bedrock-parameterisation setup, and hence do not cover known aspects of heterogeneity and model uncertainty (e.g. the sensitivity in disposal-room cross flow due to bedrock parameterisation, shown in Figure 2-3). It should therefore be emphasised that these aspects should be accounted for retrospectively, by combining the results of TD11 and TD12 in the biosphere assessment.
2) The Base case has been selected as the representative parameterisation for median disposal-room cross flow, but only in terms of *overall average characteristics*. Thus, at the *individual level*, disposal-room cross flows are not necessarily contained within the upper/lower quartiles (Figure 2-3). Hence, this individual deviation must be accounted for before drawing generalised conclusions concerning relative differences between disposal rooms in this study (cf. Chapter 4).
3) The wells are subject to the water-supply criteria (Section 1.3), and therefore in turn, their locations are compliant to local bedrock properties, which are Bedrock-case specific. In other words, studying another Bedrock case may require re-positioning of wells to fulfil the water-supply criteria.

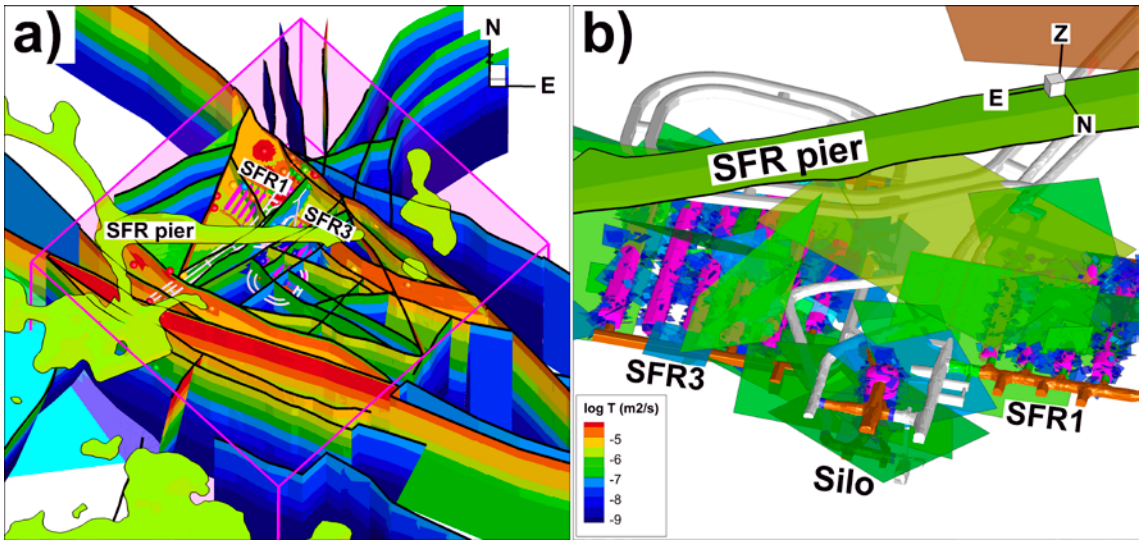


***Figure 2-2.*** *Base-case bedrock parameterisation, selected as representative for average disposal-room cross flows in TD11; a) deformation-zone parameterisation and b) rock mass outside deformation zones, modelled as a stochastic realisation of connected fractures and Unresolved PDZs (only features intersecting disposal rooms are shown).*

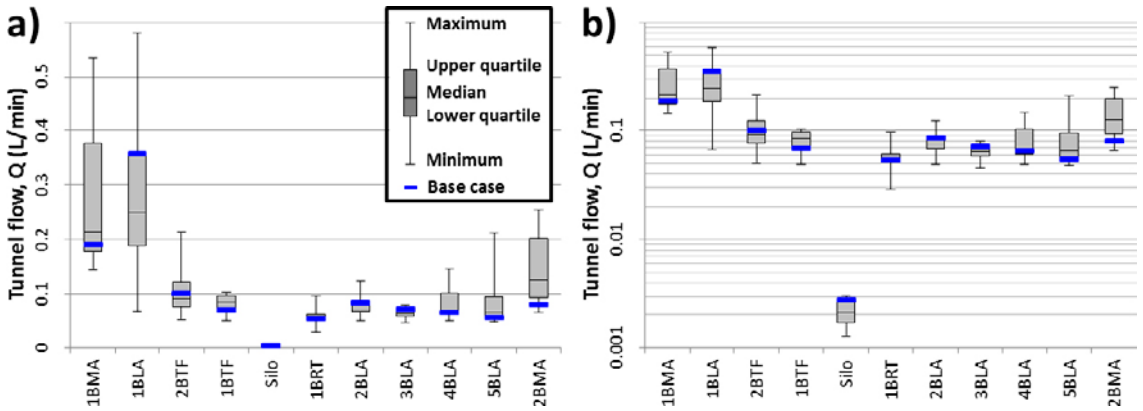


***Figure 2-3.*** *Disposal-room cross flow in the Base-case parameterisation (blue dash) compared to the bedrock-case ensemble analysed in the preceding TD11 sensitivity analysis (box-whiskers); a) linear scale and b) logarithmic scale.*

A few characteristics of the Base-case bedrock parameterisation are presented below; details are given in Öhman et al. (2014).

- Deterministic deformation zones (Figure 2-2a) are parameterised as:
  - Homogeneous, i.e. spatial heterogeneity within zones is not accounted for,
  - depth trend in transmissivity, although not delineated from SDM-PSU data, it is *assumed* based on extensive data support from SDM-Site Forsmark (Follin 2008), and
  - local conditioning at borehole intercepts, as well as rock-cavern intersections in SFR 1 (Figure 2-4; details in Öhman et al. 2013).
- The rock mass outside deformation zones is parameterised by means of a stochastic realisation of hydraulically connected fractures and "Unresolved PDZs". This particular realisation is referred to as R85, and selected as the most pessimistic realisation for rock caverns in SFR 1 (details provided in SKBdoc 1395200).
- An additional type of deterministic structures (Shallow-Bedrock Aquifer structures, or SBA-structures) is included to represent networks of predominantly sub-horizontal fractures with elevated transmissivity (see Öhman et al. 2012).

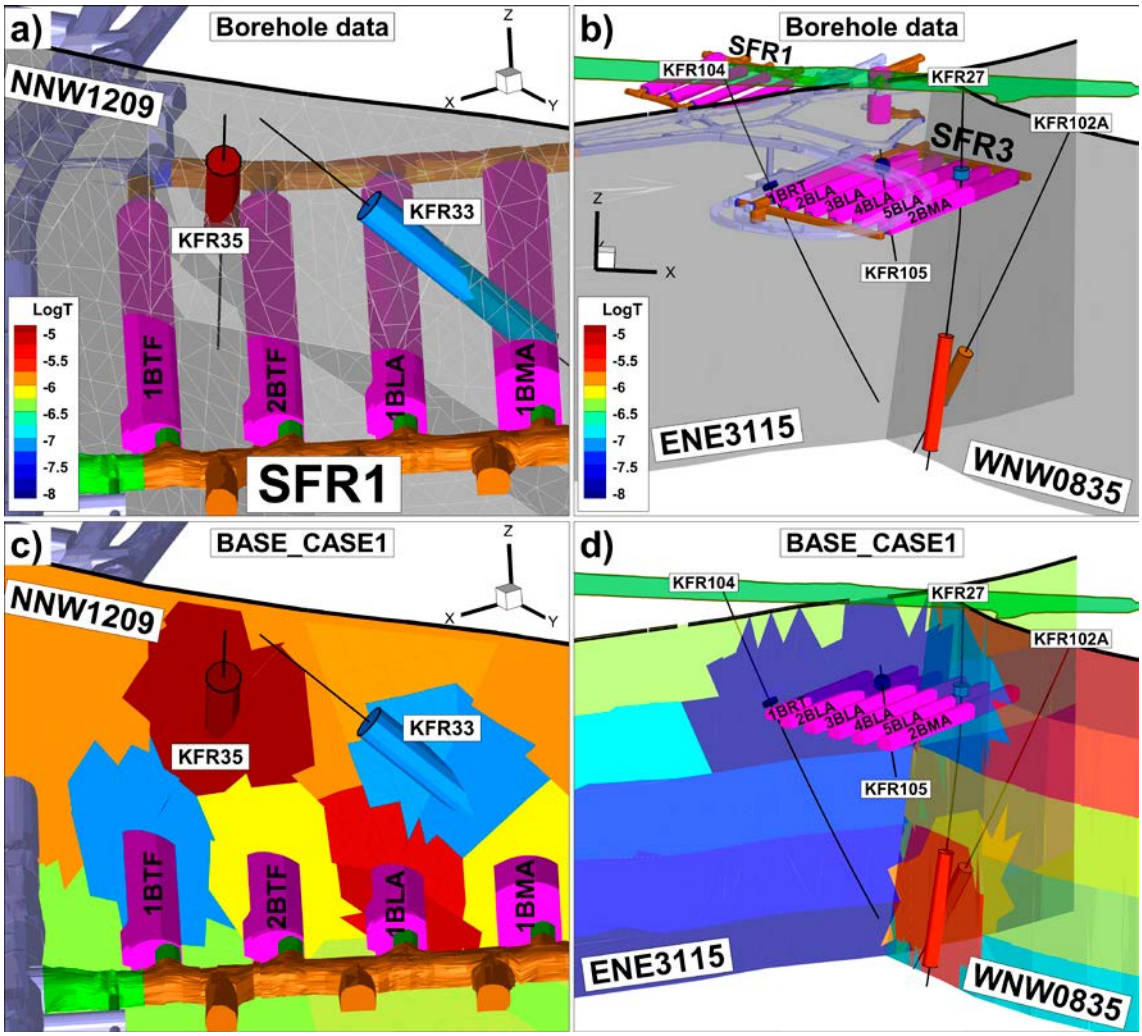


***Figure 2-4.*** *Conditioning of key deformation zones for disposal-room cross flow; a) borehole support for ZFMNNW1209, b) borehole support for ZFMENE3115 and ZFMWNW0835, c) conditioning based on borehole intercepts and rock-cavern intersections, and d) local borehole conditioning of ZFMENE3115 and ZFMWNW0835.*

Notably, in context of the full ensemble of simulated disposal-room cross flow in the preceding TD11 sensitivity analysis (Öhman et al. 2014), the Base-case parameterisation stands out somewhat in terms of high cross flow for 1BLA, but low cross flow in 4BLA, 5BLA, and 2BMA (Figure 2-3). These deviancies are intimately related to local conditioning of deformation zones applied at rock-cavern intersections (Figure 2-4), where the 1BLA intersection with ZFMNNW1209 is parameterized as highly transmissive, whereas the intersections between ZFMWNW0835 and 4BLA, 5BLA and 2BMA are parameterized as less transmissive.

### 2.2.4 Mixed boundary condition concept

A so-called *mixed* top boundary condition was applied in TD11 (described in Öhman et al. 2014). The concept is referred to as mixed, as it employs a combination of the two boundary-condition types *specified head* and *specified flux*. The top-boundary condition has two phases:

- In a preceding *recharge* phase, a realistic head-field is determined for ground-surface cells (or, less strictly speaking, the elevation of the groundwater table) by means of a flow solution with locally variable net precipitation.
- In a subsequent *steady-state* phase, the head of ground-surface cells are “frozen” and prescribed in terms of specified head, to obtain a high-convergent flow solution for the rock.

The top boundary is defined as the uppermost layer of *active cells* in the grid, i.e. immediately below either permanently deleted or temporarily inactivated cells. As described above, the purpose of the initial recharge phase is to provide a realistic top-boundary condition for the subsequent steady-state simulation (i.e. head in surface-layer cells). As such, the recharge phase has two primary targets:

- To *solve a realistic* groundwater table. Specifically, ground-surface head is solved from three components: 1) net precipitation, 2) local topography, and 3) the local conductivity of the overburden regolith (for example, the algorithm proved useful for resolving the unsaturated state of the conductive SFR pier, see Figure 2-5c).
- To *constrain an unrealistic* groundwater table. Specifically, DarcyTools does not handle surface runoff, and therefore the simulated ground-surface head may artificially exceed the local topography. To eliminate such model artefacts, the boundary-condition type for cells with excess head is permanently switched from flux to prescribed head. Hence, the approach is referred to as "mixed boundary condition". The local topographical threshold is defined by a so-called basin-filled DEM (see Öhman et al. 2014, Figure 2-5a).

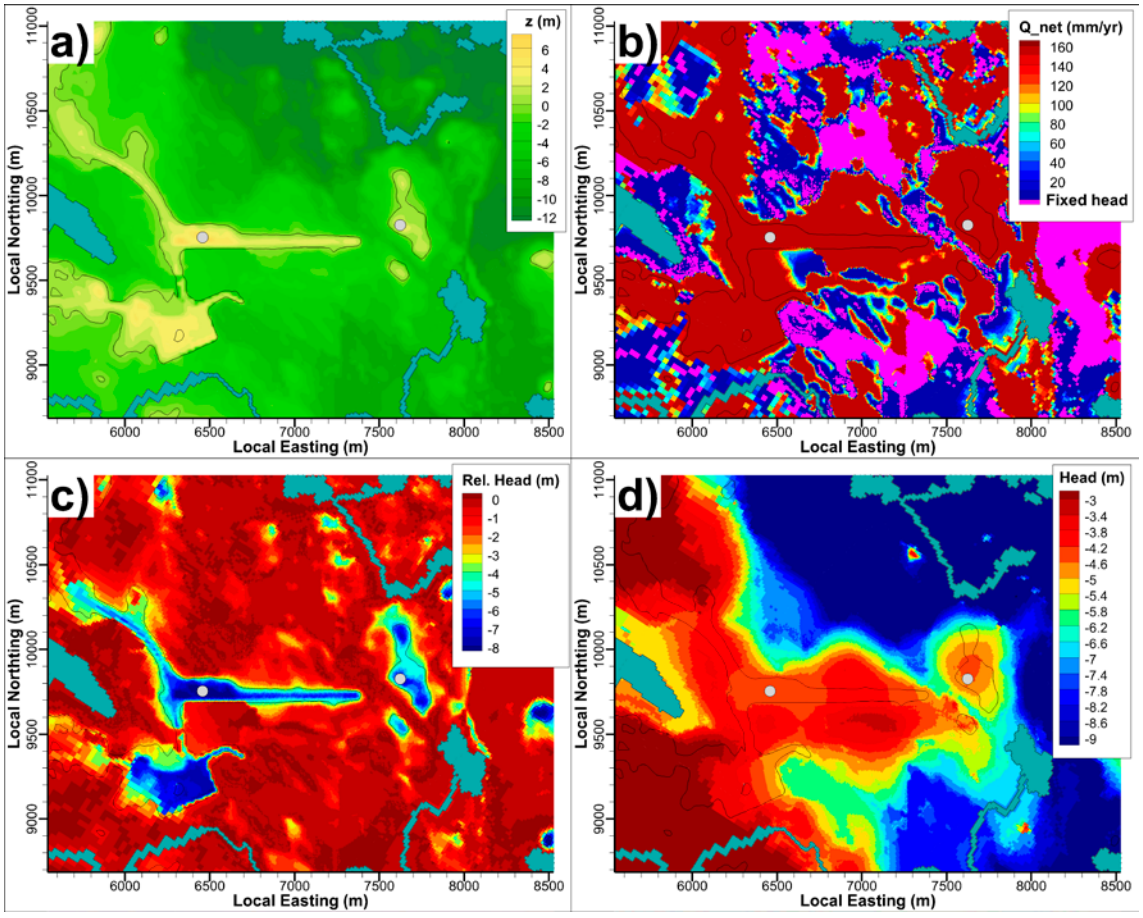


***Figure 2-5.*** *Principles of the mixed top-boundary condition; a) basin-filled topography (contoured) and surface-water objects (blue shade), b) simulated local net precipitation, c) relative head, H – z, in the uppermost layer of active cells, which can be related to the depth to the groundwater table, and d) ground-surface head.*

The determination of ground-surface head is primarily based on the following four key components:

1) Fixed head in predefined surface-water areas, i.e. streams, lakes, and the relative sea level at 5000 AD (Figure 2-5a).
2) Net precipitation, $q_{net}$ = P-PET (mm/yr), treated as a local variable in model areas where the ground-surface head must comply with the local topographical threshold. Allowed to vary from 160 to 0 mm/yr (Figure 2-5b).
3) Maximum-head in surface-layer cells, determined by the local topography (Figure 2-5b).
4) Hydraulic conductivity of the overburden regolith (spatially variable layering; see Brydsten and Strömgren 2013, Werner et al. 2013).

Lakes exceeding a certain size have been deterministically modelled based on topographical basins (Brydsten and Strömgren 2013). Below this resolution of deterministic modelling, the topographical data contain numerous local depressions, which in reality are expected to form minor lakes, wetlands, pools, and eventually become peat-filled. Irrespectively of which, special care must be taken for local topographical basins, such that the groundwater table is allowed to rise above the local basin floor, but *not* to rise above the threshold of the basin. This is achieved by employing a so-called "basin-filled" variant of topography data to define the local criterion for maximum head in the uppermost layer of active cells. In a basin-filled DEM, all local basins above sea level have been filled up till their geometrical thresholds (the filling is a standard operation), such that at any given point the DEM slopes towards the coast. The purpose of this approach is to avoid the risk of local basins in DEM data acting as unrealistic sink terms.

#### *Note on accuracy*

Based on visual inspection of results (Figure 2-5), the method is judged to provide a substantial improvement to determining realistic groundwater-table elevations for the SR-PSU purposes, in comparison to earlier modelling employing the basic top-boundary condition alternatives *prescribed head* or *free-groundwater table*.

Nonetheless, it is recognized that the newly introduced concept of mixed boundary conditions has not yet reached its fully mature potential. The computational cells are of variable size and located in a rotated coordinate system, which results in an imperfect matching to topographical data, and in turn an uncertainty to the accuracy in simulated groundwater table (or, more precisely ground-surface head). Depending on convergence criteria, another potential source of error is numerical instability during the recharge-phase convergence, which may cause unnecessary switching over to prescribed head (this switch to prescribed head is permanent during the course of simulation).

# 3 Modelling procedure

This chapter presents an overview of the modelling approach and its underlying motives, simplifications, and assumptions. A complementary detailed description of the data-file management, including specifications to source codes used and filenames is given in Appendix A.

## 3.1 Model representation of wells

### 3.1.1 Local grid refinement option

As mentioned above, DarcyTools features the possibility of unstructured computational grids, which more or less allows an unlimited local grid refinement in areas of interest (Svensson et al. 2010). The possibility of local refinement allows resolving particular phenomena in detail, that is, phenomena which are associated to areas of high property contrasts or where gradients are steep. This study focusses on water-supply wells, and therefore it would seem rational to apply a fine discretisation in the near-field around wells to improve the realism in simulation results.

For example, a high level of grid refinement is required around pumped wells to resolve the combined effects of 1) non-linear drawdown, 2) fractured-bedrock heterogeneity, and 3) particle-pathway channelling. An example of down-to-borehole-diameter refinement and a following discussion on the concept of "hydraulic choking" is provided in Appendix G, Öhman and Follin (2010). In other words, addressing certain aspects of well performance, involving dilution and radionuclide concentrations, requires a detailed modelling approach and a rigorous analysis.

Although it is tempting to make the most usage of the modelling-tool feasibilities, a project decision was taken *not* to apply the option of local grid refinement around wells, for the following reasons:

**Model uncertainty:** in the context of other model simplifications that have been formed out of necessity in the model setup (Öhman et al. 2014), it is not meaningful to model a specific phenomenon in excessive detail. An unbalanced level of details in the overall modelling approach may result in a misleading impression of the confidence level in the overall model results.

**Model complexity**: for several technical reasons, the additional effort required for grid refinement of wells is out of proportion compared to its benefits. Well-specific refinement imply handling of multiple grids (one grid per well studied). ECPM translation is grid specific (Section 2.1), which in turn implies matching grids to parallel sets of ECPM properties. The underlying DFN realisation (R85; Öhman et al. 2014) has a fracture-size cut off associated to the grid discretisation, which holds that the subset of small fractures must be complemented in areas of local grid refinement. Analysing the local fracture network around a water-supply well would require multiple DFN realisations, and so forth.

**Modelling scope and time frame**: the priorities of TD12 are to meet the objectives (Section 1.3) within the given time frame of the SR-PSU project. TD12 concerns larger-scale groundwater flow patterns and is not focused on the drawdown in or in the immediate vicinity of wells. The drawbacks of additional complexity outweigh its benefits, and therefore a more pragmatic, simplistic approach is taken (presented in further detail, below).

### 3.1.2 Numerical representation of wells

To delimit model complexity and the computational demand of simulations (Section 3.1.1), the wells are given a simplistic model representation. A "well trajectory" concept is used along with trajectory length, $L$ (m), which is a *relative* reference to the local bedrock surface. In several aspects, this trajectory length, $L$, is a useful spatial reference, as the bedrock-surface elevation varies over the model area (see TD11, Öhman et al. 2014), which complicates the use of absolute elevation.

In the computational grid, the wells are represented by the grid cells that are intersected by the well trajectory (Figure 3-1). The well trajectory is assumed to be vertical and defined as extending from its starting point, at the bedrock surface, to its lower point, 60 m deep into the bedrock (i.e. from trajectory length $L$ = 0 m to $L$ = 60 m; Figure 3-1a).

Moreover, a minimum bedrock casing is applied in order to reduce the risk of short-circuiting flow from the overlying regolith, which means that only computational cells at a certain depth below the bedrock surface are included as part of the borehole. Put more simply, the numerical representation of wells does not begin at $L$ = 0 m, but instead at $L \geq L_{casing}$ (Figure 3-1a). Based on judgment of preliminary results and consideration to common practises today (Werner et al. 2013), a minimum bedrock casing $L_{casing}$ = 4 m is assumed (see discussion in Section 3.2.2).

In the computational grid, the stack of computational cells intersected by well trajectories is tagged by means of so-called "DarcyTools markers". Owing to the unstructured DarcyTools grid (Svensson et al. 2010), this marking of cells is the key to providing direct access to cells in subsequent modelling steps. Once a cell group has been marked, they can readily be accessed by means of search algorithms, which employ inbuilt grid-search functionalities provided in the different DarcyTools modules (Svensson and Ferry 2010). For example, the local bedrock surface in the computational grid, can for a given location in the horizontal plane [x', y'] be determined as "the cell wall above the uppermost bedrock cell" (i.e. its underlying cell is marked as bedrock, but its overlying cell may be *inactivated*, *removed*, or *marked as HSD*). The elevation of this cell wall is referred to as $z_0$ (m; Table 3-1) and defines the trajectory starting point of the well, $L$ = 0 m. Any underlying cell containing the same coordinate [x', y'] is marked as a "well cell" provided its depth, $L = z0 - z_{upper\_cell\_wall}$ (m), is contained within the interval [$L_{casing}$ …60 m].

Particular subsequent modelling steps for the "well cells" (Figure 3-1a – c) include bedrock-property sampling, local parameterisation modification, boundary-condition prescription, particle tracking, and flow calculations. These modelling steps are described in sections 3.2 to 3.4, below.

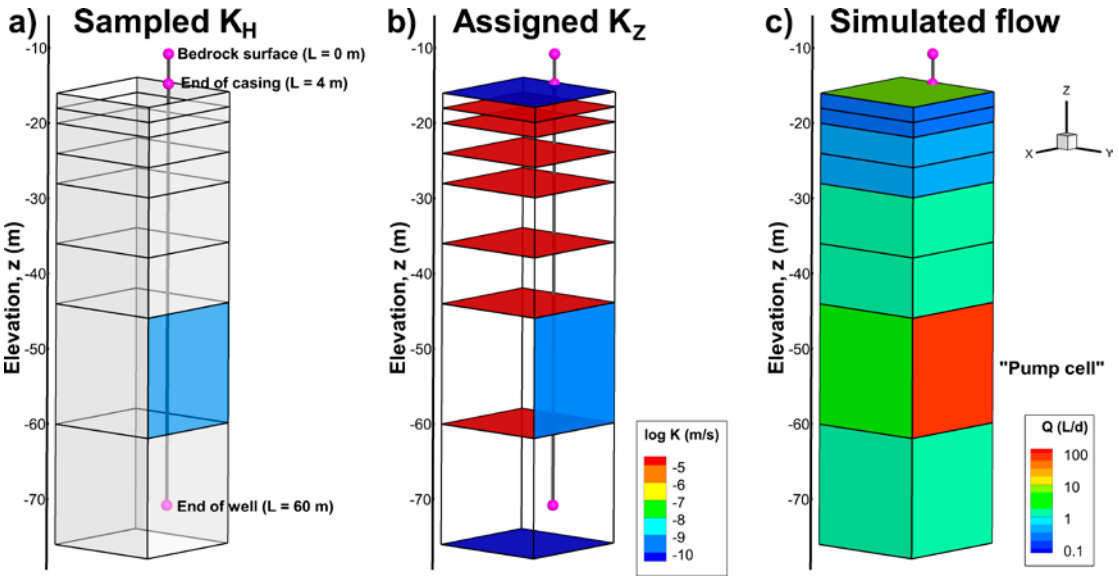


***Figure 3-1.*** *Cell walls of computational cells intersected by well trajectory (black line with pink dots); a) sampled horizontal ECPM conductivity, b) parameterised vertical cell-wall conductivity, representing the borehole, and c) simulated cell-wall flow towards the borehole.*

## 3.2 Localisation of wells in Subtask A

### 3.2.1 Geometrical sampling of bedrock properties

As discussed in Section 1.4, most wells in Subtask A are associated to settlements at potential arable land (wells 1–11), whereas one well (well 12) is located in the well-interaction area (Figure 1-2; Table 1-1). The first step in Subtask A is to determine suitable locations of these wells within given geographical boundaries, based on a water-supply requirement of 700 L/d. It should again be noted that DarcyTools honours observed bedrock heterogeneity by means of a heterogeneous parameterisation approach, as defined from an underlying stochastic DFN model. Consequently, the location of wells is therefore *not of general validity*, but applies only to the bedrock parameterisation studied (the TD11 Base case). In other words, the located wells may not necessarily fulfil the requirement of 700 L/d in an arbitrary model setup, as the well capacity at a specific location may be fully determined by the stochastic DFN realisation.

Flow simulations are complex in setup and computationally demanding to solve, and therefore do not provide a very effective approach for determining locations with sufficiently conductive bedrock to sustain the water-supply requirement. Instead, an efficient geometrical sampling method is developed, with the purpose to map out local model parameterisation that is considered relevant for finding proper well locations. The key assumption in this approach is that, for any given position, the local well capacity, $Q_{well}/s$ ($m^2/s$), can be directly evaluated from grid-cell properties (i.e. without the need for flow simulations), which for an assumed drawdown, $s$ (m), can be related to the water-supply criterion 700 L/d.

The wells are 60 m deep below bedrock surface, and therefore the theoretical maximum drawdown is c 60 m (drawdown inside the well). In practise, the drawdown in a sustainable, functioning well must be less than that. Furthermore, as the actual well geometry is not resolved in geometrical detail (Section 3.1.2), the typical non-linear drawdown pattern around a pumped well is not resolved below cell scale (typical side lengths are 8 to 16 m). This implies that the maximum drawdown, referring to the level *within* the actual well, must be associated to a realistic drawdown criterion for "well cells" (Figure 3-1). As a rule-of-thumb criterion for the "well cells", it was decided to assume a criterion of "bedrock drawdown" of $s \leq 10$ m.

The local well capacity, Q/s ($m^2/s$), is estimated from the parameterised bedrock ECPM properties of grid cells that are intersected by the borehole trajectory (Figure 3-1b). For $n$ intersected DarcyTools grid cells, the maximum well capacity is estimated as

$$\frac{Q_{\max}}{s} \approx \sum_n bK_{H,\max} \tag{3-1}$$

where b is the vertical extent of a "well cell" and $K_{Hmax}$ is its maximum horizontal cell-wall conductivity (each cell has at least 4 cell walls with horizontal conductivity). The wells are assumed to be cased in regolith and therefore only bedrock cells are included in Equation (3-1). The final calculations (Section 3.2.4) take into account a well casing that extends a few meters into the bedrock (see discussion in Section 3.2.2), which is found to be important for the estimation of well capacity. The conductivity analysis of "well cells" in the DarcyTools grid is executed by means of a Fortran code, compiled as the DarcyTools module PropGen (Table A-2 in Appendix A).

As a demonstration of principles, the well capacity is estimated at the assigned initial locations of wells 1–12 in Subtask A (Table 3-1). It should be noted that the regolith is assumed to be cased off in this example, but *no bedrock casing* is assumed at this stage. Firstly, the 12 initial locations are translated and rotated into the local DarcyTools model coordinate system ([x', y']; Table 3-1). Based on these coordinates, well cells are marked according to Section 3.1.2, after which Equation (3-1) can be applied to all marked well cells. Five of the 12 locations are inside the SFR Regional domain. For consideration to scaling issues arising from ECPM properties of varying cell size, the maximum cell side length is also recorded (cells are large compared to the typical diameter of a well; Table 3-1). At first sight, the estimated maximum well capacities appear rather similar, ranging from c $10^{-7}$ to $10^{-4}$ $m^2/s$ (Table 3-1), although well 10 stands out with $Q/s = 2.45 \cdot 10^{-7}$ $m^2/s$, which for a 10 m drawdown corresponds to a mere production of c 220 L/d.

**Table 3-1. Estimated well capacity, Q/s at the initial well locations of Subtask A (no bedrock casing).**

| Well | x' (m) | y' (m) | $z_0$ (m) | Side length, $L_{max}$ (m) | Well capacity, Q/s ($m^2$/s) | SFR Regional domain |
|---|---|---|---|---|---|---|
| 1 | 5704.89 | 12246.2 | –12 | 16 | 7.55E–06 | Outside |
| 2 | 5552.88 | 10890.97 | –17 | 16 | 2.41E–04 | Outside |
| 3 | 6223.52 | 10928 | –8 | 16 | 8.08E–05 | Outside |
| 4 | 7170.26 | 11344.48 | –15 | 16 | 2.78E–05 | Outside |
| 5 | 6693.25 | 10571.93 | –13.5 | 8 | 7.97E–06 | Inside |
| 6 | 7399.13 | 10624.38 | –13 | 8 | 7.50E–06 | Border |
| 7 | 7480.42 | 9990.34 | –9.5 | 8 | 1.76E–05 | Inside |
| 8 | 7371.7 | 9486.45 | –13 | 8 | 1.28E–05 | Inside |
| 9 | 8174.24 | 9718.18 | –14 | 16 | 7.42E–05 | Outside |
| 10 | 8986.85 | 9189.63 | –16 | 16 | 2.45E–07 | Outside |
| 11 | 6382.07 | 10618.7 | –13 | 8 | 3.27E–05 | Inside |
| 12 | 6309.1 | 10445.06 | –13 | 8 | 1.62E–05 | Inside |

In an analysis at the more detailed cell-to-cell level, the component of bedrock heterogeneity is evident in sampled well capacity (Figure 3-2 and Table 3-2). A few wells have low conductivity, but may be dominated by the conductivity of a single cell (e.g. wells 1, 4, 6, and 10, see Figure 3-2). Most notably, the dominating conductivity may belong to one of the uppermost cells (wells 1 and 6, Table 3-2). Although all sampled cells are strictly classified as bedrock in the model, some of the uppermost sampled values originate from parameterisation of till (reported as log $K_{max}$ = –5.1 in Table 3-2). This is not a parameterisation error, but a consequence of the staggered grid arrangement in DarcyTools, where a cell-wall property is not associated to a single cell, but represents the control volume *between* two cell centres. In other words, if any of the four adjacent cells should represent regolith, the sampled horizontal conductivity between the two cells will reflect the till parameterisation. As expected, this model artefact only occurs for the uppermost cell layer.

Even though this finding is a model artefact, it highlights the risk of short-circuiting flow from the overburden, which is not only a problem from a modelling perspective, but also in reality. This notion highlights the necessity to introduce bedrock casing in the sampling algorithm (see Section 3.2.2).

### 3.2.2 Bedrock casing

The results presented in Section 3.2.1 reflect bedrock properties at the initial locations of wells in Subtask A, i.e. computational cells intersected by the vertical trajectory at well locations. It should be emphasised that any well section above bedrock surface is assumed to be cased off, and therefore the cell properties of overlying regolith (i.e. cells outlined in pink lines in Figure 3-2) are not included in the analysis. At the bare minimum, the preliminary test in Section 3.2.1 has demonstrated that the uppermost bedrock cell must be "cased off" owing to the risk of introducing an artificial connection to the overlying regolith.

In reality, bedrock casing extending a few meters below the bedrock surface is important for preventing surface-water contamination (it reduces the risk of local short-circuited flow paths from overlying regolith). It is difficult to speculate on the casing standards of future wells; however, guidance can be taken from current branch standards. The current Swedish standard (Normbrunn -07) is a minimum of 2 m casing into intact rock (see Werner et al. 2013). The following information is provided in (Axelsson et al. 1991):

> Casing is carried out through the soil and some meters into the rock. According to branch standards, casing tends to be run at least three to five meters into "good rock" (non-fractured rock). This is done in order to securely seal off the surface-near groundwater.

In TD12, it was decided to apply a minimum bedrock casing of 4 m. The exact casing length for a given well is conformed to the local grid discretization. Specifically, the end of casing is taken as "the first intersected cell wall, after a minimum of 4 m trajectory length in bedrock". In other words, the end of casing coincides with a cell wall that is at least 4 m below the bedrock surface. To seal off inflow from above, this cell wall is assigned a low vertical conductivity, $K_z = 3 \cdot 10^{-11}$ m/s, and also at the bottom of the well (Figure 3-1b).

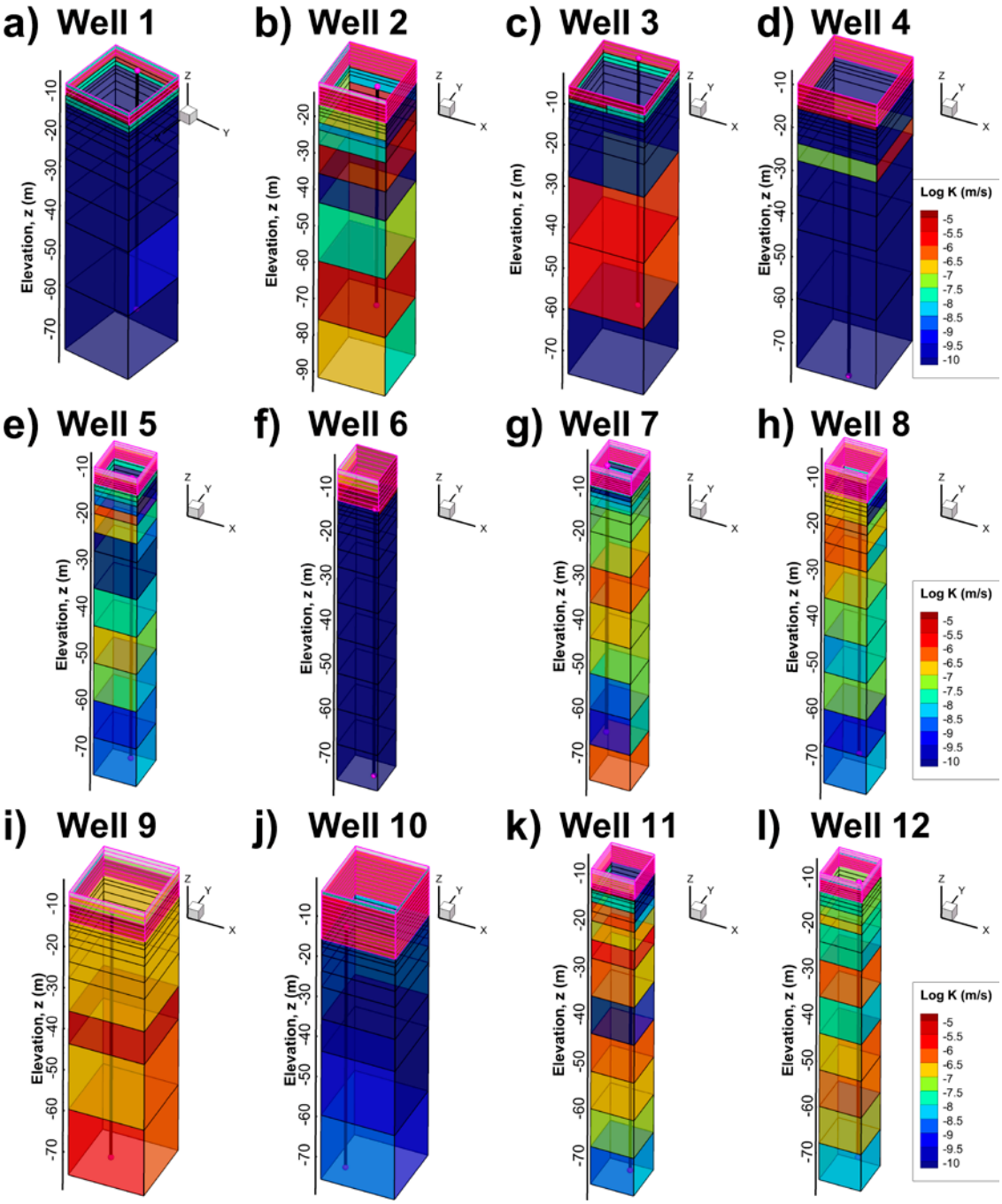


***Figure 3-2.*** *Horizontal cell-wall conductivity of intersected cells (initial locations of wells 1–12, indicated by black lines). The well capacity is estimated from intersected bedrock cells (black-edged cells), whereas the overlying regolith (pink-edged cells) is assumed to be cased off from wells, and hence not included in Equation (3-1).*

**Table 3-2. Horizontal cell-wall conductivity in well-capacity estimation at the initial well locations of Subtask A (no bedrock casing).**

| Well | Well cells1) | 1 | 2 | 3 | 4 | 5 | 6 | 7 | 8 | 9 | 10 | 11 | 12 | 13 |
|---|---|---|---|---|---|---|---|---|---|---|---|---|---|---|
| 1 | Secup (m) | 0 | 1 | 2 | 3 | 4 | 6 | 8 | 12 | 16 | 24 | 32 | 48 | |
| | Seclow (m) | 1 | 2 | 3 | 4 | 6 | 8 | 12 | 16 | 24 | 32 | 48 | 64 | |
| | Side L (m) | 16 | 16 | 16 | 16 | 16 | 16 | 16 | 16 | 16 | 16 | 16 | 16 | |
| | Log $K_{max}$ | –5.1 | –7.5 | –11 | –11 | –11 | –11 | –11 | –11 | –11 | –11 | –9 | –11 | |
| 2 | Secup (m) | 0 | 1 | 2 | 3 | 5 | 7 | 11 | 19 | 27 | 43 | 59 | | |
| | Seclow (m) | 1 | 2 | 3 | 5 | 7 | 11 | 19 | 27 | 43 | 59 | 75 | | |
| | Side L (m) | 16 | 16 | 16 | 16 | 16 | 16 | 16 | 16 | 16 | 16 | 16 | | |
| | Log $K_{max}$ | –5.1 | –7.3 | –7.3 | –7.3 | –5.2 | –4.9 | –5 | –11 | –6.8 | –5.3 | –6.7 | | |
| 3 | Secup (m) | 0 | 1 | 2 | 3 | 4 | 6 | 8 | 12 | 20 | 36 | 52 | | |
| | Seclow (m) | 1 | 2 | 3 | 4 | 6 | 8 | 12 | 20 | 36 | 52 | 68 | | |
| | Side L (m) | 8 | 8 | 16 | 16 | 16 | 16 | 16 | 16 | 16 | 16 | 16 | | |
| | Log $K_{max}$ | –5.1 | –7.5 | –7.5 | –11 | –11 | –11 | –11 | –11 | –5.8 | –5.5 | –11 | | |
| 4 | Secup (m) | 0 | 1 | 2 | 3 | 7 | 9 | 13 | 21 | 29 | 45 | | | |
| | Seclow (m) | 1 | 2 | 3 | 5 | 9 | 13 | 21 | 29 | 45 | 61 | | | |
| | Side L (m) | 16 | 16 | 16 | 16 | 16 | 16 | 16 | 16 | 16 | 16 | | | |
| | Log $K_{max}$ | –5.1 | –11 | –11 | –11 | –11 | –5.3 | –11 | –11 | –11 | –11 | | | |
| 5 | Secup (m) | 0 | 0.5 | 1.5 | 2.5 | 4.5 | 6.5 | 10.5 | 14.5 | 22.5 | 30.5 | 38.5 | 46.5 | 54.5 |
| | Seclow (m) | 0.5 | 1.5 | 2.5 | 4.5 | 6.5 | 10.5 | 14.5 | 22.5 | 30.5 | 38.5 | 46.5 | 54.5 | 62.5 |
| | Side L (m) | 8 | 8 | 8 | 8 | 8 | 8 | 8 | 8 | 8 | 8 | 8 | 8 | 8 |
| | Log $K_{max}$ | –7.5 | –7.5 | –7.9 | –8.5 | –6.3 | –6 | –8.3 | –7.5 | –7.1 | –6.8 | –7.1 | –8.3 | –8.4 |
| 6 | Secup (m) | 0 | 1 | 2 | 3 | 5 | 7 | 11 | 15 | 23 | 31 | 39 | 47 | 55 |
| | Seclow (m) | 1 | 2 | 3 | 5 | 7 | 11 | 15 | 23 | 31 | 39 | 47 | 55 | 63 |
| | Side L (m) | 8 | 8 | 8 | 8 | 8 | 8 | 8 | 8 | 8 | 8 | 8 | 8 | 8 |
| | Log $K_{max}$ | –5.1 | –11 | –11 | –11 | –11 | –11 | –11 | –11 | –11 | –11 | –11 | –11 | –11 |
| 7 | Secup (m) | 0 | 0.5 | 1.5 | 2.5 | 4.5 | 6.5 | 10.5 | 18.5 | 26.5 | 34.5 | 42.5 | 50.5 | 58.5 |
| | Seclow (m) | 0.5 | 1.5 | 2.5 | 4.5 | 6.5 | 10.5 | 18.5 | 26.5 | 34.5 | 42.5 | 50.5 | 58.5 | 66.5 |
| | Side L (m) | 8 | 8 | 8 | 8 | 8 | 8 | 8 | 8 | 8 | 8 | 8 | 8 | 8 |
| | Log $K_{max}$ | –7.5 | –7.4 | –7.1 | –7.5 | –7 | –7 | –6.9 | –6.1 | –6.6 | –6.8 | –7.3 | –7.7 | –6.2 |
| 8 | Secup (m) | 0 | 1 | 2 | 3 | 5 | 7 | 11 | 15 | 23 | 31 | 39 | 47 | 55 |
| | Seclow (m) | 1 | 2 | 3 | 5 | 7 | 11 | 15 | 23 | 31 | 39 | 47 | 55 | 63 |
| | Side L (m) | 8 | 8 | 8 | 8 | 8 | 8 | 8 | 8 | 8 | 8 | 8 | 8 | 8 |
| | Log $K_{max}$ | –6.8 | –6.7 | –6.7 | –6.7 | –6.5 | –6.3 | –6.3 | –6.1 | –7.4 | –7.6 | –7.2 | –8.5 | –8.3 |
| 9 | Secup (m) | 0 | 1 | 2 | 4 | 6 | 10 | 14 | 22 | 30 | 46 | | | |
| | Seclow (m) | 1 | 2 | 4 | 6 | 10 | 14 | 22 | 30 | 46 | 62 | | | |
| | Side L (m) | 16 | 16 | 16 | 16 | 16 | 16 | 16 | 16 | 16 | 16 | | | |
| | Log $K_{max}$ | –6.8 | –6.8 | –6.8 | –6.8 | –6.8 | –6.7 | –6.8 | –5.3 | –6.1 | –6 | | | |
| 10 | Secup (m) | 0 | 1 | 2 | 4 | 8 | 12 | 20 | 28 | 44 | | | | |
| | Seclow (m) | 1 | 2 | 4 | 8 | 12 | 20 | 28 | 44 | 60 | | | | |
| | Side L (m) | 16 | 16 | 16 | 16 | 16 | 16 | 16 | 16 | 16 | | | | |
| | Log $K_{max}$ | –8.3 | –8.3 | –8.1 | –8.1 | –8 | –7.9 | –10 | –9.3 | –8.6 | | | | |
| 11 | Secup (m) | 0.5 | 1 | 2 | 3 | 5 | 7 | 11 | 15 | 23 | 31 | 39 | 47 | 55 |
| | Seclow (m) | 1 | 2 | 3 | 5 | 7 | 11 | 15 | 23 | 31 | 39 | 47 | 55 | 63 |
| | Side L (m) | 8 | 8 | 8 | 8 | 8 | 8 | 8 | 8 | 8 | 8 | 8 | 8 | 8 |
| | Log $K_{max}$ | –5.1 | –7.5 | –7.5 | –6.1 | –6.5 | –6.5 | –5.6 | –6.2 | –7.2 | –6.1 | –6.5 | –6.6 | –8.2 |
| 12 | Secup (m) | 0 | 1 | 2 | 3 | 5 | 7 | 11 | 15 | 23 | 31 | 39 | 47 | 55 |
| | Seclow (m) | 1 | 2 | 3 | 5 | 7 | 11 | 15 | 23 | 31 | 39 | 47 | 55 | 63 |
| | Side L (m) | 8 | 8 | 8 | 8 | 8 | 8 | 8 | 8 | 8 | 8 | 8 | 8 | 8 |
| | Log $K_{max}$ | –7.2 | –7.2 | –7.1 | –7 | –6.6 | –7.2 | –7.5 | –6.3 | –7.3 | –6.3 | –6.2 | –6.8 | –8 |

[1)] Well cells, below bedrock casing, in ascending order, i.e. “cell 1” refers to the uppermost bedrock cell, just below the bedrock surface. This is not to be confused with the DarcyTools ID grid numbering (cf. Table 4-1).

As a demonstration, the well capacities are re-evaluated at the 12 initial well locations in Subtask A, using a minimum bedrock casing of 4 m. The actual casing length implemented depends on the local grid refinement, as well as the elevation of the bedrock surface, and ranges from 4 to 7 m (Table 3-3). As expected, casing off the uppermost cells, of which some may be subject to regolith influence (Table 3-2), has a significant impact on wells 1 and 6, which now fall below the criterion 700 L/d according to scoping calculations for a bedrock drawdown, $s$ = 10 m (Table 3-3).

This scoping calculation is also verified by means of a simplified test-flow simulation (Section 3.2.3), which reinforces the confidence in the sampling algorithm as an effective tool for providing advance notice on the suitability of well locations. The localisation of the 12 wells in Subtask A is described in Section 3.2.4, and an analysis of bedrock properties at the final locations is provided in Section 4.1.1.

### 3.2.3 Test simulation for initial well locations

The preliminary test of the sampling algorithm for wells indicates that the criterion 700 L/d cannot be met at the initially assigned locations of wells 1, 6, and 10. This notion is based on scoping calculations and the geometrical sampling analysis of the intersected ECPM grid-cell properties, as described in Sections 3.2.1 and 3.2.2. To test the confidence in relying on a geometrical sampling approach for predicting simulated well production, a simplified flow simulation is performed.

This simulation is performed only to test the reliability of the geometrical sampling process. No results of this test simulation are used elsewhere, and therefore only a brief presentation of the setup is given here. In essence, the TD11 Base case for the time slice 5000 AD is re-run, although 12 active pumping wells are implemented according to the example in Figure 3-1.

**Table 3-3. Re-evaluated well capacity for a minimum bedrock casing of 4 m.**

| Well | $Q_{well}/s$[1)] (no casing) | Casing (m) | $Q_{well}/s$[1)] (casing) | Estimated maximum production[2)], $Q_{max}$ (L/d) |
|---|---|---|---|---|
| 1 | 7.55E–06 | 4 | 1.57E–08 | 13.6 |
| 2 | 2.41E–04 | 5 | 2.33E–04 | 201,226 |
| 3 | 8.08E–05 | 4 | 7.32E–05 | 63,262 |
| 4 | 2.78E–05 | 7 | 2.03E–05 | 17,556 |
| 5 | 7.97E–06 | 4.5 | 7.90E–06 | 6,827 |
| 6 | 7.50E–06 | 5 | 1.74E–09 | 1.5 |
| 7 | 1.76E–05 | 4.5 | 1.74E–05 | 14,990 |
| 8 | 1.28E–05 | 5 | 1.18E–05 | 10,187 |
| 9 | 7.42E–05 | 4 | 7.36E–05 | 63,564 |
| 10 | 2.45E–07 | 4 | 2.17E–07 | 187.7 |
| 11 | 3.27E–05 | 5 | 2.73E–05 | 23,622 |
| 12 | 1.62E–05 | 5 | 1.58E–05 | 13,660 |

[1)] Calculated by Equation (3-1)

[2)] Estimated maximum well production for an assumed drawdown of 10 m. Values below 700 L/d indicate the need to relocate the well to meet requirements (Section 1.3).

***Setup:***

- A single simulation is performed, where all 12 wells are assumed to co-exist (note that wells are not assumed to co-exist in the final simulations).
- The original positions of the 12 wells are used (note that unrealistic drawdown are expected in wells 1, 6, and 10, as shown in Table 3-3).
- Cells intersected by well trajectories are assigned a vertical conductivity of $K_z = 10^{-4}$ m/s, while the upper and lower ends of the well are assigned a low vertical conductivity, $K_z = 3 \cdot 10^{-11}$ m/s (Figure 3-1b).
- Well production is simulated by introducing a sink term of –700 L/d (or more precisely, in applied SI units, –0.008101852 kg/s) in the borehole cell of maximum horizontal conductivity (marked "pump cell" in Figure 3-1c).
- The flow field is solved as a steady-state solution with prescribed head for ground-surface cells, i.e. top-boundary conditions and initial values are imported from the Base-case pressure solution at 5000 AD in TD11.

The following simulation results are examined in detail:

1) Drawdown among "well cells".
2) Well production (or more precisely, net flow across cell walls, as shown in Figure 3-1c).

The simulated drawdown is estimated as the simulated head relative to initial head, $H_0$ (m). For the purposes of this simple evaluation, it was considered sufficient to approximate the initial head as somewhere between ground surface elevation, $z_{HSD}$, and bedrock surface, $z_{rock}$. The "exact value" of the reference head, $H_0$, is not readily available due to the re-parameterisation of vertical conductivities (Figure 3-1b). However, for the purpose of identifying anomalous drawdown relative to bedrock surface, the approximation is considered adequate enough.

In most wells, the simulation results indicate that the well production has a realistic impact on groundwater levels, as the simulated head is typically contained within the bounds of the ground-surface/bedrock-surface elevations (less strictly speaking, the groundwater table is typically within the regolith). However, in line with expectations from Section 3.2.2, wells 1, 6, and 10 (marked yellow in Table 3-4) stand out with large simulated drawdown, yet without reaching the required 700 L/d. Although this scoping simulation is highly simplified, its results concur with the findings of geometrical sampling and support the sampling method as an efficient tool to find well locations with sufficiently conductive bedrock to sustain the required water demand.

**Table 3-4. Test-simulation results for the initial well locations of Subtask A.**

| Well | $z_{rock}$ (m) | $z_{HSD}$ (m) | Simulated head, $H_{bedrock}$ (m) | Simulated production, $Q_{sim}$ (L/d) |
|---|---|---|---|---|
| 1 | –12 | –9 | –61 | 102.6 |
| 2 | –17 | –11 | –12.63 | 699.9 |
| 3 | –8 | –6 | –11.82 | 700.0 |
| 4 | –15 | –10 | –13 | 700.0 |
| 5 | –13.5 | –10 | –11.83 | 700.0 |
| 6 | –13 | –6 | –311 | 152.1 |
| 7 | –9.5 | –5 | –6.7 | 700.0 |
| 8 | –13 | –7 | –8.74 | 715.4 |
| 9 | –14 | –7 | –9.26 | 700.0 |
| 10 | –16 | –4 | –38.32 | 690.9 |
| 11 | –13 | –9 | –11.14 | 700.0 |
| 12 | –13 | –9 | –10.81 | 700.0 |

### 3.2.4 Localisation of wells

Having tested out the sampling method for well-capacity estimation (Sections 3.2.1 to 3.2.3), the algorithm is applied for finding suitable final locations of the 12 wells in Subtask A (Section 1.4.2). The algorithm is expanded to examine well capacities within potential settlement areas for wells 1–11, and within 100 m for well 12, i.e. to find locations having sufficiently conductive bedrock to sustain the required water supply of 700 L/d.

The centres of potential settlement areas and the centre of the area to be investigated for well 12 are taken as the starting points for the analyses of surrounding bedrock (pink dots in Figure 3-3 to Figure 3-14). The well-trajectory sampling method is applied for all grid cells within a "search square" that encloses the areas of interest. The side length of the square is almost 100 m and it is aligned with the DarcyTools computational mesh. It should be noted that in order to include part of the Singö deformation zone, the search square for well 8 is translated 76 m to the northeast (Figure 3-10).

In the first step, the starting point of the well trajectory ($L$ = 0 m; Figure 3-1) is defined by the local bedrock-surface elevation, $z_0$ (m) in each cell (sub-figure b in Figure 3-3 to Figure 3-14). In the second step, the bedrock casing is adapted to the local discretisation of cells, with a minimum length of 4 m. Thus, the actual bedrock casing in cells ranges from 4 to 7 m (sub-figure c in Figure 3-3 to Figure 3-14). Finally, the well-trajectory sampling method, Equation (3-1), is executed to estimate well capacity of all cells. Given the well-capacity, $Q/s$ ($m^2/s$), the "required drawdown", $s$ (m), to produce 700 L/d is calculated (sub-figure d in Figure 3-3 to Figure 3-14).

The well localisation is primarily based on the mapped "drawdown requirements". As demonstrated earlier, the settlements for wells 1, 6, and 10 (Table 3-4), all have unsuitable locations with unrealistic drawdown for producing the water-supply demand (settlement-area centre indicated by a pink dot in Figure 3-3d, Figure 3-8d, and Figure 3-12d). In general, high drawdown requirements ($s$ > 10 m; yellow to red in Figure 3-3d to Figure 3-14d) indicate unsuitable locations, whereas low values ($s$ < 1 m; blue colours in Figure 3-3d to Figure 3-14d) demonstrate favourable locations for wells. Furthermore, nearby deformation zones, if present within the 100 m radius, are also considered as preferential in the judgment of suitable well locations. No well is located more than 100 m away from its settlement-area centre, or for well 12, from its assigned centre location. The location of well 2 coincides with the settlement-area centre (hence, it is not relocated). The selected, final locations of wells for Subtask A are presented in Table 3-5.

**Table 3-5. Final locations of wells 1–12 in Subtask A.**

| Well | Settlement location (RT90) | | Well location (RT90) | |
|---|---|---|---|---|
| | Easting (m) | Northing (m) | Easting (m) | Northing (m) |
| 1 | 1633455 | 6704141 | 1633480 | 6704167 |
| 2 | 1632597 | 6703081 | 1632597 | 6703081 |
| 3 | 1633182 | 6702751 | 1633215 | 6702740 |
| 4 | 1634204 | 6702592 | 1634260 | 6702567 |
| 5 | 1633386 | 6702198 | 1633357 | 6702170 |
| 6 | 1634009 | 6701862 | 1633964 | 6701886 |
| 7 | 1633736 | 6701284 | 1633706 | 6701291 |
| 8 | 1633373 | 6700918 | 1633410 | 6700994 |
| 9 | 1634174 | 6700681 | 1634204 | 6700665 |
| 10 | 1634574 | 6699798 | 1634539 | 6699824 |
| 11 | 1633149 | 6702405 | 1633141 | 6702412 |
| 12[1)] | 1632994 | 6702298 | 1632971 | 6702264 |

[1)] Well 12 is located in the well-interaction area (Figure 1-3, and not associated to any potential agricultural settlement (Table 1-1)

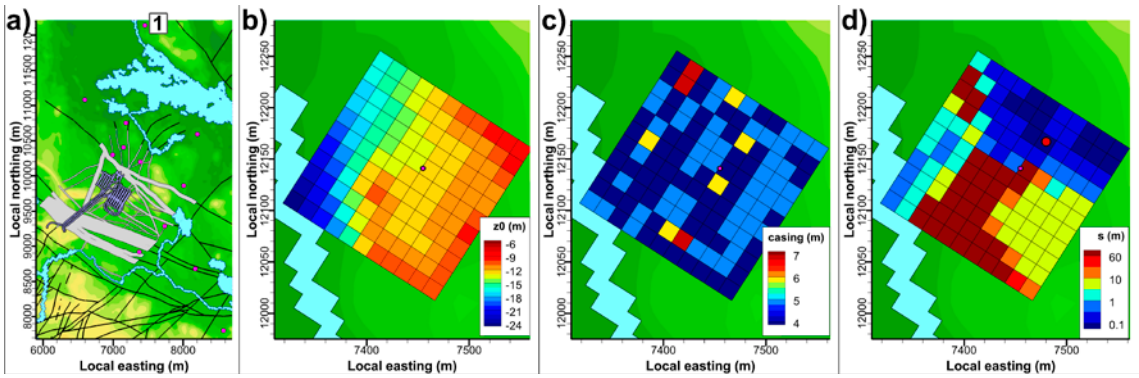


***Figure 3-3.*** *Localisation of well 1; a) initial location, b) bedrock elevation, $z_0$ (m), c) casing length, $L_{casing}$ (m), and d) required drawdown in "well cells" for a production of 700 L/d. The large red dot marks the selected, final well location.*

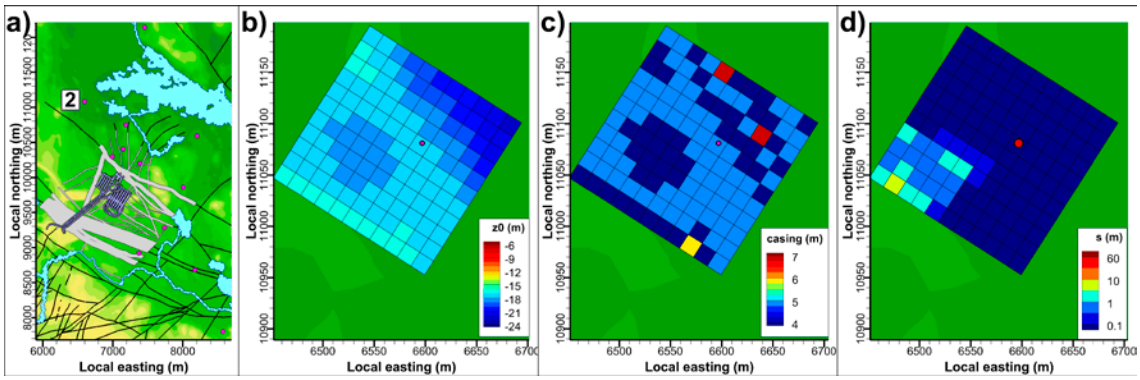


***Figure 3-4.*** *Localisation of well 2; a) initial location, b) bedrock elevation, $z_0$ (m), c) casing length, $L_{casing}$ (m), and d) required drawdown in "well cells" for a production of 700 L/d. The large red dot marks the selected, final well location.*

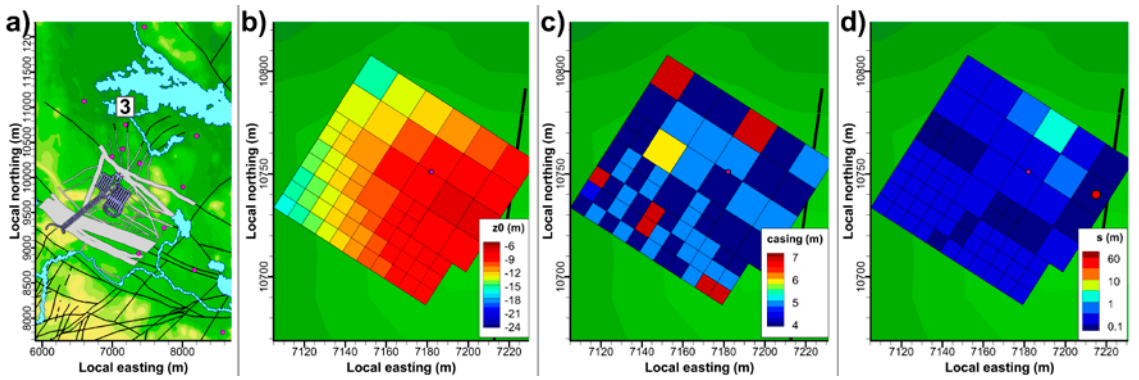


***Figure 3-5.*** *Localisation of well 3; a) initial position, b) bedrock elevation, $z_0$ (m), c) casing length, $L_{casing}$ (m), and d) required drawdown in "well cells" for a 700 L/d production. Large red dot marks selected well position.*

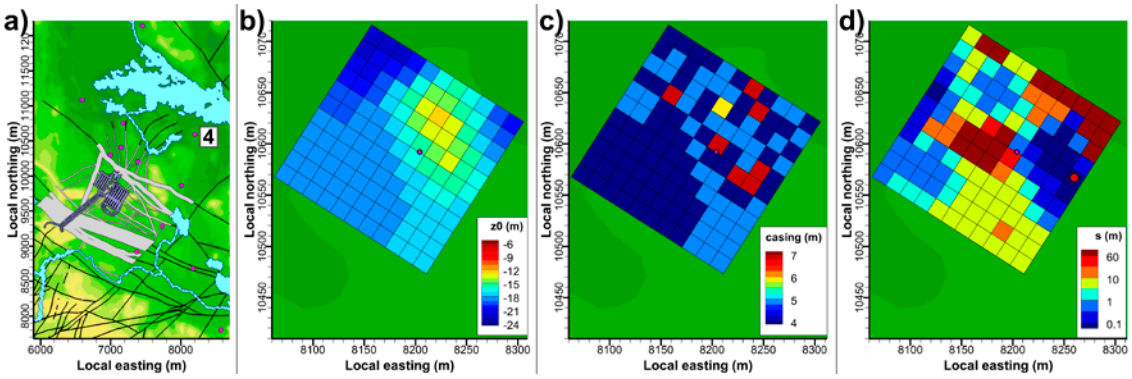


***Figure 3-6.*** *Localisation of well 4; a) initial location, b) bedrock elevation, $z_0$ (m), c) casing length, $L_{casing}$ (m), and d) required drawdown in "well cells" for a production of 700 L/d. The large red dot marks the selected, final well location.*

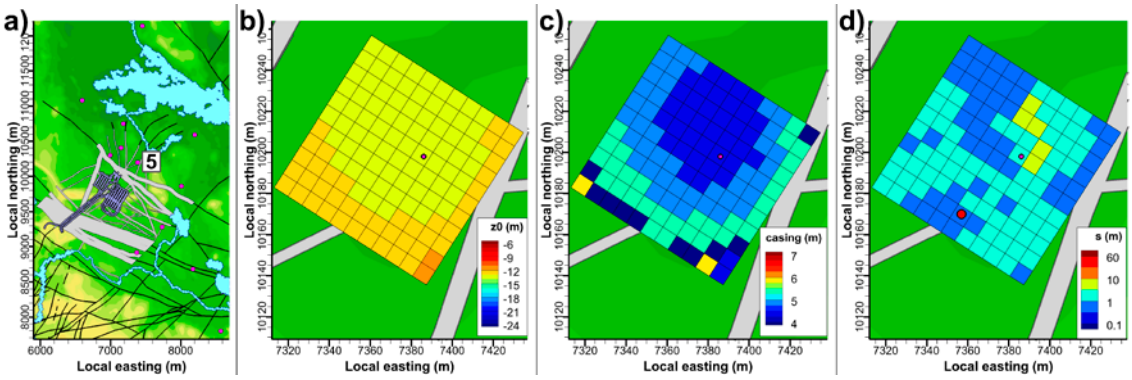


***Figure 3-7.*** *Localisation of well 5; a) initial location, b) bedrock elevation, $z_0$ (m), c) casing length, $L_{casing}$ (m), and d) required drawdown in "well cells" for a production of 700 L/d. The large red dot marks the selected, final well location.*

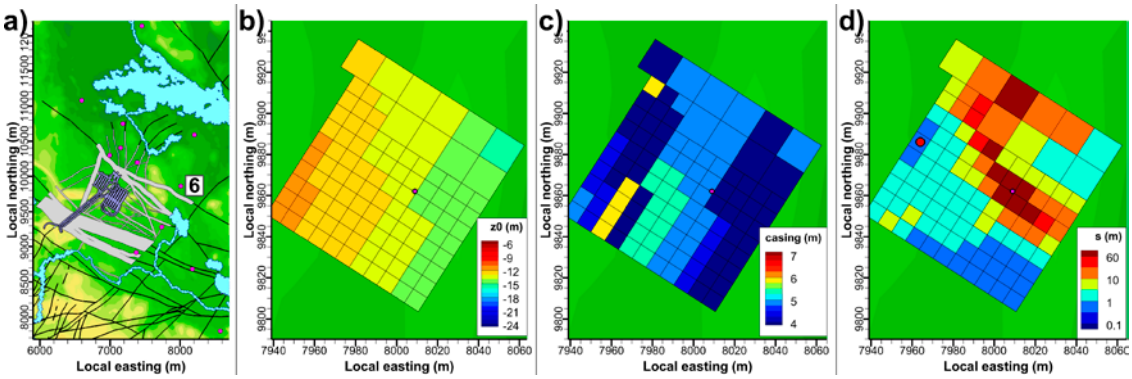


***Figure 3-8.*** *Localisation of well 6; a) initial location, b) bedrock elevation, $z_0$ (m), c) casing length, $L_{casing}$ (m), and d) required drawdown in "well cells" for a production of 700 L/d. The large red dot marks the selected, final well location.*

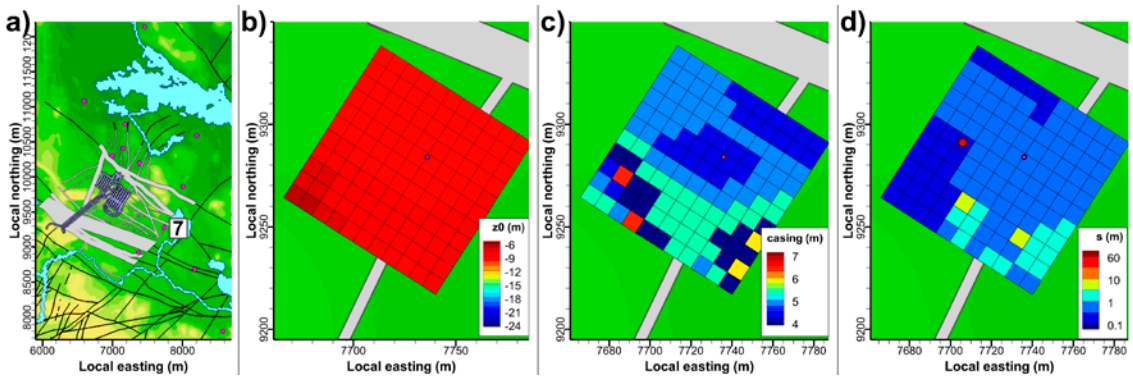


***Figure 3-9.*** *Localisation of well 7; a) initial location, b) bedrock elevation, $z_0$ (m), c) casing length, $L_{casing}$ (m), and d) required drawdown in "well cells" for a production of 700 L/d. The large red dot marks the selected, final well location.*

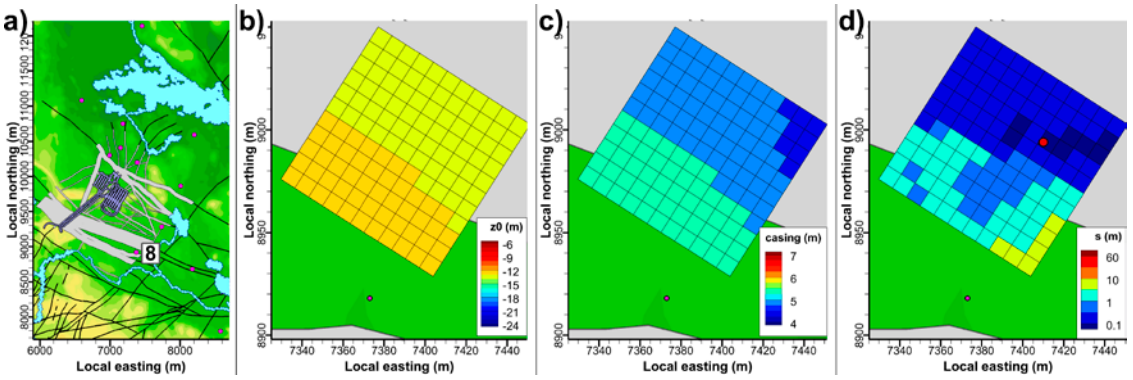


***Figure 3-10.*** *Localisation of well 8; a) initial location, b) bedrock elevation, $z_0$ (m), c) casing length, $L_{casing}$ (m), and d) required drawdown in "well cells" for a production of 700 L/d. The large red dot marks the selected, final well location. Search area centred 76 m north-east of the original settlement position (small pink dot) to cover part of Singö deformation zone.*

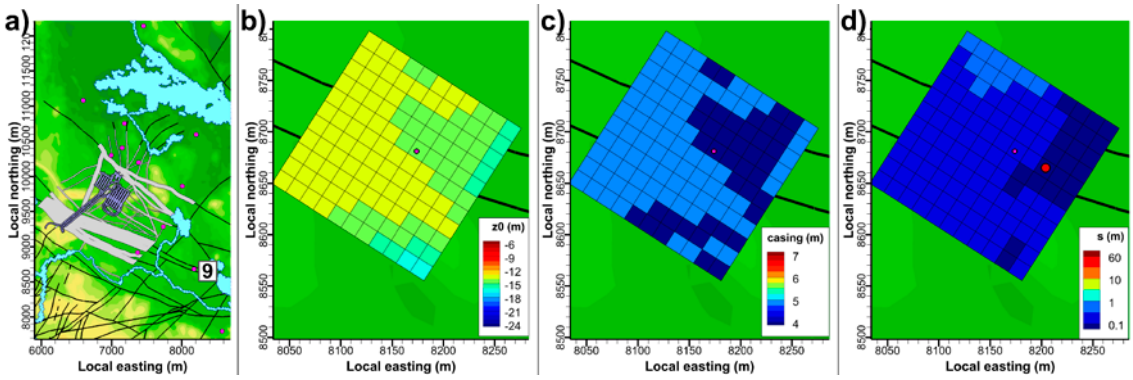


***Figure 3-11.*** *Localisation of well 9; a) initial location, b) bedrock elevation, $z_0$ (m), c) casing length, $L_{casing}$ (m), and d) required drawdown in "well cells" for a production of 700 L/d. The large red dot marks the selected, final well location.*

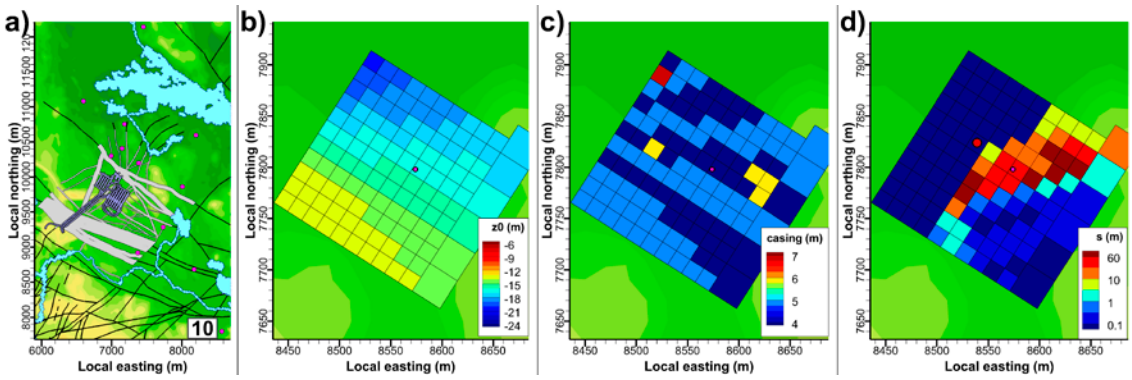


***Figure 3-12.*** *Localisation of well 10; a) initial location, b) bedrock elevation, $z_0$ (m), c) casing length, $L_{casing}$ (m), and d) required drawdown in "well cells" for a production of 700 L/d. The large red dot marks the selected, final well location.*

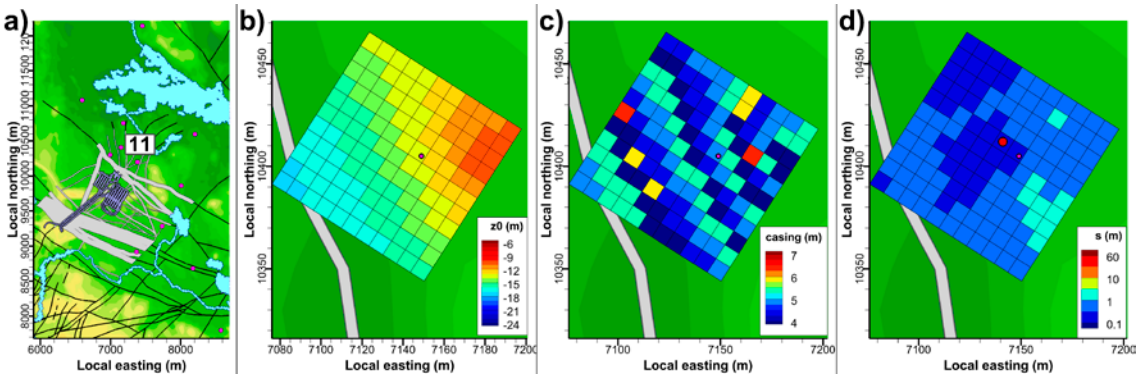


***Figure 3-13.*** *Localisation of well 11; a) initial location, b) bedrock elevation, $z_0$ (m), c) casing length, $L_{casing}$ (m), and d) required drawdown in "well cells" for a production of 700 L/d. The large red dot marks the selected, final well location.*

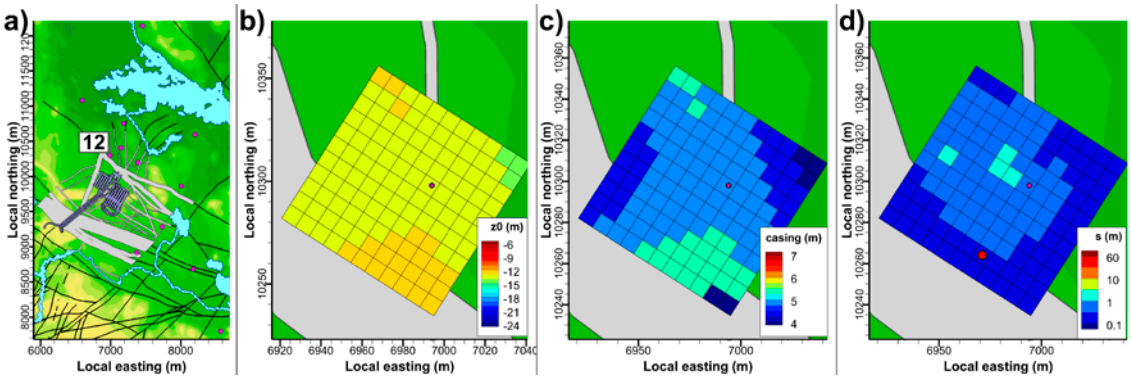


***Figure 3-14.*** *Localisation of well 12; a) initial location, b) bedrock elevation, $z_0$ (m), c) casing length, $L_{casing}$ (m), and d) required drawdown in "well cells" for a production of 700 L/d. The large red dot marks the selected, final well location.*

## 3.3 Flow simulation procedure

### 3.3.1 Well scenarios

This study does not address the potential interaction between co-existing wells. Instead, each well is modelled separately and independently of the others. Hence, each "well scenario" requires a separate flow solution, in which only the studied well is implemented. In other words, Subtask A consists of 12 separate flow simulations, Subtask B consists of 4 flow simulations (all addressing the same well, but with variable water abstraction rates), and Subtask C consists of 8 flow simulations.

As mentioned previously, the framework for all well simulations in TD12 is the Base case bedrock parameterisation as defined in TD11 (Section 2.2.3). The details of this model setup are comprehensive and therefore not presented here; the reader is instead referred to Öhman et al. (2014). However, in order to meet the TD12 objectives, a few adaptations must be made to the modelling approach. The adaptations are primarily related to the following:

1) Introduction of wells into the pre-existing computational grid (Section 3.3.2).
2) Minor modifications of boundary conditions (Section 3.3.3).
3) Evaluation of well interaction by means of particle tracking (Section 3.4).

It is beyond the scope of TD12 to address transient effects of the successively altering flow regime; therefore the flow field is solved as a steady-state solution for the stage of shoreline retreat at 5000 AD.

### 3.3.2 Parameterisation of "well cells"

The water-supply wells are introduced by means of a highly simplistic representation in the computational grid, in terms of a stack of "well cells" as described in Section 3.1 (Figure 3-1). The conductivity enhancement associated to the drilled well is represented by modifying the vertical conductivity of these cells (i.e. well characteristics are accounted for, but at the scale of effective cell properties). In other words, the well itself is a highly conductive conduit, but its cross-sectional area is very small in relation to the representative "well cells".

In order to provide good hydraulic communication along the well trajectory, the well cells are assigned a high vertical conductivity, $K_z = 10^{-4}$ m/s (Figure 3-1b). It is expected that this parameterisation will result in a realistic, low simulated hydraulic gradient along the well trajectory. On the contrary, the upper and lower ends of each well are assigned a very low vertical conductivity, $K_z = 3 \cdot 10^{-11}$ m/s, which is intended to seal off vertical inflow (Figure 3-1b).

### 3.3.3 Boundary conditions

The prescribed boundary conditions in TD12 are essentially identical to the TD11 setup:

- No-flow across the model bottom (z = –1,100 m).
- No-flow across the vertical sides that outline the flow-model domain (Figure 2-1).
- Mixed boundary condition at the top of the model domain (i.e. ground surface or seafloor, according to Section 2.2.4). However, as explained further below, the ground-surface head is re-solved within a 700 m radius around the well to account for potential local drawdown.
- Water abstraction from wells is simulated by introducing a –700 L/d sink term (i.e. prescribed as $Q_{well} = –0.00810$ kg/s) to the well cell of maximum horizontal conductivity. As mentioned previously, this cell is referred to as the "pump cell" (Figure 3-1c), and is addressed by its unique DarcyTools cell number (Table 4-1 and Table 4-3).

To reduce simulation time, the existing flow solution for *undisturbed conditions* is used as initial values, i.e. for the TD11 Base case model setup at the 5000 AD time slice, but without wells. The concept of mixed boundary conditions is summarized in Section 2.2.4, and a description on how the concept is modified to account for the potential drawdown around the studied water-supply wells is given below.

### *Significance of local drawdown in top-boundary condition*

The purpose of the recharge phase is to allow the groundwater table to conform to local hydrogeological conditions. It is therefore of interest to examine the potential influence that water abstraction from wells may have on the local groundwater table, as well as placing the significance of this in context of the uncertainties and potential errors discussed above.

All simulated wells in TD12 are parameterised to mimic a minimum of 4 m bedrock casing (Figure 3-1b; Section 3.3.2). The intention of this is to seal off its hydraulic contact to the overlying regolith. Nevertheless, three potential effects on the flow field are considered for each implemented well:

1) Water abstraction causes local drawdown in the bedrock, which may propagate to ground surface.
2) The modified vertical conductivity of "well cells" may affect the hydraulic connectivity in bedrock (e.g. it may short-circuit flow paths between large-scale structures).
3) Even minor modifications to the model setup affects the numerical convergence progress, leading to slightly different outcomes in different flow simulations. This may potentially demonstrate that the sensitivity to numerical instability exceeds the actual hydraulic impact of the well.

A scoping simulation is performed to evaluate the potential significance of drawdown around wells. This setup very similar to the preceding scoping simulation (Section 3.2.3), where all 12 wells of Subtask A are included and simultaneously pumped; however, the well locations have been updated to their final positions (Table 3-5). The model top-boundary condition is solved according to the two-phase approach developed in TD11 (Section 2.2.4). The resulting ground-surface head $H$ (the elevation of the groundwater table) is compared with the pre-existing flow solution in TD11, with an identical model setup but without wells, here referred to as the "reference case". Thus, the simulated drawdown at ground surface can be expressed as $s = H_{All\ wells} - H_{No\ wells}$ (Figure 3-15). The following is noted:

- In most of the wells, the water abstraction causes a local drawdown at ground surface (note that no drawdown is observed for wells 2 and 8).
- The simulated ground-surface drawdown is quite small, $s \approx 0.001$ to 0.1 m.
- Drawdown is not necessarily centred on the well, but depends on the local topography.
- The maximum influence radius of a well is estimated to 700 m (in reality, it is expected to be considerably smaller).
- Areas of "unexpected drawdown", i.e. simulated "drawdown" not associated to well pumping, as well as "negative drawdown" (higher elevation of the groundwater table for pumped conditions; blue colours in Figure 3-15) reflect the limitations of this modelling approach. The limitations are due to 1) the precision in the recharge algorithm and 2) water abstraction from wells can be subordinate to the impact of altering the "well-cell" conductivity (see e.g. well 2 in Table 4-5).

A second scoping simulation is tested to examine the effect that the top-boundary condition has below the ground surface, or more precisely, in the well "pump cell" (Table 4-1 and Table 4-3). Similarly to the previous simulation, all 12 wells of Subtask A are assumed to be active simultaneously. However, in this second test simulation, the top-boundary condition is taken directly from the TD11 reference case (without wells). In other words, this second simulation *neglects* local drawdown in the top-boundary condition (grey dots in Figure 3-16) and is compared against the preceding scoping simulation, where the top-boundary condition is adapted to water abstraction in wells (grey dots in Figure 3-16). In both simulation cases, the simulated head in the "pump cell" of wells is related to its corresponding value in the TD11 reference case (i.e. without wells), to determine the local drawdown. It is noted that owing to the high vertical conductivity of well cells (Section 3.3.2), the gradient along well cells is very low. The simulated drawdown is compared to the estimation based on the geometrical sampling, Equation (3-1), see Figure 3-16. The following can be noted:

- The estimated drawdown, based on the geometrical sampling of local bedrock properties, Equation (3-1), agrees well with simulation results, which places confidence in the approach for finding final locations of wells (Section 3.2.4).
- In most wells, the type of top-boundary condition is insignificant for the simulated drawdown in the "pump cell". The exceptions from this are wells 1, 3, 4, and 9 (cf. grey and blue dots in Figure 3-16).

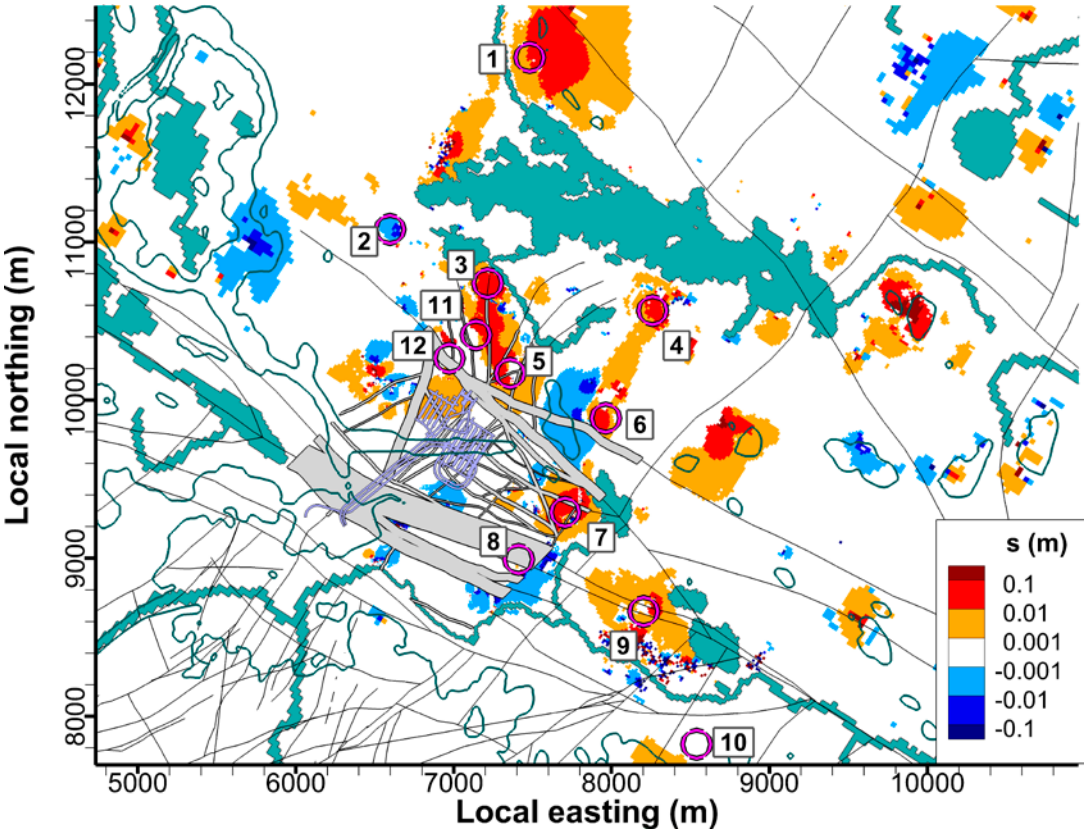


***Figure 3-15.*** *Simulated drawdown at ground surface due to water abstraction from wells, s (m), expressed as the difference in ground-surface head between 1) the scoping case (12 wells of Subtask A simultaneously pumped) and 2) the reference case from TD11 (without wells).*

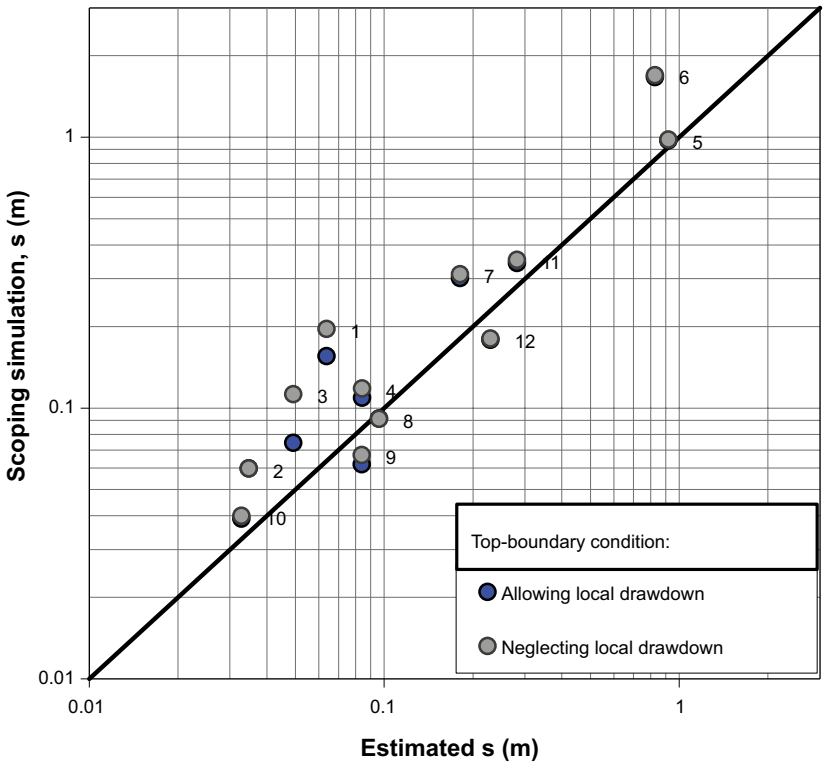


***Figure 3-16.*** *Drawdown in pumped wells of Subtask A; scoping simulation versus estimation in geometrical sampling, Equation (3-1). Drawdown calculated as simulated head in "pump cell" relative to its head in the TD11 reference case, without wells. Two boundary conditions for ground-surface cells are compared.*

### *Accounting for local drawdown in top-boundary condition*

Based on the results of the scoping simulations, it was decided to account for local drawdown in the top-boundary condition, but only within a radius of 700 m from each well. In essence, this is done by incorporating a well-production component into the *recharge phase*. For this numerical model implementation, the reference-head solution (the solution from corresponding TD11 case *without wells*) is used in three different ways:

1) As initial values for the entire model volume (to shorten the simulation time).
2) As top-boundary condition in areas farther than 700 m radius from each well (i.e. outside of the maximum radius of influence).
3) As criteria for maximum ground-surface head inside the 700 m radius area. Hence, it is assumed that well production cannot lead to an increased groundwater level, and the difficult step of referring to basin-filled DEM can therefore be omitted.

The following approach is taken to re-solve ground-surface head within 700 m radius from each well. The initial head values are taken from the reference-head solution and the recharge is set to 0.0 mm/yr. Beyond the 700 m radius, the ground-surface head is prescribed from the reference-head solution. Inside the 700 m radius, local recharge is successively increased by iteration, from a starting value of 0.0 to a maximum of 160 mm/yr, as long as the simulated ground-surface head does not exceed the reference-head solution. Thus, remaining ground-surface head below the reference head is interpreted as 1) actual well drawdown or 2) a consequence of that the well short-circuits structures in the bedrock. In each iteration, any ground-surface head exceeding the reference head is permanently switched to a constant-head boundary condition, where head is prescribed from the reference-head solution (i.e. the hydraulic head is not allowed to exceed the ground-surface elevation).

Well 1 can be taken as an example to demonstrate the simulated local top-boundary condition. The well is located in a hill slope, c 150 m east of the effluent stream of biosphere object 116 (also referred to as Charlie's lake; Figure 3-17a). Drawdown, *s* (m), is defined as the difference in simulated ground-surface head between the TD12 scenario *with* well pumping, and the TD11 reference case *without wells*. The foothill, west of well 1, is a saturated area owing to discharge from the elevated groundwater table of the hill, and hence, the drawdown is very limited to the west. Instead, the drawdown spreads eastwards, uphill in a smooth, semi-concentric pattern, with only a few centimetres in magnitude (Figure 3-17c). Further to the east, closer to the 700 m perimeter (i.e. more precisely, at the foothill east of the hill), a few abrupt decimetre-scale changes can be observed. These discrete changes signify cells that were of "prescribed-head type" in the TD11 reference solution, but could be solved with the "variable-recharge approach" under the pumped conditions in TD12.

In other words, the decimetre changes reflect the tolerance (or limited accuracy) in the mapping between rotated grid cells and the basin-filled topography data. Hence, the largest benefit of re-solving the local top-boundary condition around wells is perhaps not accounting for the actual drawdown, as its impact is small indeed, but rather focusing the flow solution to the target area improves the simulated groundwater table near wells.

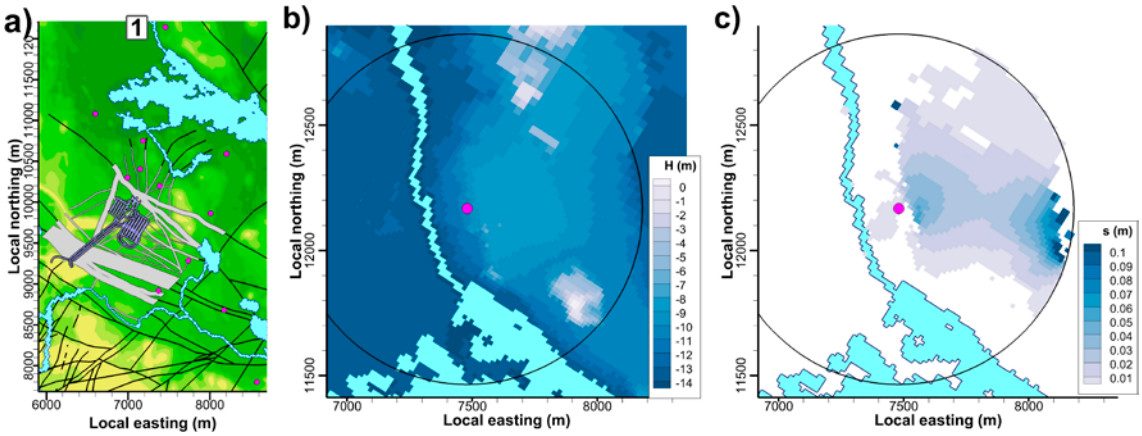


***Figure 3-17.*** *Solving the local groundwater table around well 1; a) map of well locations, b) simulated head in ground-surface layer, and c) head difference within a 700 m radius, expressed as drawdown.*

Having determined the elevation of the groundwater table (or more precisely head in ground-surface cells) by means of a *recharge phase*, which has been adapted to include near-field influence of *water abstraction from wells*, the groundwater table is applied as a top-boundary condition to obtain a highly convergent steady-state solution. This steady-state solution is analysed by means of a particle-tracking method to determine the potential interactions between the disposal rooms and hypothetical water-supply wells (Section 3.4).

## 3.4 Evaluation of well interaction

Once steady-state flow solutions have been determined for each of the specified wells (Section 3.3), well interaction is evaluated by means of a particle-tracking method. Well interaction refers to a hydraulic connection between the SFR facility and a pumped water-supply well, which in turn can be related to the risk of radionuclide transport to the well (Werner et al. 2013). The particle-tracking method has been thoroughly described in TD11 (Öhman et al. 2014). In this method, each particle represents a water parcel (a discrete water volume) and each tracked particle trajectory corresponds to a groundwater flow path. In this study, particle trajectories refer only to groundwater flow paths within bedrock. Thus, passages through backfill or regolith are neither included as part of the particle trajectory, nor in its performance measures. As an example, typical starting/termination points of particle trajectories are passages across the disposal-room wall, bedrock/regolith interface, or entry to a water-supply well.

The particle tracking concept can be applied to traverse the flow field in either direction: *forwards* refers to tracking particles downstream, along with the hydraulic gradient, while *backwards* refers to tracking particles upstream, against the hydraulic gradient. Both concepts are used in this study:

1. 1,000,000 particles tracked forwards from SFR 1 (uniformly distributed per volume, among disposal rooms 1BTF, 2BTF, 1BLA, 1BMA, and Silo).
2. 1,000,000 particles tracked forwards from SFR3 (uniformly distributed per volume, among disposal rooms 2BLA, 3BLA, 4BLA, 5BLA, 2BMA, and 1BRT.
3. 1,000,000 particles tracked backwards from well (all released in the “pump cell”, i.e. the most conductive cell intersected by the well).

Interactions are defined as the fraction of released particles that reach a disposal room, $i$, or a pumped well, $j$. The interactions are denoted:

- $f_{ij}$ [0…1], in forward tracking from a disposal room, $i$ = 1…11, to a well, $j$ = 1…20, or
- $f_{ji}$ [0…1], in backward tracking from a well, $j$ = 1…20, to a disposal room, $i$ = 1…11.

In theory, mass conservation holds that for any flow across a disposal room, $Q_i$, the particle-tracking direction is interchangeable, such that

$$Q_i f_{ij} = Q_j f_{ji} \tag{3-2}$$

where $Q_j$ is the water abstraction from a well, $j$, which is set to 700 L/d in Subtasks A and C. For example, in a case where a disposal-room cross flow is low, $Q_i$ = 7 L/d and all of its released particles reach a pumped well in forward tracking, $f_{ij}$ = 1.0, whereas the fraction of abstracted water that originate at the disposal room $i$ is only 1%, $f_{ji} = f_{ij} \cdot Q_i/Q_j = 0.01$ (i.e. 99% of the pumped water has not passed through the disposal room). In other words, unlike the *forward* interactions, $f_{ij}$, the *backward* interactions, $f_{ji}$, incorporates dilution in well production.

“Well cells” may have a cross-flow term under pumped conditions, i.e. an outward-directed flow component, $Q_{out}$, such that $Q_{in} = 700 + |Q_{out}|$ (Section 4.2.1). In backward particle tracking, this cross-flow term adds to the dilution of pumped water and, in effect, $Q_{in}$ must be used instead of $Q_j$ for equivalence in Equation (3-2). Although a natural cross-flow term may exist in reality, this effect is expected to be highly exaggerated here by the coarse discretisation of well cells (Section 3.1), in combination with the “well-property parameterisation” (Section 3.3.2).

# 4 Results

## 4.1 Bedrock properties of “well cells”

### 4.1.1 Final well locations for Subtask A

As a preceding modelling step of Subtask A, the locations of wells 1 to 12 were determined in a geometrical analysis, where the “required drawdown”, *s*, to sustain the target well production of 700 L/d was estimated in the surroundings of hypothetical future settlements for wells 1–11 and for well 12 in the well-interaction area (Section 3.2.4). The resulting, final locations of wells 1 to 12 are presented in Table 3-5.

To demonstrate the outcome of the localisation of wells, the corresponding bedrock properties are evaluated at the final locations, in analogy with the principles explained in Sections 3.1 and 3.2. The primary conclusions of this bedrock-property analysis (Table 4-1, Table 4-2, and Figure 4-1) are

- All wells are expected to fulfil the criterion of a sustainable production of 700 L/d at their final locations, and
- Based on maximum horizontal cell-wall conductivity, a “pump cell” (Figure 3-1c) can be selected for representing the sink term in well production (Section 3.3.3), as well as the release point in backward-particle tracking (Section 3.4).

**Table 4-1. Estimated well capacities for final well location in Subtask A.**

| Well | Casing (m) | Estimated well capacity[1], Q/s ($m^2$/s) | Estimated maximum production[2], Q (L/d) | $Z_0$ (m) | Pump cell ID[3] |
|---|---|---|---|---|---|
| 1 | 6 | 1.27E–04 | 109,814 | –12 | 556315 |
| 2 | 5 | 2.33E–04 | 201,226 | –17 | 465536 |
| 3 | 4 | 1.65E–04 | 142,387 | –8 | 286099 |
| 4 | 4 | 9.62E–05 | 83,151 | –16 | 4309302 |
| 5 | 5.5 | 8.81E–06 | 7,612 | –12.5 | 2070009 |
| 6 | 4.5 | 9.78E–06 | 8,452 | –11.5 | 1942252 |
| 7 | 4.5 | 4.49E–05 | 38,750 | –9.5 | 1703837 |
| 8 | 5 | 8.44E–05 | 72,904 | –13 | 1488008 |
| 9 | 4 | 9.65E–05 | 83,341 | –14 | 307287 |
| 10 | 4 | 2.47E–04 | 213,235 | –16 | 472893 |
| 11 | 4.5 | 2.87E–05 | 24,831 | –13.5 | 1934412 |
| 12 | 5.5 | 3.53E–05 | 30,491 | –12.5 | 2219115 |

[1] Calculated from sampled cell properties (Table 4-2), using Equation (3-1).

[2] Estimated maximum well production, based on the estimated well capacity and assuming a maximum 10 m drawdown in the rock mass around the well.

[3] In flow simulations (Section 3.3), water abstraction from wells is imposed as a flux boundary condition in a single grid cell (the most conductive cell out of those intersected by the well scanline; Table 4-2). This grid cell, identified via a unique DarcyTools ID grid cell number, is referred to as the “Pump cell”.

**Table 4-2. Sampled cell-wall conductivity for the final well locations in Subtask A.**

| Well | Well cell[1)] | 1 | 2 | 3 | 4 | 5 | 6 | 7 | 8 | 9 |
|---|---|---|---|---|---|---|---|---|---|---|
| **1** | Secup (m) | 6 | 8 | 16 | 32 | 48 | | | | |
| | Seclow (m) | 8 | 16 | 32 | 48 | 64 | | | | |
| | Side L (m) | 16 | 16 | 16 | 16 | 16 | | | | |
| | Log $K_{max}$ | –10.5 | –10.5 | –5.2 | –5.9 | –10.5 | | | | |
| **2** | Secup (m) | 5 | 7 | 11 | 19 | 27 | 43 | 59 | | |
| | Seclow (m) | 7 | 11 | 19 | 27 | 43 | 59 | 75 | | |
| | Side L (m) | 16 | 16 | 16 | 16 | 16 | 16 | 16 | | |
| | Log $K_{max}$ | –5.2 | –4.9 | –5.0 | –10.5 | –6.8 | –5.3 | –6.7 | | |
| **3** | Secup (m) | 4 | 6 | 8 | 12 | 20 | 36 | 52 | | |
| | Seclow (m) | 6 | 8 | 12 | 20 | 36 | 52 | 68 | | |
| | Side L (m) | 16 | 16 | 16 | 16 | 16 | 16 | 16 | | |
| | Log $K_{max}$ | –5.6 | –5.6 | –5.6 | –5.6 | –5.6 | –5.6 | –5.6 | | |
| **4** | Secup (m) | 4 | 6 | 8 | 12 | 20 | 28 | 44 | | |
| | Seclow (m) | 6 | 8 | 12 | 20 | 28 | 44 | 60 | | |
| | Side L (m) | 16 | 16 | 16 | 16 | 16 | 16 | 16 | | |
| | Log $K_{max}$ | –4.8 | –4.5 | –7.3 | –8.2 | –10.5 | –10.5 | –10.5 | | |
| **5** | Secup (m) | 5.5 | 7.5 | 11.5 | 15.5 | 23.5 | 31.5 | 39.5 | 47.5 | 55.5 |
| | Seclow (m) | 7.5 | 11.5 | 15.5 | 23.5 | 31.5 | 39.5 | 47.5 | 55.5 | 63.5 |
| | Side L (m) | 8 | 8 | 8 | 8 | 8 | 8 | 8 | 8 | 8 |
| | Log $K_{max}$ | –6.6 | –7.0 | –7.2 | –6.2 | –7.2 | –7.1 | –7.1 | –7.5 | –7.6 |
| **6** | Secup (m) | 4.5 | 8.5 | 16.5 | 24.5 | 32.5 | 40.5 | 48.5 | 56.5 | |
| | Seclow (m) | 8.5 | 16.5 | 24.5 | 32.5 | 40.5 | 48.5 | 56.5 | 64.5 | |
| | Side L (m) | 8 | 8 | 8 | 8 | 8 | 8 | 8 | 8 | |
| | Log $K_{max}$ | –6.4 | –6.1 | –8.0 | –7.0 | –7.0 | –7.2 | –7.7 | –9.1 | |
| **7** | Secup (m) | 4.5 | 6.5 | 10.5 | 18.5 | 26.5 | 34.5 | 42.5 | 50.5 | 58.5 |
| | Seclow (m) | 6.5 | 10.5 | 18.5 | 26.5 | 34.5 | 42.5 | 50.5 | 58.5 | 66.5 |
| | Side L (m) | 8 | 8 | 8 | 8 | 8 | 8 | 8 | 8 | 8 |
| | Log $K_{max}$ | –8.3 | –8.2 | –7.2 | –5.8 | –5.5 | –7.6 | –7.4 | –7.9 | –6.2 |
| **8** | Secup (m) | 5 | 7 | 11 | 15 | 23 | 31 | 39 | 47 | 55 |
| | Seclow (m) | 7 | 11 | 15 | 23 | 31 | 39 | 47 | 55 | 63 |
| | Side L (m) | 8 | 8 | 8 | 8 | 8 | 8 | 8 | 8 | 8 |
| | Log $K_{max}$ | –5.8 | –5.9 | –5.7 | –5.9 | –5.8 | –5.9 | –5.8 | –5.9 | –5.9 |
| **9** | Secup (m) | 4 | 6 | 10 | 14 | 22 | 30 | 46 | | |
| | Seclow (m) | 6 | 10 | 14 | 22 | 30 | 46 | 62 | | |
| | Side L (m) | 16 | 16 | 16 | 16 | 16 | 16 | 16 | | |
| | Log $K_{max}$ | –5.3 | –5.8 | –6.7 | –6.0 | –5.2 | –6.0 | –6.7 | | |
| **10** | Secup (m) | 4 | 6 | 8 | 12 | 20 | 28 | 44 | | |
| | Seclow (m) | 6 | 8 | 12 | 20 | 28 | 44 | 60 | | |
| | Side L (m) | 16 | 16 | 16 | 16 | 16 | 16 | 16 | | |
| | Log $K_{max}$ | –8.2 | –7.6 | –7.6 | –7.5 | –7.6 | –7.6 | –4.8 | | |
| 11 | Secup (m) | 4.5 | 6.5 | 10.5 | 14.5 | 22.5 | 30.5 | 38.5 | 46.5 | 54.5 |
| | Seclow (m) | 6.5 | 10.5 | 14.5 | 22.5 | 30.5 | 38.5 | 46.5 | 54.5 | 62.5 |
| | Side L (m) | 8 | 8 | 8 | 8 | 8 | 8 | 8 | 8 | 8 |
| | Log $K_{max}$ | –5.8 | –6.6 | –5.6 | –6.2 | –7.4 | –6.2 | –6.7 | –6.5 | –8.9 |
| **12** | Secup (m) | 5.5 | 7.5 | 11.5 | 15.5 | 23.5 | 31.5 | 39.5 | 47.5 | 55.5 |
| | Seclow (m) | 7.5 | 11.5 | 15.5 | 23.5 | 31.5 | 39.5 | 47.5 | 55.5 | 63.5 |
| | Side L (m) | 8 | 8 | 8 | 8 | 8 | 8 | 8 | 8 | 8 |
| | Log $K_{max}$ | –5.7 | –5.9 | –6.2 | –6.3 | –6.4 | –6.2 | –6.2 | –6.3 | –6.3 |

[1)] Well cells, below bedrock casing, in ascending order, i.e. “cell 1” refers to the uppermost bedrock cell, just below the bottom end of the well casing. This is not to be confused with the DarcyTools ID grid numbering (cf., Table 4-1).

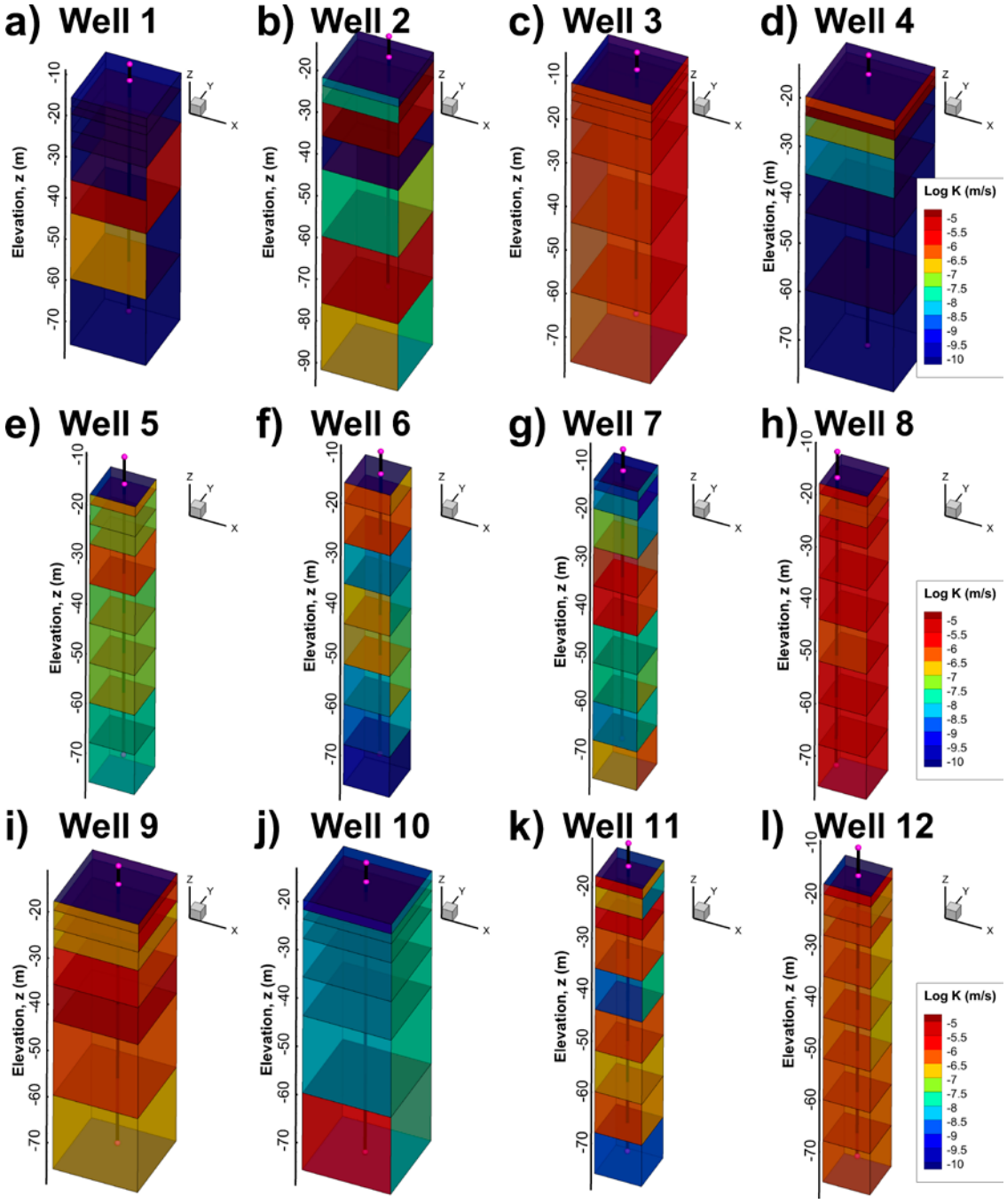


***Figure 4-1.*** *Cell-wall conductivity of computational cells intersected by wells 1 to 12 (final locations). Vertical cell walls reflect the upscaled horizontal conductivity of the bedrock, i.e. the local ECPM property based on an underlying stochastic fracture network realisation (Section 3.1). Horizontal cell walls reflect the vertical conductivity parameterised to mimic well properties (e.g. Figure 3-1b). Borehole scanline symbols are explained in Figure 3-1a.*

### 4.1.2 Well locations in Subtask C

As explained earlier (Section 1.4), there is a conceptual difference between Subtasks A and C. The purpose in Subtask C is not to address the water supply for settlements associated to arable land, but instead to study wells in the area in which wells drilled in the rock may have the highest concentrations of radionuclides originating from SFR (Figure 1-3). As such, the 8 wells in Subtask C have pre-defined final locations (Table 1-1) and therefore do not need to undergo the localisation step undertaken in Subtask A.

In analogy with Section 4.1.1, the bedrock properties are evaluated at the 8 well locations of Subtask C (Table 4-3, Table 4-4, and Figure 4-2). Again, the following can be confirmed:

- All wells are expected to fulfil the 700 L/d criterion.
- Based on maximum horizontal cell-wall conductivity, a "pump cell" (Figure 3-1c) can be selected for representing the sink term in well production (Section 3.3.3), as well as the release point in backward-particle tracking (Section 3.4).

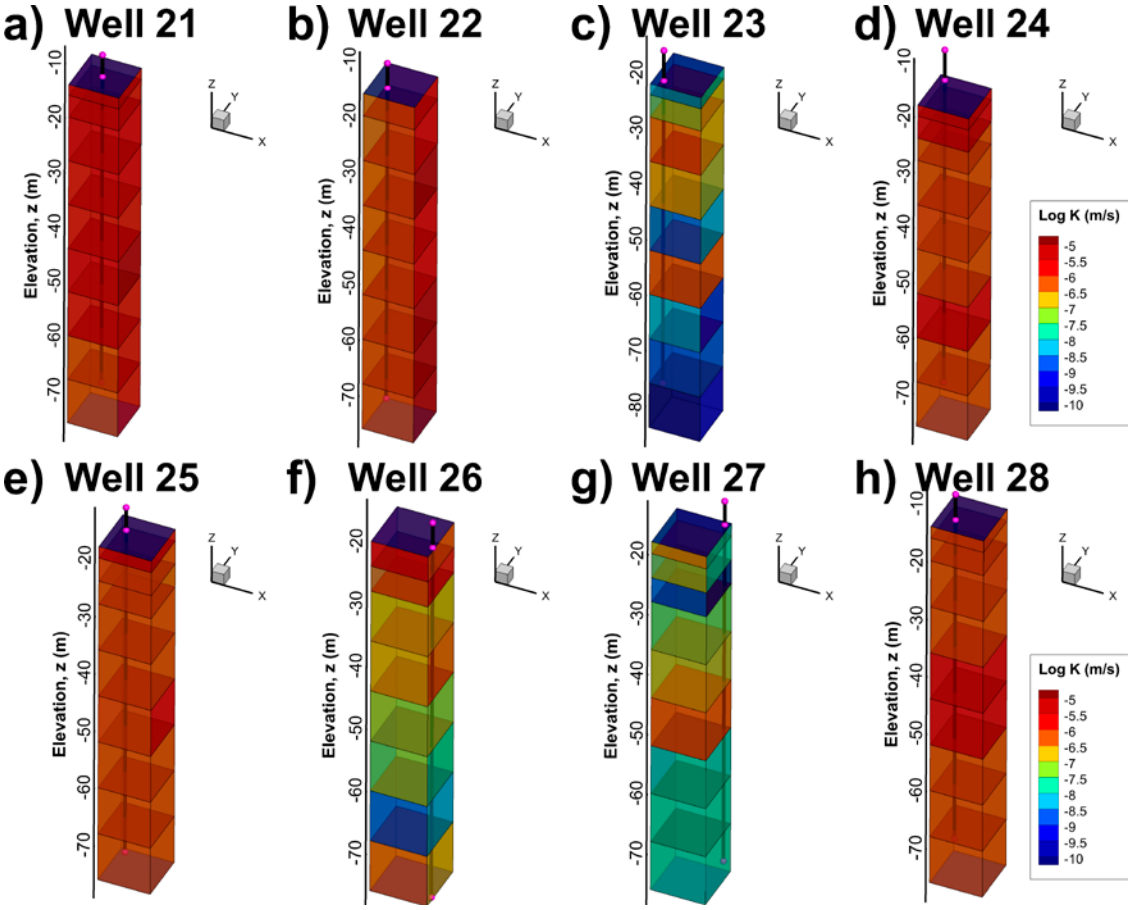


***Figure 4-2.*** *Cell-wall conductivity of computational cells intersected by wells 21 to 28. Vertical cell walls reflect the upscaled horizontal conductivity of the bedrock, i.e. the local ECPM property based on an underlying stochastic fracture network realisation (Section 3.1). Horizontal cell walls reflect the vertical conductivity parameterised to mimic well properties (e.g. Figure 3-1b). Borehole trajectory symbols are explained in Figure 3-1a.*

**Table 4-3. Estimated well capacity in Subtask C (minimum bedrock casing 4 m).**

| Well | Casing (m) | Estimated well capacity[1], Q/s ($m^2$/s) | Estimated maximum production[2], Q (L/d) | $Z_0$ (m) | Pump cell ID |
|---|---|---|---|---|---|
| 21 | 4 | 1.78E–04 | 153,619 | –10 | 2470206 |
| 22 | 4.5 | 1.96E–04 | 169,690 | –11.5 | 248395 |
| 23 | 5.5 | 1.06E–05 | 9,167 | –16.5 | 2080626 |
| 24 | 5.5 | 5.70E–05 | 49,239 | –12.5 | 1922491 |
| 25 | 4 | 4.64E–05 | 40,090 | –14 | 2469149 |
| 26 | 4 | 2.08E–05 | 18,006 | –16 | 4636411 |
| 27 | 4 | 6.79E–06 | 5,863 | –14 | 2105097 |
| 28 | 4.5 | 6.36E–05 | 54,985 | –9.5 | 1690396 |

[1] Calculated from sampled cell properties (Table 4-4), using Equation (3-1).

[2] Estimated maximum well production, assuming a maximum 10 m drawdown in the rock mass around the well.

[3] In flow simulations (Section 3.3), well production is imposed as a flux boundary condition in a single grid cell (the most conductive cell out of those intersected by the well scanline; Table 4-4). This grid cell, identified via a unique DarcyTools ID grid cell number, is referred to as the "Pump cell".

**Table 4-4. Sampled cell-wall conductivity for wells 21 to 28.**

| Well | Bedrock cell | 1 | 2 | 3 | 4 | 5 | 6 | 7 | 8 | 9 |
|---|---|---|---|---|---|---|---|---|---|---|
| 21 | Secup (m) | 4 | 6 | 10 | 18 | 26 | 34 | 42 | 50 | 58 |
| | Seclow (m) | 6 | 10 | 18 | 26 | 34 | 42 | 50 | 58 | 66 |
| | Side L (m) | 8 | 8 | 8 | 8 | 8 | 8 | 8 | 8 | 8 |
| | Log $K_{max}$ | –5.5 | –5.5 | –5.5 | –5.5 | –5.5 | –5.4 | –5.5 | –5.6 | –5.7 |
| 22 | Secup (m) | 4.5 | 8.5 | 16.5 | 24.5 | 32.5 | 40.5 | 48.5 | 56.5 | |
| | Seclow (m) | 8.5 | 16.5 | 24.5 | 32.5 | 40.5 | 48.5 | 56.5 | 64.5 | |
| | Side L (m) | 8 | 8 | 8 | 8 | 8 | 8 | 8 | 8 | |
| | Log $K_{max}$ | –5.5 | –5.5 | –5.5 | –5.5 | –5.5 | –5.5 | –5.5 | –5.5 | |
| 23 | Secup (m) | 5.5 | 7.5 | 11.5 | 19.5 | 27.5 | 35.5 | 43.5 | 51.5 | 59.5 |
| | Seclow (m) | 7.5 | 11.5 | 19.5 | 27.5 | 35.5 | 43.5 | 51.5 | 59.5 | 67.5 |
| | Side L (m) | 8 | 8 | 8 | 8 | 8 | 8 | 8 | 8 | 8 |
| | Log $K_{max}$ | –7.9 | –6.7 | –6.4 | –6.5 | –7.3 | –6.4 | –7.6 | –8.7 | –9.2 |
| 24 | Secup (m) | 5.5 | 7.5 | 11.5 | 15.5 | 23.5 | 31.5 | 39.5 | 47.5 | 55.5 |
| | Seclow (m) | 7.5 | 11.5 | 15.5 | 23.5 | 31.5 | 39.5 | 47.5 | 55.5 | 63.5 |
| | Side L (m) | 8 | 8 | 8 | 8 | 8 | 8 | 8 | 8 | 8 |
| | Log $K_{max}$ | –5.7 | –5.9 | –6.1 | –6.1 | –5.9 | –6.1 | –5.9 | –6.1 | –6.2 |
| 25 | Secup (m) | 4 | 6 | 10 | 14 | 22 | 30 | 38 | 46 | 54 |
| | Seclow (m) | 6 | 10 | 14 | 22 | 30 | 38 | 46 | 54 | 62 |
| | Side L (m) | 8 | 8 | 8 | 8 | 8 | 8 | 8 | 8 | 8 |
| | Log $K_{max}$ | –5.8 | –6 | –6.3 | –6.3 | –6.3 | –5.7 | –6.3 | –6.1 | –6.3 |
| 26 | Secup (m) | 4 | 8 | 12 | 20 | 28 | 36 | 44 | 52 | |
| | Seclow (m) | 8 | 12 | 20 | 28 | 36 | 44 | 52 | 60 | |
| | Side L (m) | 8 | 8 | 8 | 8 | 8 | 8 | 8 | 8 | |
| | Log $K_{max}$ | –5.8 | –5.8 | –6.6 | –6.5 | –7 | –7.4 | –8.4 | –6.5 | |
| 27 | Secup (m) | 4 | 6 | 10 | 14 | 22 | 30 | 38 | 46 | 54 |
| | Seclow (m) | 6 | 10 | 14 | 22 | 30 | 38 | 46 | 54 | 62 |
| | Side L (m) | 8 | 8 | 8 | 8 | 8 | 8 | 8 | 8 | 8 |
| | Log $K_{max}$ | –6.7 | –7.4 | –7.9 | –7.2 | –6.8 | –6.3 | –7.8 | –7.6 | –7.7 |
| 28 | Secup (m) | 4.5 | 6.5 | 10.5 | 18.5 | 26.5 | 34.5 | 42.5 | 50.5 | 58.5 |
| | Seclow (m) | 6.5 | 10.5 | 18.5 | 26.5 | 34.5 | 42.5 | 50.5 | 58.5 | 66.5 |
| | Side L (m) | 8 | 8 | 8 | 8 | 8 | 8 | 8 | 8 | 8 |
| | Log $K_{max}$ | –6 | –6.1 | –6 | –6 | –5.8 | –5.8 | –6.1 | –6.2 | –6.2 |

[1] Well cells, below bedrock casing, in ascending order, i.e. "cell 1" refers to the uppermost bedrock cell, just below the end of the well casing. This is not to be confused with the DarcyTools ID grid numbering (cf. Table 4-3).

## 4.2 Flow simulations

### 4.2.1 Flow across well cells

As borehole geometry is not explicitly resolved in the model, the "well cells" in this study represent both the well and its surrounding bedrock (Section 3.1.2). A consequence of this is that the natural bedrock flow through these cells cannot be differentiated from the flow induced by water abstraction in the well. Therefore it is of interest to compare the cross flow over well cells under natural conditions versus pumped conditions. Under non-pumped conditions (without wells), the natural flow across "well cells" ranges from 4.2 L/d in well 26 to 156.7 L/d in well 2 (see off-diagonal values, $Q_{in} = Q_{out}$ in Table 4-5 and Table 4-6). As expected, activation of the well production (Section 3.3.3) renders a net flow of $Q_{in} - |Q_{out}| = 700$ L/d (along the diagonal in Table 4-5 and Table 4-6). During pumping, the outward-directed flow component, $Q_{out}$, is generally small in relation to the well production. The most notable exception is well 2, where the cross-flow term over "well cells", $Q_{out} = 1210.6$ L/d, significantly exceeds the pumping rate, $Q_{in} + Q_{out} = 700$ L/d.

A high cross-flow term during pumping, $Q_{out}$, as for example in well 2, implies a significant contribution to dilution in pumped water. It is therefore important to interpret if the cross-flow is realistic or should be rejected as an artefact of coarse model discretisation. Expectations are that the cross-flow term should decrease under pumped conditions. However, in some cases the cross-flow term *increases* during pumping (e.g. the cross-flow term in well 2 is 156.7 L/d under non-pumped conditions, but increases to 1210.6 L/d during pumping; Table 4-5). This is due to the implementation of well conductivities (Section 3.3.2), which is intended to mimic well properties. On the one hand, a drilled well indeed can short-circuit hydraulic connectivity between structures and enhance the local cross flow, but on the other, this effect is very exaggerated due to the coarse discretisation of wells (Section 3.1).

**Table 4-5. Simulated flow across "well cells" in Subtask A.**

| Simulated well scenario | Q (L/d) | Observation in well 1 | 2 | 3 | 4 | 5 | 6 | 7 | 8 | 9 | 10 | 11 | 12 |
|---|---|---|---|---|---|---|---|---|---|---|---|---|---|
| 1 | In | 700.5 | 156.7 | 104.4 | 32.6 | 17.0 | 4.5 | 12.6 | 24.4 | 39.7 | 4.7 | 27.3 | 29.2 |
| | Out | –0.5 | –156.7 | –104.4 | –32.6 | –17.0 | –4.5 | –12.6 | –24.4 | –39.7 | –4.7 | –27.3 | –29.2 |
| 2 | In | 143.3 | 1910.6 | 105.0 | 32.6 | 17.0 | 4.5 | 12.6 | 24.4 | 39.7 | 4.7 | 27.3 | 29.2 |
| | Out | –143.3 | –1210.6 | –105.0 | –32.6 | –17.0 | –4.5 | –12.6 | –24.4 | –39.7 | –4.7 | –27.3 | –29.2 |
| 3 | In | 143.3 | 156.7 | 700 | 32.6 | 17.0 | 4.5 | 12.6 | 24.4 | 39.7 | 4.7 | 27.3 | 29.2 |
| | Out | –143.3 | –156.7 | 0.0 | –32.6 | –17.0 | –4.5 | –12.6 | –24.4 | –39.7 | –4.7 | –27.3 | –29.2 |
| 4 | In | 143.3 | 156.7 | 104.4 | 700 | 17.0 | 4.5 | 12.6 | 24.4 | 39.7 | 4.7 | 27.3 | 29.2 |
| | Out | –143.3 | –156.7 | –104.4 | 0.0 | –17.0 | –4.5 | –12.6 | –24.4 | –39.7 | –4.7 | –27.3 | –29.2 |
| 5 | In | 143.3 | 156.7 | 104.4 | 32.6 | 700 | 4.5 | 12.6 | 24.4 | 39.7 | 4.7 | 27.3 | 29.2 |
| | Out | –143.3 | –156.7 | –104.4 | –32.6 | 0.0 | –4.5 | –12.6 | –24.4 | –39.7 | –4.7 | –27.3 | –29.2 |
| 6 | In | 143.3 | 156.7 | 104.4 | 32.7 | 17.0 | 700 | 12.6 | 24.4 | 39.7 | 4.7 | 27.3 | 29.2 |
| | Out | –143.3 | –156.7 | –104.4 | –32.7 | –17.0 | 0.0 | –12.6 | –24.4 | –39.7 | –4.7 | –27.3 | –29.2 |
| 7 | In | 143.3 | 156.7 | 104.4 | 32.6 | 17.0 | 4.5 | 700 | 24.3 | 39.7 | 4.7 | 27.3 | 29.2 |
| | Out | –143.3 | –156.7 | –104.4 | –32.6 | –17.0 | –4.5 | 0.0 | –24.3 | –39.7 | –4.7 | –27.3 | –29.2 |
| 8 | In | 143.3 | 156.7 | 104.4 | 32.6 | 17.0 | 4.5 | 12.6 | 712.7 | 39.6 | 4.7 | 27.3 | 29.2 |
| | Out | –143.3 | –156.7 | –104.4 | –32.6 | –17.0 | –4.5 | –12.6 | –12.7 | –39.6 | –4.7 | –27.3 | –29.2 |
| 9 | In | 143.3 | 156.7 | 104.4 | 32.6 | 17.0 | 4.5 | 12.6 | 24.4 | 760.7 | 4.7 | 27.3 | 29.2 |
| | Out | –143.3 | –156.7 | –104.4 | –32.6 | –17.0 | –4.5 | –12.6 | –24.4 | –60.7 | –4.7 | –27.3 | –29.2 |
| 10 | In | 143.3 | 156.7 | 104.4 | 32.6 | 17.0 | 4.5 | 12.6 | 24.4 | 39.7 | 710.8 | 27.3 | 29.2 |
| | Out | –143.3 | –156.7 | –104.4 | –32.6 | –17.0 | –4.5 | –12.6 | –24.4 | –39.7 | –10.8 | –27.3 | –29.2 |
| 11 | In | 143.3 | 156.7 | 104.7 | 32.6 | 17.0 | 4.5 | 12.6 | 24.4 | 39.7 | 4.7 | 700 | 29.2 |
| | Out | –143.3 | –156.7 | –104.7 | –32.6 | –17.0 | –4.5 | –12.6 | –24.4 | –39.7 | –4.7 | 0.0 | –29.2 |
| 12 | In | 143.3 | 156.7 | 104.4 | 32.6 | 17.0 | 4.5 | 12.6 | 24.4 | 39.7 | 4.7 | 27.3 | 700 |
| | Out | –143.3 | –156.7 | –104.4 | –32.6 | –17.0 | –4.5 | –12.6 | –24.4 | –39.7 | –4.7 | –27.3 | 0.0 |

**Table 4-6. Simulated flow across "well cells" in Subtask C.**

| Simulated well scenario | | Q (L/d) | Observation in well 21 | 22 | 23 | 24 | 25 | 26 | 27 | 28 |
|---|---|---|---|---|---|---|---|---|---|---|
| | 21 | In | 812.8 | 29.7 | 6.2 | 74.7 | 19.7 | 4.2 | 5.8 | 31.7 |
| | | Out | –112.8 | –29.7 | –6.2 | –74.7 | –19.7 | –4.2 | –5.8 | –31.7 |
| | 22 | In | 78.5 | 746.7 | 6.2 | 74.7 | 19.7 | 4.2 | 5.7 | 31.7 |
| | | Out | –78.5 | –46.7 | –6.2 | –74.7 | –19.7 | –4.2 | –5.7 | –31.7 |
| | 23 | In | 78.9 | 29.9 | 700.0 | 74.7 | 19.7 | 4.1 | 5.9 | 31.7 |
| | | Out | –78.9 | –29.9 | 0.0 | –74.7 | –19.7 | –4.1 | –5.9 | –31.7 |
| | 24 | In | 78.9 | 29.9 | 6.2 | 945.3 | 19.4 | 4.1 | 5.8 | 31.7 |
| | | Out | –78.9 | –29.9 | –6.2 | –245.3 | –19.4 | –4.1 | –5.8 | –31.7 |
| | 25 | In | 78.9 | 29.9 | 6.2 | 74.5 | 700.0 | 4.0 | 5.8 | 31.7 |
| | | Out | –78.9 | –29.9 | –6.2 | –74.5 | 0.0 | –4.0 | –5.8 | –31.7 |
| | 26 | In | 78.9 | 29.9 | 6.2 | 74.7 | 19.9 | 700.0 | 5.8 | 31.7 |
| | | Out | –78.9 | –29.9 | –6.2 | –74.7 | –19.9 | 0.0 | –5.8 | –31.7 |
| | 27 | In | 78.8 | 29.6 | 6.2 | 74.7 | 19.7 | 4.2 | 700.0 | 31.7 |
| | | Out | –78.8 | –29.6 | –6.2 | –74.7 | –19.7 | –4.2 | 0.0 | –31.7 |
| | 28 | In | 78.9 | 29.9 | 6.2 | 74.4 | 19.7 | 4.2 | 5.8 | 700.0 |
| | | Out | –78.9 | –29.9 | –6.2 | –74.4 | –19.7 | –4.2 | –5.8 | 0.0 |

### 4.2.2 Effect on disposal-room cross flow

As may be expected, the flow across disposal rooms is largely unaffected by the pumping in remote water-supply wells associated to settlements (wells 1 to 11; Table 4-7). Pumping within the well-interaction area, wells 12 to 28, has a small, but noticeable effect on disposal-room cross flow (Table 4-7). For the water abstraction rate of 700 L/d, the increase in disposal-room cross flow is below 1% in all well scenarios.

**Table 4-7. Effects on disposal-room cross flow for all simulated wells.**

| Subtask/scenario[1)] | | 1BTF | 2BTF | 1BLA | 1BMA | Silo | 1BRT | 2BLA | 3BLA | 4BLA | 5BLA |
|---|---|---|---|---|---|---|---|---|---|---|---|
| A | Well 1 | 0% | 0% | 0% | 0% | 0% | 0% | 0% | 0% | 0% | 0% |
| | Well 2 | 0% | 0% | 0% | 0% | 0% | 0% | 0% | 0% | 0% | 0% |
| | Well 3 | 0% | 0% | 0% | 0% | 0% | 0% | 0% | 0% | 0% | 0% |
| | Well 4 | 0% | 0% | 0% | 0% | 0% | 0% | 0% | 0% | 0% | 0% |
| | Well 5 | 0% | 0% | 0% | 0% | 0% | 0% | 0% | 0% | 0% | 0% |
| | Well 6 | 0% | 0% | 0% | 0% | 0% | 0% | 0% | 0% | 0% | 0% |
| | Well 7 | 0% | 0% | 0% | 0% | 0% | 0% | 0% | 0% | 0% | 0% |
| | Well 8 | 0% | 0% | 0% | 0% | 0% | 0% | 0% | 0% | 0% | 0% |
| | Well 9 | 0% | 0% | 0% | 0% | 0% | 0% | 0% | 0% | 0% | 0% |
| | Well 10 | 0% | 0% | 0% | 0% | 0% | 0% | 0% | 0% | 0% | 0% |
| | Well 11 | 0% | 0% | 0% | 0% | 0% | 0% | 0% | 0% | 0% | 0% |
| | Well 12 | 0.2% | 0.2% | 0.1% | 0.1% | 0.4% | 0.1% | 0.1% | 0.1% | 0% | 0% |
| B | $Q_{well}$ = 1,000 L/d | 0.3% | 0.2% | 0.2% | 0.1% | 0.5% | 0.1% | 0.1% | 0.1% | 0.1% | 0.1% |
| | $Q_{well}$ = 1,400L/d | 0.4% | 0.3% | 0.2% | 0.1% | 0.7% | 0.1% | 0.2% | 0.1% | 0.1% | 0.1% |
| | $Q_{well}$ = 2,800 L/d | 0.7% | 0.6% | 0.4% | 0.2% | 1.3% | 0.3% | 0.3% | 0.3% | 0.2% | 0.1% |
| C | Well 21 | 0.1% | 0% | 0% | 0% | 0.1% | 0.2% | 0.1% | 0.2% | 0.3% | 0.3% |
| | Well 22 | 0.2% | 0.1% | 0% | 0% | 0.2% | 0.1% | 0.2% | 0.1% | 0.1% | 0.1% |
| | Well 23 | 0% | 0% | 0% | 0% | 0.1% | 0% | 0% | 0% | 0% | 0% |
| | Well 24 | 0.1% | 0.2% | 0.2% | 0.2% | 0.2% | 0.1% | 0.1% | 0.1% | 0% | 0% |
| | Well 25 | 0% | 0% | 0% | 0% | 0.1% | 0% | 0% | 0% | 0% | 0% |
| | Well 26 | 0% | 0% | 0% | 0% | 0% | 0% | 0% | 0% | 0% | 0% |
| | Well 27 | 0.1% | 0.1% | 0% | 0% | 0.2% | 0.1% | 0.1% | 0.1% | 0.1% | 0% |
| | Well 28 | 0% | 0.3% | 0.5% | 0.7% | 0.1% | 0.1% | 0% | 0% | 0% | 0% |

[1)] The abstraction rate, $Q_{well}$, is 700 L/d in Subtask A and C. Subtask B addresses variable abstraction rates in well 12.

However, the effect on disposal-room cross flows is clearly related to the distance between wells and disposal rooms (c.f. Table 4-7 and Figure 1-4b). For example, pumping in well 28 has the strongest effect on 1BMA, whereas pumping in well 21 has the strongest effect on 5BLA (Figure 4-3). Note that the effect is not evaluated for 2BMA, as the cross flow through this rock vault is affected by the identified error in DarcyTools related to the parameter <nbgrad> (see Section 2.1.1 and Öhman et al. 2014). The error in the separate algorithm for determining cross flow through 2BMA has been estimated to c 4%, which is considerably larger than the observed effects from pumping (Figure 4-3), and hence it was not considered meaningful to include 2BMA in this study. However, based on structural geology, the cross flow in 2BMA is expected to follow similar patterns as 4BLA and 5BLA.

The analysis of variable pumping rates in Subtask B demonstrates a linear dependency between the pumping rate in well 12 and its effect on disposal-room cross flow (Figure 4-4). Even at the highest pumping rate, $Q_{well}$ = 2,800 L/d, the flow across the Silo has not increased much more than 1% (Figure 4-4b). The proportionality between the water abstraction rate and influence on disposal-room cross flow suggests that the principle of superpositioning applies, i.e. additive disturbance from the abstraction rate in wells.

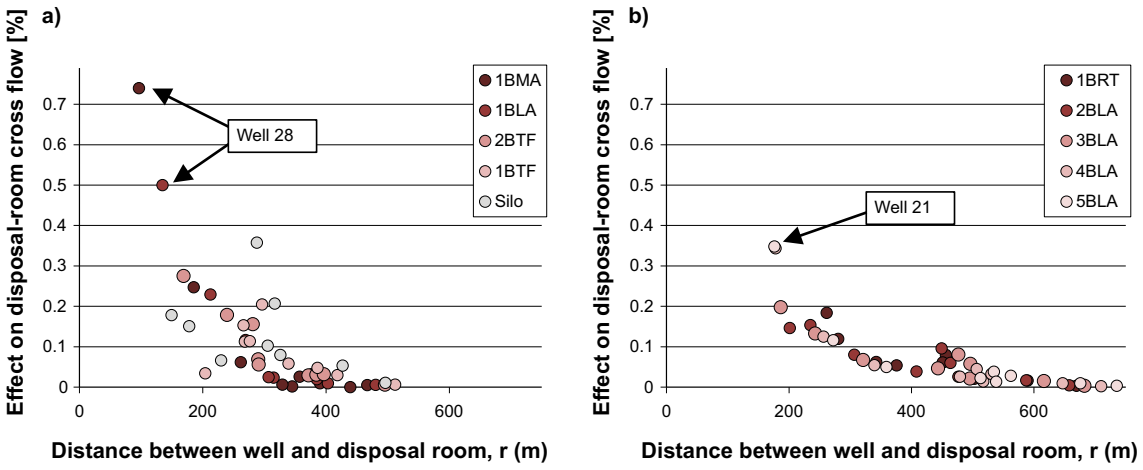


***Figure 4-3.*** *Influence on disposal-room cross flow versus distance to pumping well for wells in the well-interaction area; a) SFR 1 and b) SFR 3.*

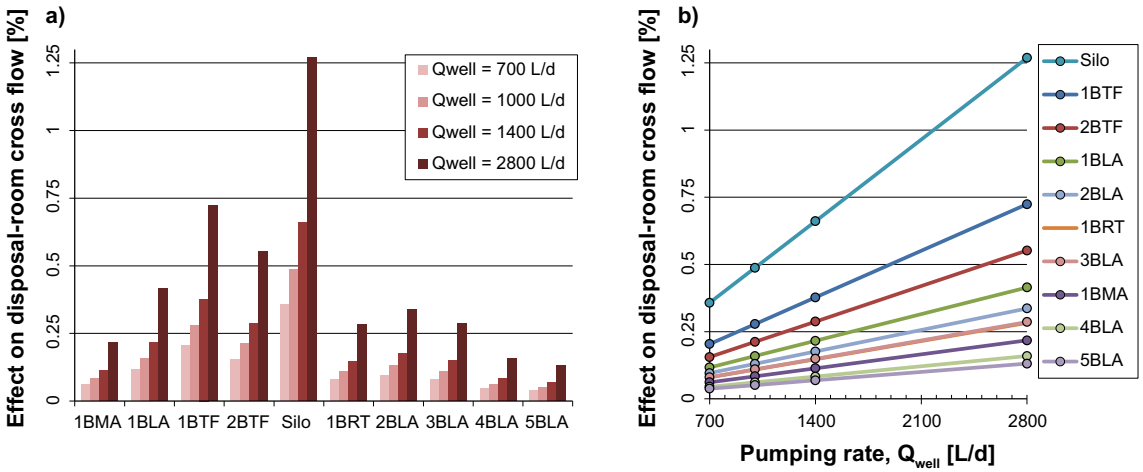


***Figure 4-4.*** *Influence of pumping rate in well 12 on disposal-room cross flow; a) overview bar plot and b) linear dependence.*

## 4.3 Well interactions

### 4.3.1 Wells in Subtask A

Well interactions are evaluated by means of particle tracking according to the principles described in Section 3.4. The resulting statistics for wells 1 to 12 are summarised in Table 4-8. However, to place the outcome in a hydrogeological context (i.e. topography, surface waters, and deformation zones), an overview of the particle-tracking results is also given in terms of exit locations at the bedrock/regolith interface for particles released from disposal rooms, as well as recharge locations for the pumped wells (Figure 4-5 through Figure 4-16). The overview has the following organisation of figures: a) map of well location, b) SFR 1 exit locations, c) SFR 3 exit locations, d) well recharge locations.

Interactions are likely to be found where exit locations and recharge locations overlap or cross-over. For example, well 1 is located north of biosphere object 116 (also referred to as Charlie's lake) and its recharge locations are concentrated to a nearby hilltop, to the east of well 1 (Figure 4-5a and d). The forward particle trajectories from SFR 1 and SFR 3, on the other hand, do not cross north of biosphere object 116 (Figure 4-5b and c), and hence the simulated well interaction is negligible.

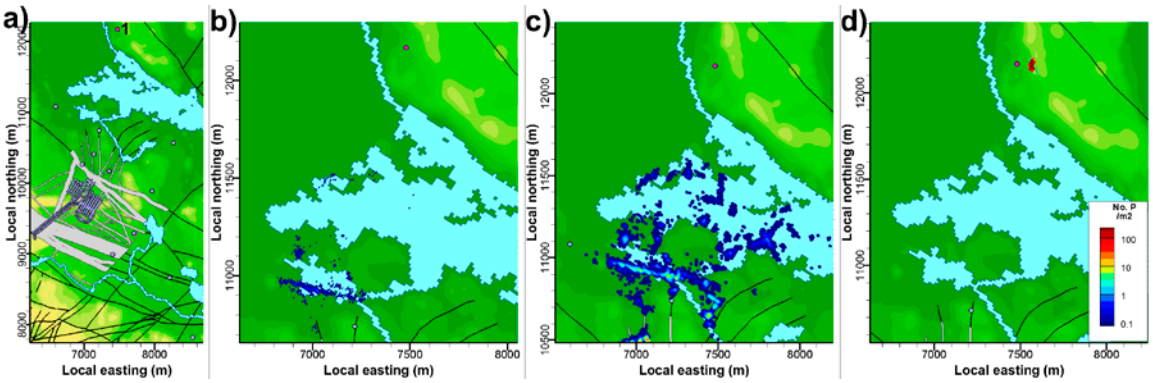


*Figure 4-5. Particle-tracking results for well 1; a) map of well location, b) exit locations for particles released within SFR 1 disposal rooms, c) corresponding exit locations for SFR 3, and d) recharge locations for well production.*

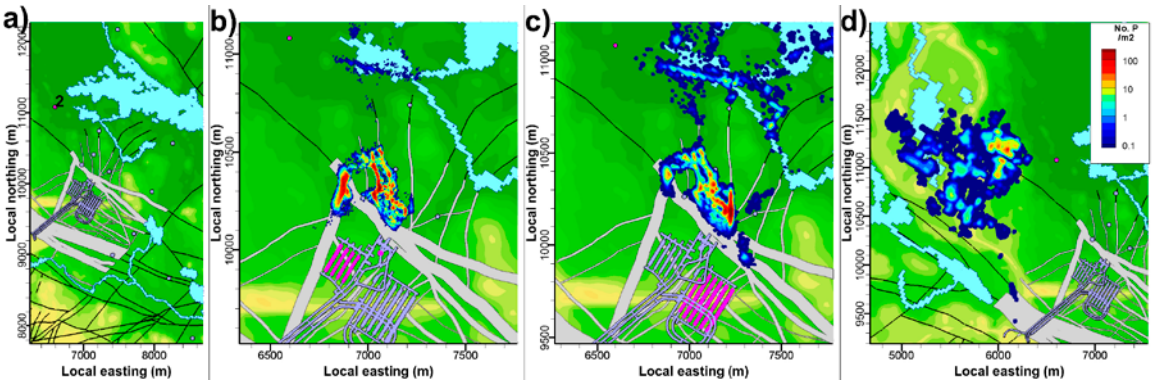


*Figure 4-6. Particle-tracking results for well 2; a) map of well location, b) exit locations for particles released within SFR 1 disposal rooms, c) corresponding exit locations for SFR 3, and d) recharge locations for well production.*

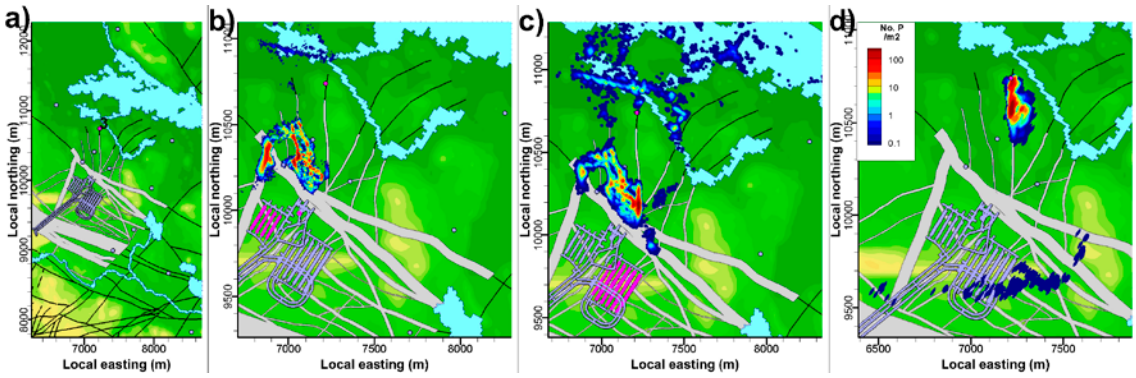


***Figure 4-7.*** *Particle-tracking results for well 3; a) map of well location, b) exit locations for particles released within SFR 1 disposal rooms, c) corresponding exit locations for SFR 3, and d) recharge locations for well production.*

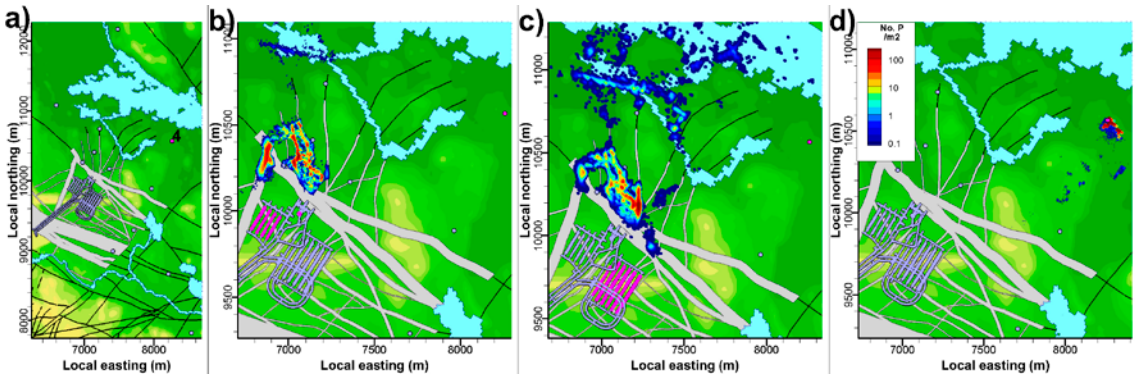


***Figure 4-8.*** *Particle-tracking results for well 4; a) map of well location, b) exit locations for particles released within SFR 1 disposal rooms, c) corresponding exit locations for SFR 3, and d) recharge locations for well production.*

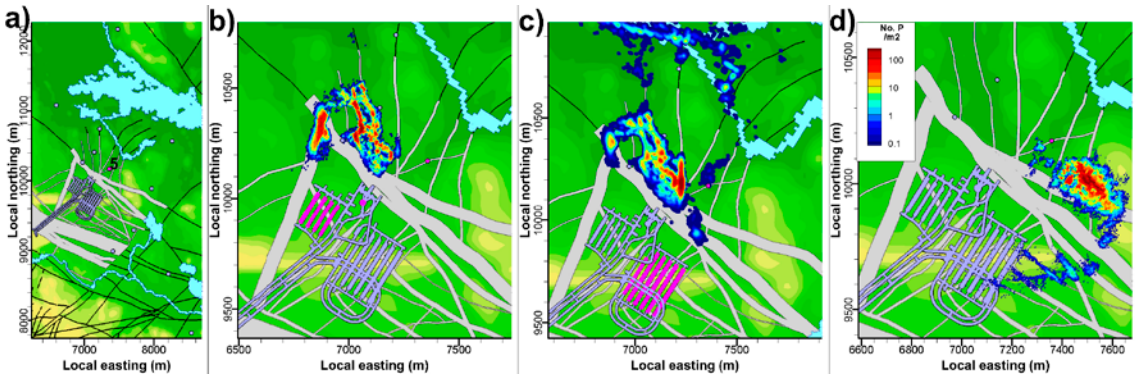


***Figure 4-9.*** *Particle-tracking results for well 5; a) map of well location, b) exit locations for particles released within SFR 1 disposal rooms, c) corresponding exit locations for SFR 3, and d) recharge locations for well production.*

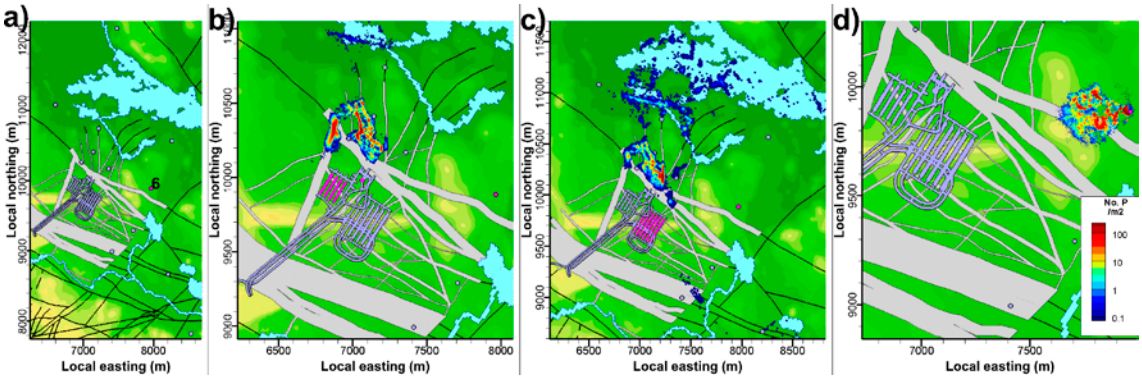


***Figure 4-10.*** *Particle-tracking results for well 6; a) map of well location, b) exit locations for particles released within SFR 1 disposal rooms, c) corresponding exit locations for SFR 3, and d) recharge locations for well production.*

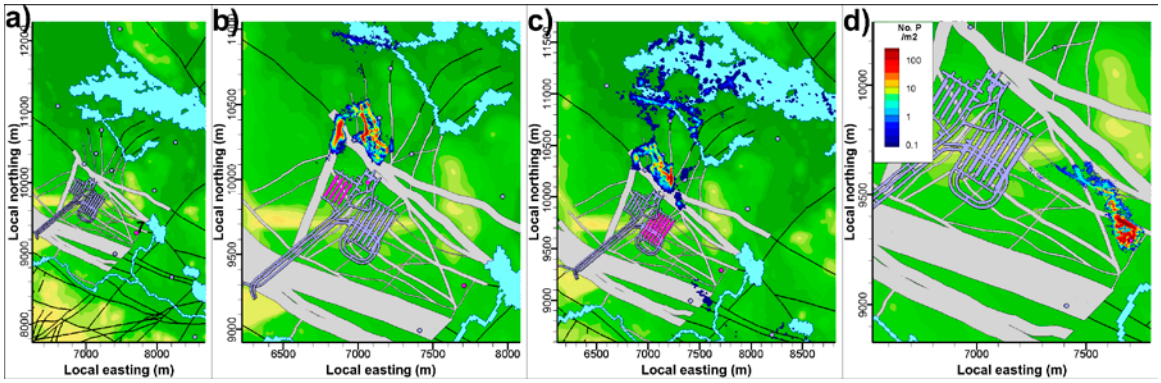


***Figure 4-11.*** *Particle-tracking results for well 7; a) map of well location, b) exit locations for particles released within SFR 1 disposal rooms, c) corresponding exit locations for SFR 3, and d) recharge locations for well production.*

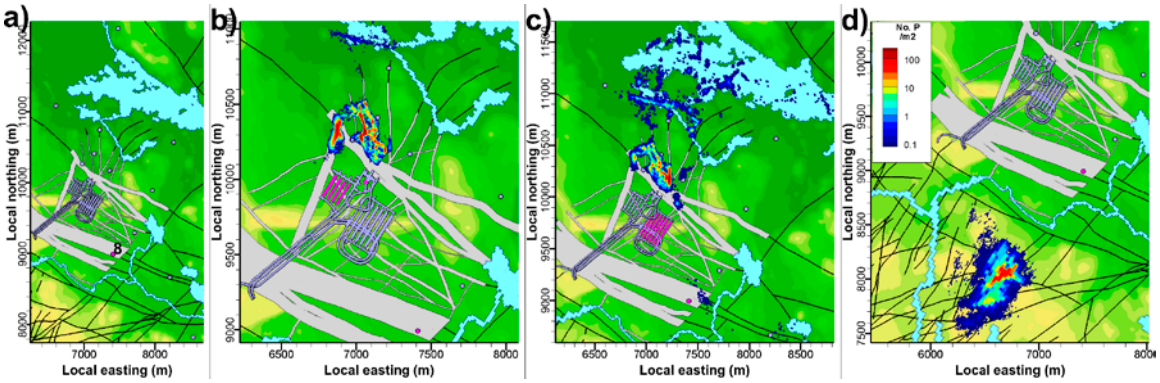


***Figure 4-12.*** *Particle-tracking results for well 8; a) map of well location, b) exit locations for particles released within SFR 1 disposal rooms, c) corresponding exit locations for SFR 3, and d) recharge locations for well production.*

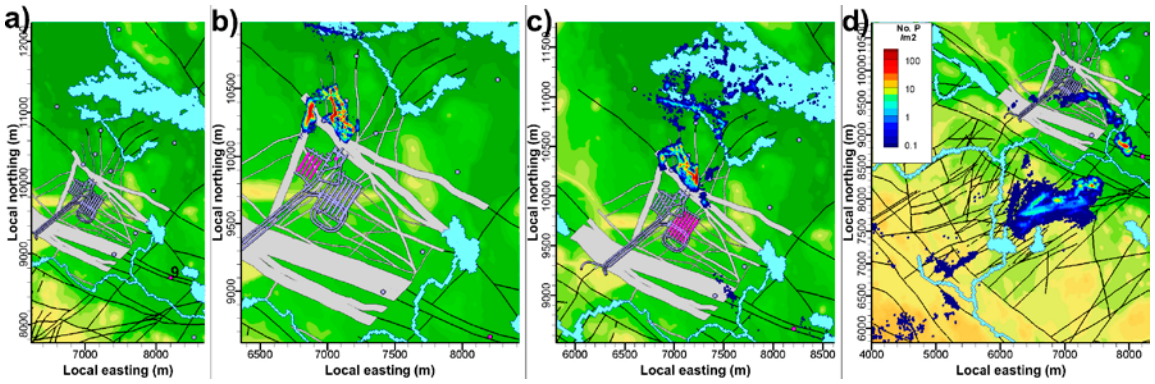


***Figure 4-13.*** *Particle-tracking results for well 9; a) map of well location, b) exit locations for particles released within SFR 1 disposal rooms, c) corresponding exit locations for SFR 3, and d) recharge locations for well production.*

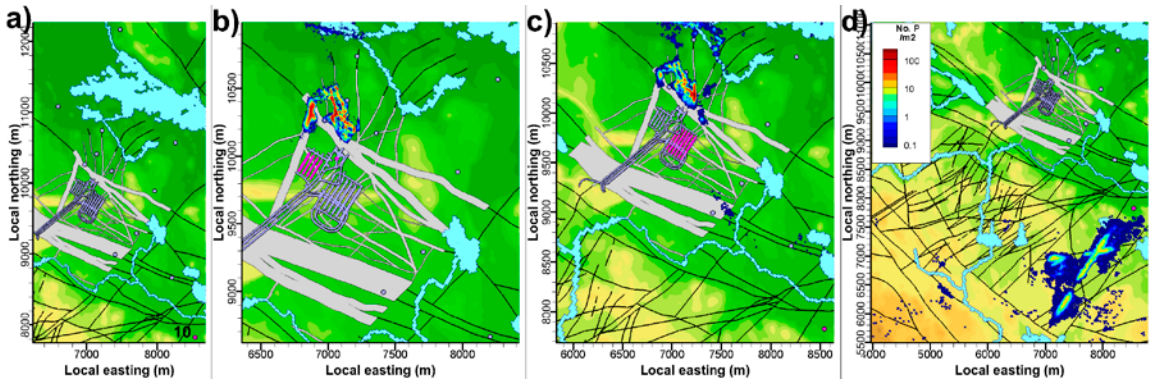


***Figure 4-14.*** *Particle-tracking results for well 10; a) map of well location, b) exit locations for particles released within SFR 1 disposal rooms, c) corresponding exit locations for SFR 3, and d) recharge locations for well production.*

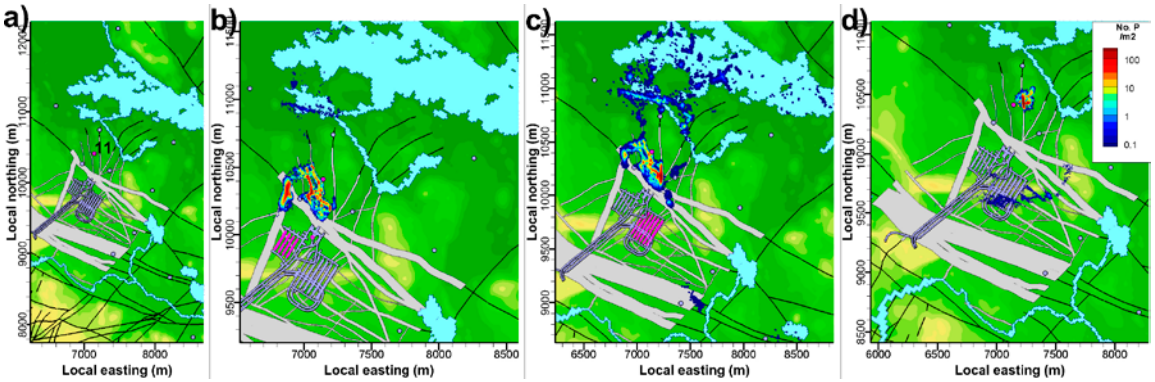


***Figure 4-15.*** *Particle-tracking results for well 11; a) map of well location, b) exit locations for particles released within SFR 1 disposal rooms, c) corresponding exit locations for SFR 3, and d) recharge locations for well production.*

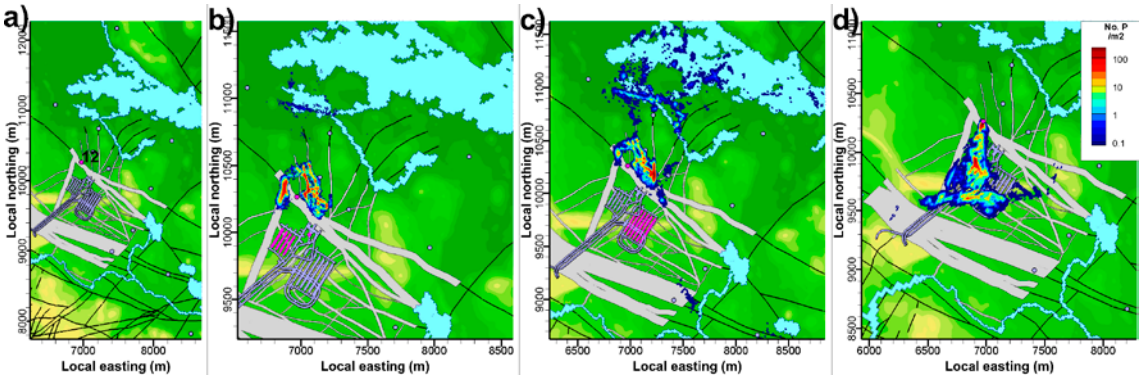


***Figure 4-16.*** *Particle-tracking results for well 12; a) map of well location, b) exit locations for particles released within SFR 1 disposal rooms, c) corresponding exit locations for SFR 3, and d) recharge locations for well production.*

Among the water-supply wells associated to hypothetical settlements, well 11 has interactions with both SFR 1 and SFR 3, whereas wells 3 and 5 only have interactions with SFR 3. As expected, well 12, which is located in the well-interaction area, stands out in Subtask A with high interactions (Table 4-8).

**Table 4-8. Interaction between disposal facilities and wells in Subtask A.**

| Well | Facility | Disp. room | Forward tracking | | | Backward tracking | |
|---|---|---|---|---|---|---|---|
| | | | Released | Captured | | Flow ratio | |
| | | | No. particles | No. particles | $f_{ij}$ | $Q_j/Q_i$ | $f_{ji}$ |
| **3** | SFR 3 | 2BLA | | 0 | – | 5.8 | 0.0002% |
| | | 3BLA | 169,697 | 6 | 0.004% | 6.8 | 0.0004% |
| | | 4BLA | 169,204 | 5 | 0.003% | 7.6 | 0.0001% |
| | | 5BLA | 165,794 | 4 | 0.002% | 9.0 | 0.0001% |
| | | 2BMA | 213,510 | 4 | 0.002% | 6.2 | 0.001% |
| | | 1BRT | 110,240 | 2 | 0.002% | 9.1 | – |
| **5** | SFR 3 | 3BLA | 169,829 | 2 | 0.001% | 6.8 | – |
| | | 4BLA | 168,604 | 4 | 0.002% | 7.6 | 0.001% |
| | | 5BLA | 166,498 | 35 | 0.021% | 9.0 | 0.002% |
| | | 2BMA | 213,614 | 195 | 0.091% | 6.2 | 0.012% |
| **11** | SFR 1 | 1BTF | 131,287 | 2 | 0.002% | 7.1 | 0.0001% |
| | | 2BTF | 144,823 | 1 | 0.001% | 4.9 | – |
| | | Silo | 254,256 | 23 | 0.009% | 175.8 | 0.0003% |
| | SFR 3 | 2BLA | 171,296 | 203 | 0.119% | 5.8 | 0.016% |
| | | 3BLA | 169,640 | 292 | 0.172% | 6.8 | 0.021% |
| | | 4BLA | 168,674 | 171 | 0.101% | 7.6 | 0.008% |
| | | 5BLA | 166,652 | 94 | 0.056% | 9.0 | 0.005% |
| | | 2BMA | 213,974 | 92 | 0.043% | 6.2 | 0.007% |
| | | 1BRT | 109,764 | 95 | 0.087% | 9.1 | 0.011% |
| **12** | SFR 1 | 1BTF | 130,914 | 30,134 | 23.02% | 7.1 | 2.80% |
| | | 2BTF | 144,899 | 46,076 | 31.80% | 4.9 | 6.02% |
| | | 1BLA | 185,613 | 58,064 | 31.28% | 1.4 | 18.98% |
| | | 1BMA | 284,636 | 47,497 | 16.69% | 2.6 | 5.18% |
| | | Silo | 253,938 | 3,618 | 1.43% | 175.2 | 0.007% |
| | SFR 3 | 2BLA | 171,891 | 2,900 | 1.69% | 5.8 | 0.25% |
| | | 3BLA | 169,615 | 713 | 0.420% | 6.8 | 0.058% |
| | | 4BLA | 168,177 | 185 | 0.110% | 7.5 | 0.008% |
| | | 5BLA | 166,445 | 72 | 0.043% | 9.0 | 0.006% |
| | | 2BMA | 213,774 | 77 | 0.036% | 6.2 | 0.006% |
| | | 1BRT | 110,098 | 6,128 | 5.57% | 9.1 | 0.52% |

As discussed in Section 3.4, particles are distributed proportionally to disposal-room volume. A comparison between the two types of interactions, those determined by forward tracking, $f_{ij}$, and those determined by backward tracking, $f_{ji}$, requires consideration to the flow ratio between $Q_j$, the water abstraction from a well, $j$ = 1 to 12, and $Q_i$, the cross flow of disposal-room $i$ = 1 to 11. Hence, the flow ratio, $Q_j/Q_i$, is presented along with both types of evaluated interaction, $f_{ij}$ and $f_{ji}$, in Table 4-8.

Neither of the wells 3, 5, 11, and 12 have a cross-flow term during pumped conditions (Table 4-5), and therefore, forward-tracking results, re-scaled by the flow ratio according to Equation (3-2), are more or less identical to backward-tracking results (Figure 4-17 and Figure 4-18).

### 4.3.2 Variable production rates in Subtask B

The analysis of variable pumping rates in well 12 provides further insight into how dilution affects the determined interactions.

*Forward*-tracked interactions (i.e. the fraction of particles released within disposal facilities that reach well 12) strictly increases with higher production rate (Figure 4-19). This finding is in line with expectations, as larger pumping rates will expand the cone of depression and re-direct a larger fraction of flow towards the well. However, as discussed in Section 3.4, the forward tracking does not account for the increasing dilution in the abstracted water, as higher pumping rates also increase flow that do not cross the disposal facilities. The dilution effects in the abstracted water must be demonstrated by means of back-tracked interactions.

*Backward*-tracked interactions, i.e. the fraction of particles in abstracted water that originate via flow paths that cross disposal rooms, exhibits a clearly different relation to pumping rate (Figure 4-20). The increasing pumping rates decrease back-tracked interactions, at least for the SFR 1 rock vaults, where interactions were high under the initial 700 L/d pumping rate (e.g. 1BLA). This signifies increased dilution, i.e. the increased inflow via rock vaults observed during forward tracking is proportionally less than the increase in abstraction rate. In other disposal rooms, where interactions are low under the initial 700 L/d pumping rate (i.e. the Silo and most disposal rooms in SFR 3), a modest increase can be observed with higher abstraction rate. This signifies, vice-versa, that the increasing flow via these disposal rooms is proportionally larger in relation to the increasing abstraction rate. It is not fully clear why, but may indicate that the impact on the flow field towards the well is asymmetrical, possibly due to bedrock heterogeneity.

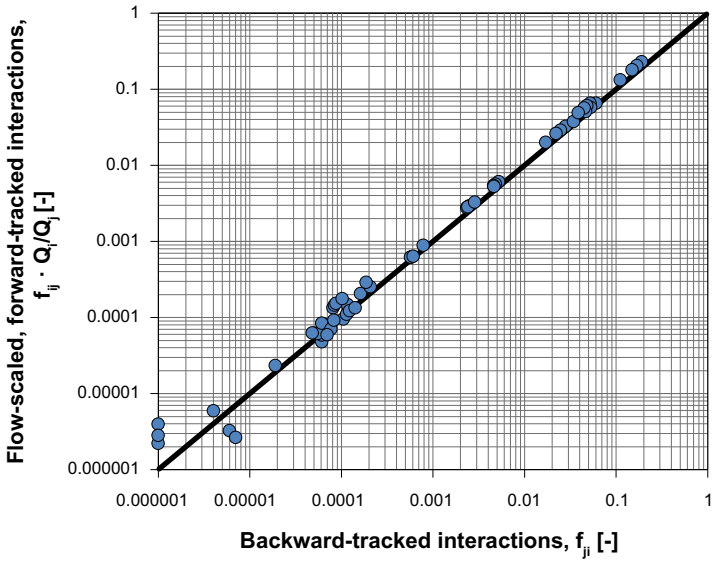


***Figure 4-17.*** *Interactions between disposal rooms and water-supply wells; flow-scaled fraction of forward-tracked trajectories from disposal rooms to wells, $f_{ij} \cdot Q_i/Q_j$ versus fraction of backward-tracked trajectories from wells to disposal rooms, $f_{ji}$, (four values omitted, indicated by '–' in Table 4-8).*

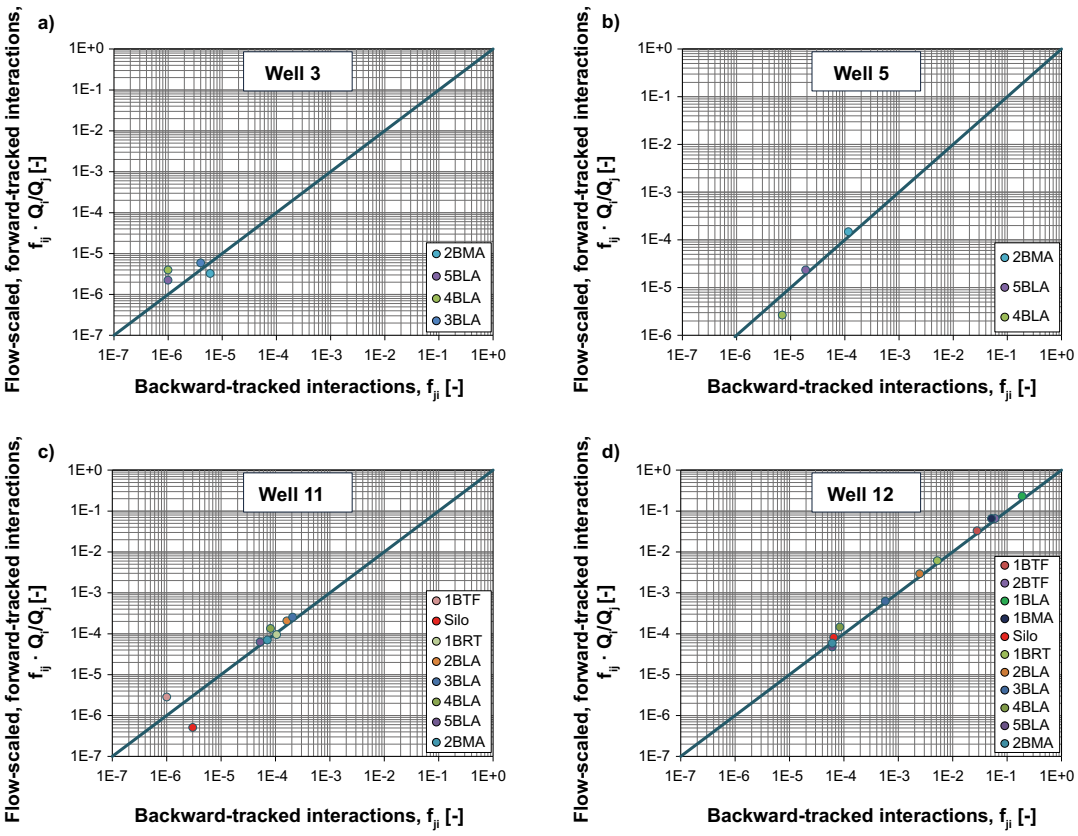


***Figure 4-18.*** *Interactions between disposal rooms and water-supply wells; flow-scaled fraction of forward-tracked trajectories from disposal rooms to wells, $f_{ij} \cdot Q_i/Q_j$, versus fraction of backward-tracked trajectories from wells to disposal rooms, $f_{ji}$ (four values omitted, indicated by '–' in Table 4-8).*

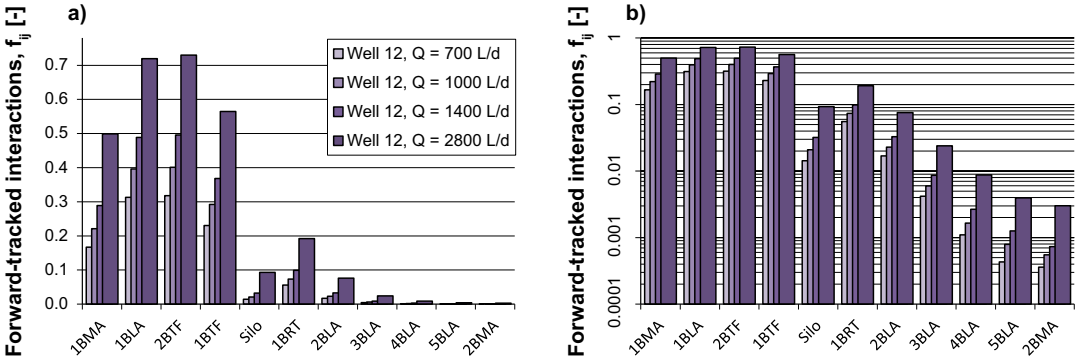


***Figure 4-19.*** *Fraction of particles reaching well 12 for forward tracking from disposal rooms; a) linear scale and b) logarithmic scale.*

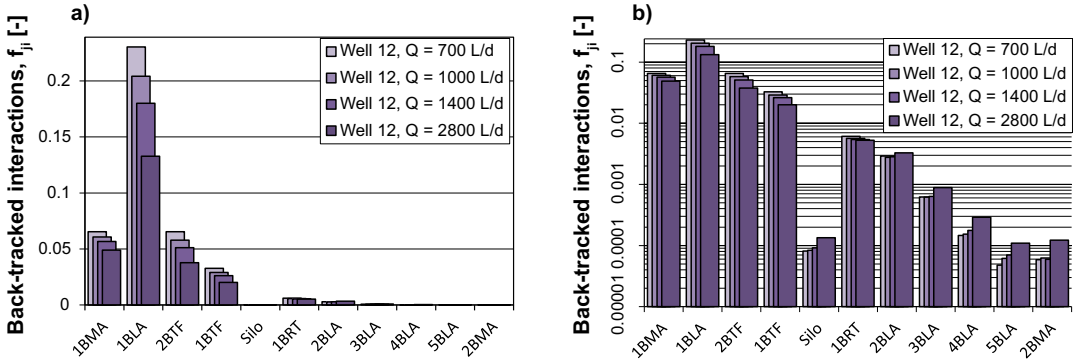


***Figure 4-20.*** *Fraction of particles with upstream flow paths passing disposal rooms, obtained by backward particle tracking from well 12; a) linear scale and b) logarithmic scale.*

The proportionality between flow-scaled (i.e. multiplied by the ratio $Q_i/Q_j$) forward interaction and back-tracked interaction, according to Equation (3-2), can be confirmed (Figure 4-21a). However, it can be noted that the interaction values as determined from flow-scaled forward tracking are on average c 20% higher, which is interpreted to reflect the limitation in accuracy (cf. Table 4-10 and Table 4-11).

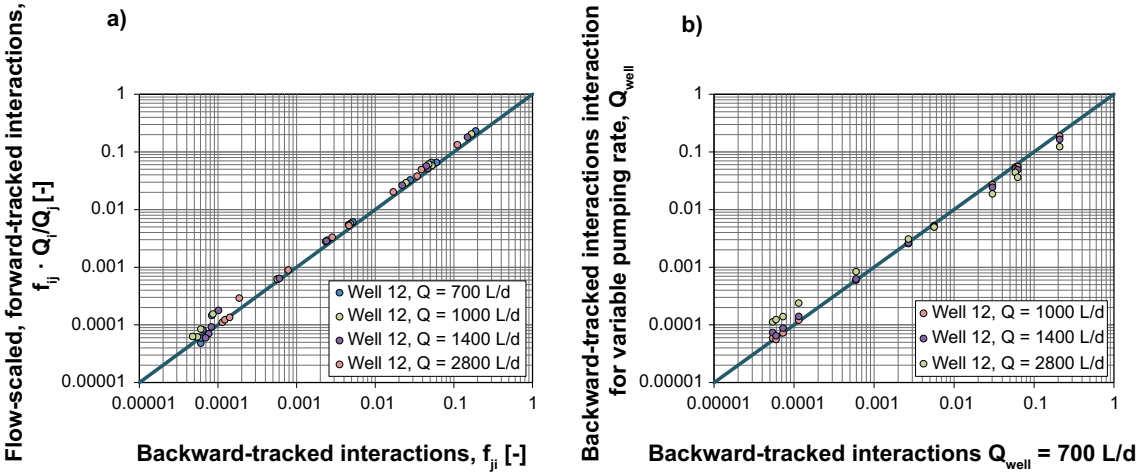


***Figure 4-21.*** *Back-tracked interactions and variable pumping rate in well 12; a) backward tracking from well 12, versus flow-scaled forward tracking from facilities, and b) different production rates, versus the original 700 L/d rate.*

**Table 4-9. Forward-tracked interactions, $f_{ij}$ [–], with variable pumping rates in well 12.**

| Tunnel\\$Q_{well}$ [L/d] | 700 | 1000 | 1400 | 2800 |
|---|---|---|---|---|
| 1BTF | 23% | 29% | 37% | 56% |
| 2BTF | 32% | 40% | 50% | 73% |
| 1BLA | 31% | 40% | 49% | 72% |
| 1BMA | 17% | 22% | 29% | 50% |
| Silo | 1.4% | 2.1% | 3.2% | 9.3% |
| 1BRT | 5.6% | 7.4% | 9.9% | 19% |
| 2BLA | 1.7% | 2.3% | 3.3% | 7.6% |
| 3BLA | 0.4% | 0.6% | 0.86% | 2.4% |
| 4BLA | 0.1% | 0.2% | 0.3% | 0.87% |
| 5BLA | 0.04% | 0.08% | 0.1% | 0.4% |
| 2BMA | 0.04% | 0.06% | 0.07% | 0.3% |

**Table 4-10. Flow-scaled forward-tracked interactions, $f_{ij} \cdot Q_i/Q_j$ [–], with variable pumping rates in well 12.**

| Tunnel\$Q_{well}$ [L/d] | 700 | 1000 | 1400 | 2800 |
|---|---|---|---|---|
| 1BTF | 3.3% | 2.9% | 2.6% | 2.0% |
| 2BTF | 6.5% | 5.8% | 5.1% | 3.8% |
| 1BLA | 23% | 20% | 18% | 13% |
| 1BMA | 6.5% | 6.1% | 5.7% | 4.9% |
| Silo | 0.008% | 0.008% | 0.009% | 0.013% |
| 1BRT | 0.61% | 0.56% | 0.54% | 0.53% |
| 2BLA | 0.29% | 0.28% | 0.28% | 0.33% |
| 3BLA | 0.062% | 0.062% | 0.064% | 0.089% |
| 4BLA | 0.015% | 0.015% | 0.018% | 0.029% |
| 5BLA | 0.005% | 0.006% | 0.007% | 0.011% |
| 2BMA | 0.006% | 0.006% | 0.006% | 0.012% |

**Table 4-11. Back-tracked interactions, $f_{ji}$ [–], with variable pumping rates in well 12.**

| Tunnel\$Q_{well}$ [L/d] | 700 | 1000 | 1400 | 2800 |
|---|---|---|---|---|
| 1BTF | 2.8% | 2.5% | 2.2% | 1.7% |
| 2BTF | 6.0% | 5.3% | 4.7% | 3.4% |
| 1BLA | 19% | 17% | 15% | 11% |
| 1BMA | 5.2% | 4.8% | 4.5% | 3.9% |
| Silo | 0.007% | 0.006% | 0.008% | 0.014% |
| 1BRT | 0.52% | 0.48% | 0.46% | 0.46% |
| 2BLA | 0.25% | 0.23% | 0.24% | 0.29% |
| 3BLA | 0.058% | 0.057% | 0.061% | 0.079% |
| 4BLA | 0.008% | 0.009% | 0.010% | 0.019% |
| 5BLA | 0.006% | 0.006% | 0.008% | 0.011% |
| 2BMA | 0.006% | 0.005% | 0.007% | 0.012% |

### 4.3.3 Wells in the well-interaction area in Subtask C

Forward particle tracking to the additional wells 21 to 28 provides a deeper insight to the pattern of well interactions in the well-interaction area (Figure 1-3). Altogether, none of the wells 21 to 28 exceed well 12 in terms of total interaction strength. In particular, well 12 stands out with exceptionally high forward-tracked interactions from the four rock caverns of SFR 1 (Table 4-12). On the other hand, wells 23, 25, 26, and 27 all exceed well 12 in terms of interactions with the Silo, as well as in terms of total interaction strength with the disposal rooms of SFR 3.

A common factor for the wells with highest interactions (wells 12, 23, 25, 26, and 27) is that they enclose an area just northeast of deformation zone ZFMNW0805A/B (Figure 4-22). Wells 24 and 28, located in ZFMNNE0869, have essentially no interactions with the Silo or any disposal room of SFR 3. On the contrary, wells 21 and 22, which are located southeast of ZFMNE0870, have essentially no interactions with any disposal room of SFR 1 (deformation zone ZFMNE0870 is parallel to the access tunnels and terminates against ZFMNW0805A/B near the Silo, see Figure 4-22).

Based on earlier confirmations on the agreement between flow-scaled forward-tracking and backtracked interactions (Sections 4.3.1 and 4.3.2), the backward particle tracking was considered redundant for the analysis in Subtask C. Instead, scaling the results by the flow ratio, $Q_i/Q_j$, is therefore considered adequate for addressing dilution aspects (Table 4-13). The effect of flow-ratio dilution in wells can be observed by comparing Table 4-12 and Table 4-13. For example, owing to the technical barriers in the Silo it has an exceptionally low cross flow, and in turn, the dilution is particularly strong for silo interactions (c.f. Table 4-12 and Table 4-13).

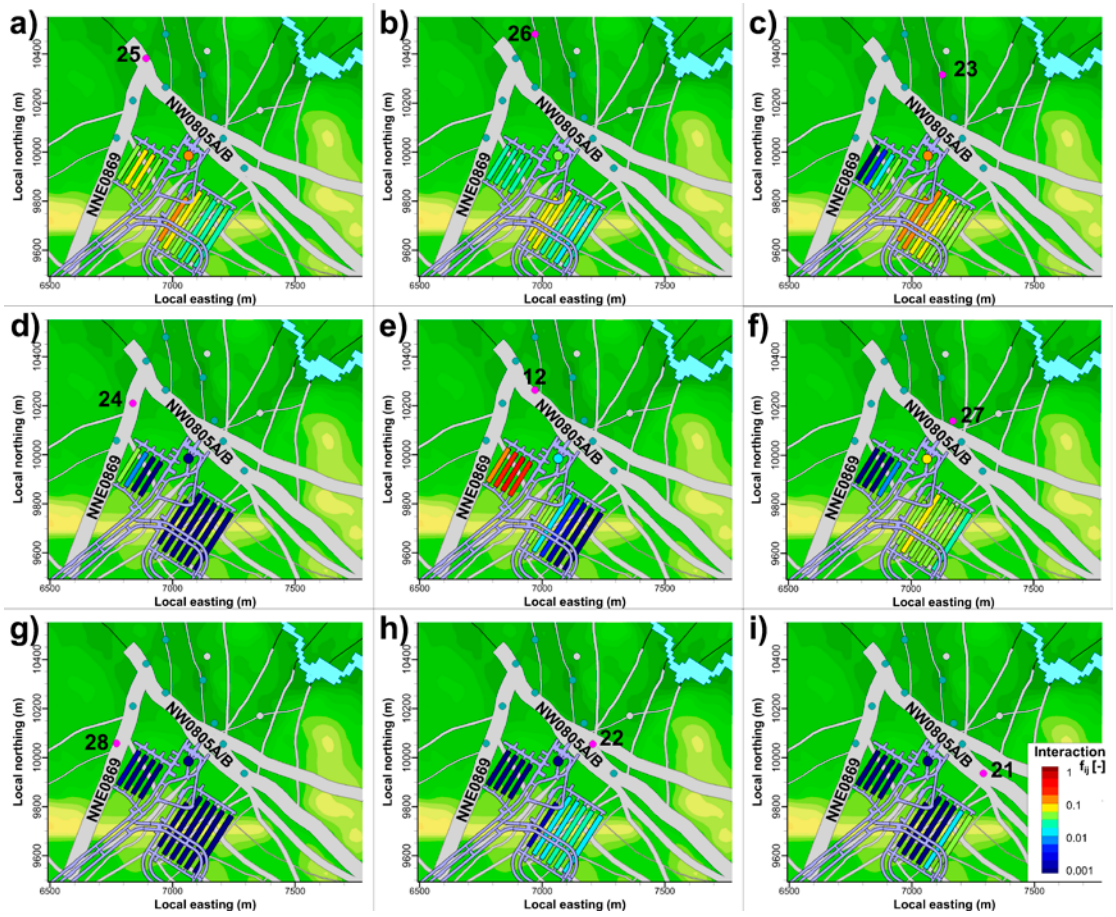


***Figure 4-22.*** *Fraction of particles, which are uniformly released in disposal rooms of SFR 1 and SFR 3, that reach water-supply wells in the well-interaction area, $f_{ij}$ [–].*

**Table 4-12. Forward-tracked interactions in well-interaction area, $f_{ij}$ [%].**

| Well | 1BMA | 1BLA | 2BTF | 1BTF | Silo | 1BRT | 2BLA | 3BLA | 4BLA | 5BLA | 2BMA |
|---|---|---|---|---|---|---|---|---|---|---|---|
| **12** | 17 | 31 | 32 | 23 | 1.4 | 5.6 | 1.7 | 0.42 | 0.11 | 0.043 | 0.036 |
| **21** | <0.001 | <0.001 | <0.001 | <0.001 | <0.001 | <0.001 | 0.001 | 0.024 | 0.091 | 1.2 | 4.2 |
| **22** | <0.001 | <0.001 | <0.001 | <0.001 | <0.001 | 0.10 | 1.04 | 1.36 | 2.0 | 2.1 | 1.3 |
| **23** | 0.015 | 0.48 | 1.4 | 5.4 | 17 | 12 | 12 | 9.8 | 6.3 | 3.8 | 3.3 |
| **24** | 4.9 | 0.85 | 0.030 | <0.001 | <0.001 | <0.001 | <0.001 | <0.001 | <0.001 | <0.001 | <0.001 |
| **25** | 4.7 | 6.2 | 5.8 | 4.8 | 10 | 13 | 9.3 | 4.4 | 2.5 | 1.8 | 2.0 |
| **26** | 1.8 | 2.4 | 2.3 | 2.0 | 5.4 | 8.5 | 6.2 | 3.2 | 2.0 | 1.6 | 1.9 |
| **27** | <0.001 | <0.001 | 0.008 | 0.73 | 6.6 | 3.4 | 6.5 | 4.5 | 4.4 | 3.9 | 2.1 |
| **28** | 0.11 | 0.006 | <0.001 | <0.001 | <0.001 | <0.001 | <0.001 | <0.001 | <0.001 | <0.001 | <0.001 |

**Table 4-13. Flow-scaled forward interactions in well-interaction area, $f_{ij} \cdot Q_i/Q_j$ [%].**

| Well | 1BMA | 1BLA | 2BTF | 1BTF | Silo | 1BRT | 2BLA | 3BLA | 4BLA | 5BLA | 2BMA |
|---|---|---|---|---|---|---|---|---|---|---|---|
| **12** | 7 | 23 | 7 | 3 | 0.01 | 0.6 | 0.29 | 0.06 | 0.01 | 0.005 | 0.006 |
| **21** | 0 | 0 | 0 | 0 | 0 | <0.001 | <0.001 | 0.003 | 0.012 | 0.1 | 0.7 |
| **22** | 0 | 0 | 0 | 0 | 0 | 0.01 | 0.18 | 0.20 | 0.3 | 0.2 | 0.2 |
| **23** | 0.006 | 0.35 | 0.3 | 0.8 | 0.10 | 1 | 2 | 1.45 | 0.8 | 0.4 | 0.5 |
| **24** | 1.9 | 0.63 | 0.006 | 0 | 0 | <0.001 | 0 | 0 | 0 | 0 | 0 |
| **25** | 1.8 | 4.5 | 1.2 | 0.7 | 0.06 | 1 | 1.6 | 0.65 | 0.3 | 0.2 | 0.3 |
| **26** | 0.7 | 1.8 | 0.5 | 0.3 | 0.03 | 0.9 | 1.1 | 0.5 | 0.3 | 0.2 | 0.3 |
| **27** | 0 | 0 | 0.002 | 0.1 | 0.04 | 0.4 | 1.1 | 0.7 | 0.6 | 0.4 | 0.3 |
| **28** | 0.04 | 0.005 | 0 | 0 | 0 | 0 | 0 | 0 | 0 | 0 | 0 |

In general, somewhat lower cross flows are simulated for the disposal rooms of SFR 3 (Table 4-8), and consequently, the interactions from SFR 3 are subject to a comparatively higher degree of dilution in wells, relative to those from SFR 1. Therefore, based on the outlook of flow-scaled data, well 12 certainly stands out in terms of SFR 1 interactions, particularly with regard to 1BLA that also has the highest cross flow (Figure 4-23). However, it must be emphasised that this pattern in relative disposal-room cross flows is not entirely of general character, but depends on the underlying bedrock parameterisation variant (e.g. Figure 2-3). In particular, the magnitudes in disposal-room cross flows is largely controlled by the local parameterisation at intersections between deformation zones and disposal rooms. The present study is based on the Base-case parameterisation, in which the 1BLA intersection with ZFMNNW1209 is parameterized as highly transmissive, whereas deformation-zone intersections with SFR 3 disposal rooms are parameterized as less transmissive (Figure 2-4).

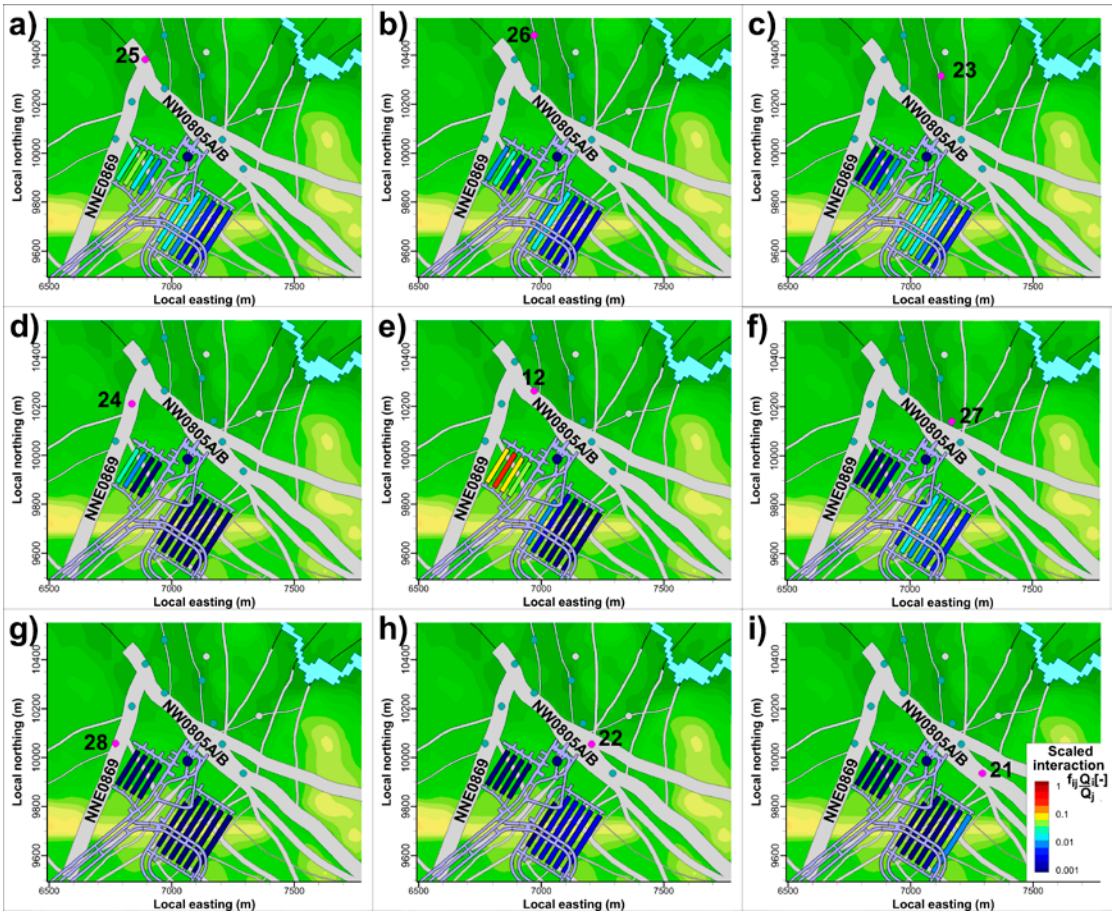


***Figure 4-23.*** *Flow-scaled fraction of particles, which are uniformly released in disposal rooms of SFR1 and SFR3, that reach water-supply wells in the well-interaction area, $f_{ij} \cdot Q_i/Q_j$[–].*

# 5 Summary and conclusions

This document presents an analysis of potential future water-supply wells which is part of the radiological safety assessment for the SFR repository after closure (the SR-PSU project). The groundwater flow model that was developed in SDM-PSU is used as a numerical tool to assess flow-path interactions between the backfilled repository (i.e. the existing SFR 1, as well as its planned extension, SFR 3) and potential water-supply wells.

SFR is hosted in a dynamic hydrogeological setting, which is induced by the ongoing shore-line displacement (Öhman et al. 2014). The current study addresses the time slice 5000 AD, which is a stage of shoreline retreat when areas of arable land have recently emerged from the sea and the groundwater flow regime has reached a more or less stationary state (unaffected by further shoreline retreat). The simulations employ a model setup that was defined as the "Base case" in the preceding sensitivity analysis in which the combined effects of heterogeneity and uncertainty in bedrock parameterisation were addressed (Öhman et al. 2014). The output of this study, combined with the previous simulation results, will facilitate dose assessments that can be related to radionuclide transport to water-supply wells.

The specific objectives of TD12 were to study:

(1) The influence that the water abstraction from water-supply wells may have on groundwater flow through the facility (SFR 1 and SFR 3).

(2) Groundwater-flow interaction between the facility (SFR 1 and SFR 3) and water-supply wells.

The analysed well locations fall into two categories: 1) water-supply wells for settlements associated to potential arable land and 2) wells drilled in the well-interaction area downstream from SFR, i.e. the area where the highest radionuclide concentrations originating from SFR can be expected. The wells for settlements associated to areas of arable land (Figure 1-2) are located where the bedrock is sufficiently conductive for sustaining the assumed water demand of a self-sustaining community of modern farmers, 700 L/d.

The results demonstrate that for all wells associated to potential arable land, both the influences on disposal-room cross flow and groundwater-flow interactions are very small (i.e. wells 1 to 11; Table 4-7). Owing to the remote emplacements of many wells, these results are in line with expectations.

Water abstraction from wells in the well-interaction area, wells 12 to 28, has a small, but noticeable effect on the flow through disposal rooms of SFR 1 and SFR 3. However, the influence of the water abstraction does not exceed 1% for any disposal room for the water abstraction rate of 700 L/d; Table 4-7). The highest influence on disposal-room cross flow is 1.4%, which occurs for an abstraction rate of 2,800 L/d from well 12. For this well, the influence on disposal-room cross flow is directly proportional to the water abstraction rate (Figure 4-4), suggesting that the principle of superpositioning applies.

Well interactions are determined by means of a particle-tracking approach that is described in Öhman et al. (2014). It is confirmed that either particle-tracking direction can be used in the determination of well interaction (i.e. upstream or downstream the direction of flow); forward-tracking and backward-tracking output are interchangeable in terms of "flow-ratio scaling", $Q_i/Q_j$, where $Q_i$ is the disposal-room cross flow and $Q_j$ is the well abstraction, Equation (3-2). In physical terms, flow-ratio scaling corresponds to the dilution in pumped water from a well. For example, the technical barriers render a very low cross flow in the Silo, which implies that the silo interaction in a downstream well is subject to strong dilution, i.e. even if 17% of the Silo cross flow reaches well 23 (Table 4-12), only 0.1% of the abstracted water from well 23 has passed through the Silo (Table 4-13).

This study employs crude geometrical representations of the studied wells, where each well is represented by the computational cells intersected by the well trajectory (i.e. no local grid refinement is employed; Section 3.1). A potential additional dilution component is therefore discussed for the water pumped from wells, which is referred to as the cross-flow term for well cells (Section 4.2.2). This refers to the flow across those cells that have been identified as part of a well, but where the flow is not induced by pumping. In other words, the total inflow into these well cells may exceed the prescribed abstraction rate (Table 4-5 and Table 4-6). Accounting for this type of dilution implies that flow-ratio scaling should not apply to the production rate, but to the larger total inflow into well cells. On the one hand, a well drilled into the bedrock may short-circuit the hydraulic connectivity between structures and induce a natural-driven flow along the well, causing dilution of the water inside the well. On the other hand, this effect is likely to be highly exaggerated owing to the coarse discretisation of well cells. It is therefore difficult to clearly state if the simulated cross-flow terms are realistic. Fortunately, the wells most strongly associated to well interactions have low or none cross-flow terms.

The highest interactions in the well-interaction area are found in an area just northeast of deformation zone ZFMNW0805A/B (Figure 4-22). Wells located in ZFMNNE0869 or southeast of ZFMNE0870 demonstrate considerably less interactions. Well 12 has the highest interactions with disposal rooms in SFR 1, a finding which is accentuated in terms of flow-scaled interactions (Figure 4-23), particularly with regard to disposal room 1BLA.

It should be emphasized that interpretations based on flow-scaled interaction output, concerning the relative interaction strengths between the different disposal rooms of SFR 1 and SFR 3, requires consideration of the uncertainty in disposal-room cross flow related to bedrock parameterisation (e.g. Figure 2-3). In other words, care must be taken not to overgeneralise simulation output based on a single bedrock parameterisation variant, as disposal-room cross flow is largely controlled by the local parameterisation at intersections between deformation zones and disposal rooms.

# References

SKB's (Svensk Kärnbränslehantering AB) publications can be found at www.skb.se/publications. References to SKB's unpublished documents are listed separately at the end of the reference list. Unpublished documents will be submitted upon request to document@skb.se.


**Axelsson C-L, Byström J, Eriksson Å, Holmén J, Haitjema H M, 1991.** Hydraulic evaluation of the groundwater conditions at Finnsjön. The effects on dilution in a domestic well. SKB TR 91-54, Svensk Kärnbränslehantering AB.

**Brydsten L, Strömgren M, 2013.** Landscape development in the Forsmark area from the past into the future (8500 BC – 40,000 AD). SKB R-13-27, Svensk Kärnbränslehantering AB.

**Dershowitz W, Winberg A, Hermanson J, Byegård J, Tullborg E-L, Andersson P, Mazurek M, 2003.** Äspö Hard Rock Laboratory. Äspö Task Force on modelling of groundwater flow and transport of solutes. Task 6c. A semi-synthetic model of block scale conductive structures at the Äspö HRL. SKB IPR-03-13, Svensk Kärnbränslehantering AB.

**Follin S, 2008.** Bedrock hydrogeology Forsmark. Site descriptive modelling, SDM-Site Forsmark. SKB R-08-95, Svensk Kärnbränslehantering AB.

**Gentzschein B, Levén J, Follin S, 2007.** A comparison between well yield data from the site investigation in Forsmark and domestic wells in northern Uppland. SKB P-06-53, Svensk Kärnbränslehantering AB.

**Joyce S, Simpson T, Hartley L, Applegate D, Hoek J, Jackson P, Swan D, Marsic N, Follin S, 2010.** Groundwater flow modelling of periods with temperate climate conditions – Forsmark. SKB R-09-20, Svensk Kärnbränslehantering AB.

**Saetre P, Ekström P-A, Nordén S, Keesman S, 2013.** The biosphere model for radionuclide transport and dose assessment in SR-PSU. SKB TR-13-46, Svensk Kärnbränslehantering AB.

**SKB, 2008.** Geovetenskapligt undersökningsprogram för utbyggnad av SFR. SKB R-08-67, Svensk Kärnbränslehantering AB. (In Swedish.)

**SKB, 2013.** Site description of the SFR area at Forsmark at completion of the site investigation phase, SDM-PSU Forsmark. SKB TR-11-04, Svensk Kärnbränslehantering AB.

**SKB, 2014.** Initial state report for the safety assessment SR-PSU. SKB TR-14-02, Svensk Kärnbränslehantering AB.

**Svensson U, Ferry M, 2010.** Darcy Tools version 3.4. User's guide. SKB R-10-72, Svensk Kärnbränslehantering AB.

**Svensson U, Ferry M, Kuylenstierna H-O, 2010.** DarcyTools version 3.4. Concepts, methods and equations. SKB R-07-38, Svensk Kärnbränslehantering AB.

**Werner K, Sassner M, Johansson E, 2013.** Hydrology and near-surface hydrogeology at Forsmark – synthesis for the SR-PSU project. SR-PSU Biosphere. SKB R-13-19, Svensk Kärnbränslehantering AB.

**Öhman J, Follin S, 2010.** Site investigation SFR. Hydrogeological modelling of SFR. Model version 0.2. SKB R-10-03, Svensk Kärnbränslehantering AB.

**Öhman J, Bockgård N, Follin S, 2012.** Site investigation SFR. Bedrock hydrogeology. SKB R-11-03, Svensk Kärnbränslehantering AB.

**Öhman J, Follin S, Odén M, 2013.** Bedrock hydrogeology – Groundwater flow modelling. Site investigation SFR. SKB R-11-10, Svensk Kärnbränslehantering AB.

**Öhman J, Follin S, Odén M, 2014.** SR-PSU Hydrogeological modelling. TD11 – Temperate climate conditions. SKB P-14-04, Svensk Kärnbränslehantering AB.

### Unpublished documents

| SKBdoc id, version | Title | Issuer, year |
|---|---|---|
| 1395200 ver 1.0 | TD05-Effects in ECPM translation | SKB, 2013 |
| 1396127 ver 1.0 | Detailed study of nbgrad | SKB, 2013 |
| 1395214 ver 2.0 | TD08- SFR3 effect on the performance of the existing SFR1 | SKB, 2013 |

# Appendix A

## Model sequence and management of model data files

### Source data

The input data specifically delivered for TD12 are initial locations of wells associated to potential agricultural settlements (wells 1–11), the initial location of well 12 (in the well-interaction area), and locations of 8 further wells in the well-interaction area (Table 1-1). All additional input data for modelling (complete list in Table A-2 through Table A-5) are model files taken from the preceding modelling task, TD11, where traceability from data input deliveries to model files are described in Öhman et al. (2014).

### Management of model data files

In order to facilitate the handling of large number of modelling files in TD11, naming conventions were used that were agglomerated from variable parameters. TD12 studies a single bedrock case and a selected stage of shoreline retreat, and hence, the following two parameters are constant in TD12: 1) <**Bedrock case**> = BASE_CASE1_DFN_R85 and 2) <**time slice**> = 5000AD. A remaining variable parameter is <**Layout**>, which refers to individual disposal rooms, the entire SFR 1 or the entire SFR 3 (note that the notation "SFR2" is used to refer to the planned extension, SFR 3). Another remaining variable parameter is <**File type**> of particle-tracking output, which, depending on particle-tracking direction, refers to recharge areas, discharge areas, or even so-called "Exit locations" (Section 1.5).

The most important variable parameter is the newly introduced <**Well**>, which can take on the well numbering 1 to 28. Note that, particularly for Subtask B, file-name conventions were adjusted to include specifications to well abstraction rate.

This study employs the modelling sequence developed in TD11 (Table A-1; details for the numerical approach given in Öhman et al. 2014). All relevant model input/output files on each modelling step, along with references to the main report, are summarized in Table A-2 to Table A-5. The corresponding source code is also provided for each modelling step (i.e. *.f). Note that the executables may involve additional input/output files, which are not specified in Table A-2 to Table A-5, however, non-listed files were never actually used in the final analysis.

**Table A-1. Modelling sequence in TD12[1)].**

| Source code for modelling step | Description |
|---|---|
| prpgen_TD12_Get_well-capacity.f | Used to survey bedrock properties, according to the well-trajectory sampling method (Section 3.2.4; see Table A-2). Compiled as DarcyTools module PropGen. |
| prpgen_TD12_Get_well-capacity_FINAL.f | Used to sample bedrock properties along a final set of well trajectories (Section 4.1; see Table A-2). Compiled as DarcyTools module PropGen. |
| fif-RECHARGE_TD12_second_delivery.f | Used to account for potential drawdown near wells in the model top-boundary condition (Sections 2.2.4 and 3.3.3; Table A-3). Compiled as Fortran Input File for DarcyTools solver module. |
| fif_TD12_Steady_state_second_delivery.f | Used to freeze model-top boundary and obtain a high-convergent steady state solution (Sections 2.2.4 and 3.3.3; Table A-4). Compiled as Fortran Input File for DarcyTools solver module. |
| P_track_random_TD12_deplete_loops_second_delivery.f | Particle tracking to determine groundwater-flow interactions between wells and the upstream SFR facility (Sections 1.5 and 3.4; Table A-5). Compiled as DarcyTools module PropGen. Note that "deplete_loops" refers to a method to eliminate artefacts related to an identified error concerning the inbuilt DarcyTools parameter <nbgrad> (Section 2.1.1), described in SKBdoc 1396127. |

[1)] Note that these files have been developed in iterative, successive versions. "second_delivery" refers to the final versions that were updated to accommodate the delivery of the well-interaction locations of Subtask C.

**Table A-2. Sampling bedrock properties along well trajectories [prpgen_TD12_Get_well-capacity.f][1] and [prpgen_TD12_Get_well-capacity_FINAL.f][2]**

| Input files | Description |
|---|---|
| Well_coordinates.txt | Coordinates where bedrock well capacity is to be calculated (RT90; i.e. Table 1-1 and Table 3-5). |
| xyz_5000AD_L1BC | DarcyTools computational grid. Cell-inactivation applied to topography data at 5000 AD. Local grid refinement for layout L1BC (i.e. the extension SFR 3). Grid generation explained in Öhman et al. (2014). |
| BASE_CASE1_DFN_R85_L1BC_condx.dat<br>BASE_CASE1_DFN_R85_L1BC_condy.dat<br>BASE_CASE1_DFN_R85_L1BC_condz.dat | Cell-wall ECPM conductivity in x-,y-, and z-directions (as gridded in rotated coordinate system). Used to estimate local well capacity of bedrock. L1BC refers to layout used in gridding for the planned extension SFR3. BASE_CASE1_DFN_R85 refers to the TD11 base-case parameterization (Öhman et al. 2014). |
| Output files | Description |
| xyz_5000AD_L1BC | DarcyTools computational grid. Grid cells intersected by well trajectories are "tagged" for convenient access in subsequent modelling. Tagging by means of so-called DarcyTools markers. |
| NEW_Well_coordinates.txt | Translated rotated model coordinates (see Section 2.2.2), and sampled bedrock properties (e.g. well capacity and selected pumping cell). Provided for specified points in variant[2] (Table 4-1 and Table 4-3), and for extended survey area in variant[1]. |
| Well_stats.txt | Detailed sampled bedrock properties (i.e. Table 4-2 and Table 4-4). Only for variant[2] |
| BASE_CASE1_DFN_R85_L1BC_ECPM_K.plt[2] | Output for 3D visualisation of bedrock properties of cells intersected by well trajectory (Figure 3-2, Figure 4-1, and Figure 4-2). Only produced in variant[2]. Tecplot format. |
| MAP.plt[1] | 2D map of bedrock properties around a given reference point (i.e. Figure 3-3 to Figure 3-14). Only produced in variant[1]. Tecplot format. |

[1] Variant to **survey** the near-field around a given coordinate, used in the localisation of wells for Subtask A.

[2] Variant to extract bedrock properties **only** at specified locations.

**Table A-3. Solving local drawdown for top-boundary condition [fif-RECHARGE_TD12_second_delivery.f]**

| Input files | Description |
|---|---|
| [DTS_setup.txt] | Defines <Well> and, particularly for Subtask B, specifications also include well abstraction rate. |
| cif_RECHARGE.xml | Input specifications for DarcyTools execution, as "Compact Input File" in DarcyTools format. |
| xyz_5000AD_L1BC | DarcyTools computational grid. Cell-inactivation applied to topography data at 5000AD. Local grid refinement for layout L1BC (i.e. the extension SFR 3). Grid generation explained in Öhman et al. (2014). Vertical conductivity along well trajectory (Section 3.3.2) assigned by means of identifying pre-defined DarcyTools markers |
| BASE_CASE1_DFN_R85_L1BC_PERMX_SFR2_5000AD<br>BASE_CASE1_DFN_R85_L1BC_PERMY_SFR2_5000AD<br>BASE_CASE1_DFN_R85_L1BC_PERMZ_SFR2_5000AD | Cell-wall ECPM permeability in x-,y-, and z-directions (as gridded in rotated coordinate system). L1BC refers to layout used in gridding for the planned extension SFR 3.<br>"SFR2" refers to coexistence of both facilities (i.e. parameterised backfill and plugging of SFR 1 and SFR 3). |
| REFERENCE_P | Initial pressure solution, as determined in TD11 (without wells). Used for pressure initialisation and as reference ground-surface head in individual well-simulations. |
| PIER.txt | Used to freeze ground-surface head in areas of fill material, e.g. the SFR pier. As a precaution, water abstraction in wells is not allowed to cause drawdown in fill material. [subroutine Check_Fill] |
| Hard coded values | Description |
| $z_{sea}$= –16.59634 m | Relative sea level at 5000 AD, used in top-boundary condition (SKBdoc 1359616) |
| ID numbers for selected "pumping cell" in all <Well> | Id numbers taken from Table 4-1 and Table 4-3. Used to prescribe sink term (Section 3.3.3). |
| Output files | Description |
| RECHARGE_rstslv | Flow solution stored in a standardised "DarcyTools restart format". The head solution in ground-surface cells is propagated as a top-boundary condition for the "Steady-state phase". |
| GWT_Recharge5000AD.dat | Tecplot ground-surface output for visualisation (e.g. Figure 3-17b and c) |

**Table A-4. Steady-state flow solution [fif_TD12_Steady_state_second_delivery.f]**

| Input files | Description |
|---|---|
| [DTS_setup.txt] | Defines <Well> and, particularly for Subtask B, specifications also include well abstraction rate |
| cif_STEADY_STATE.xml | Input specifications for DarcyTools execution, as "Compact Input File" in DarcyTools format. |
| xyz_5000AD_L1BC | DarcyTools computational grid. Cell-inactivation applied to topography data at 5000 AD. Local grid refinement for layout L1BC (i.e. the extension SFR 3). Grid generation explained in Öhman et al. (2014). Vertical conductivity along well trajectory (Section 3.3.2) assigned by means of identifying pre-defined DarcyTools markers. |
| BASE_CASE1_DFN_R85_L1BC_PERMX_SFR2_5000AD<br>BASE_CASE1_DFN_R85_L1BC_PERMY_SFR2_5000AD<br>BASE_CASE1_DFN_R85_L1BC_PERMZ_SFR2_5000AD | Cell-wall ECPM permeability in x-,y-, and z-directions (as gridded in rotated coordinate system). L1BC refers to layout used in gridding for the planned extension SFR 3. "SFR2" refers to coexistence of both facilities (i.e. parameterised backfill and plugging of SFR 1 and SFR 3). |
| RECHARGE_rstslv | Ground-surface head solution stored in the standardised "DarcyTools restart format". Determined in the preceding "Recharge phase" (Table A-3), and here used as top-boundary condition. |
| Hard coded values | Description |
| $z_{sea}$= –16.59634 m | Relative sea level at 5000 AD, used in top-boundary condition (SKBdoc 1359616) |
| ID numbers for selected "pumping cells" in all <Well> | Id numbers taken from Table 4-1 and Table 4-3. Used to prescribe sink term (Section 3.3.3). |
| Output files | Description |
| Flow_solution.dat | Final steady-state flow solution, accessible for particle-tracking post processing (Section 3.4). Contains cell-wall Darcy velocity and cell-centre pressure. |
| Tunnel_flows.dat | Tabulated cross flow over cell-domain boundaries defined by so-called "DarcyTools markers". Contains cross flows through disposal rooms, as well as, "well cells" (Table 4-5, Table 4-6, and Table 4-7). |
| Tunnel_walls.plt | Output for 3D visualisation of tunnel-wall flow and flow over well cells. Tecplot format. |

**Table A-5. Particle tracking [P_track_random_TD12_deplete_loops_second_delivery.f][1)]**

| Input files | Description |
|---|---|
| [DTS_setup.txt] | Defines <Well>. Particularly for Subtask B, specifications also include well abstraction rate |
| cif_STEADY_STATE.xml | Input specifications for DarcyTools execution, as "Compact Input File" in DarcyTools format. |
| xyz_5000AD_L1BC | DarcyTools computational grid. Cell-inactivation applied to topography data at 5000 AD. Local grid refinement for layout L1BC (i.e. the extension SFR 3). Grid generation explained in Öhman et al. (2014). Vertical conductivity along well trajectory (Section 3.3.2) assigned by means of identifying pre-defined DarcyTools markers. |
| Flow_solution.dat | Final steady-state flow solution, accessible for particle-tracking post processing (Section 3.4). Contains cell-wall Darcy velocity and cell-centre pressure. |
| BASE_CASE1_DFN_R85_L1BC_5000AD_PORO | Bedrock cell porosity, calculated as intersectional volume sum of fracture aperture per cell volume. |
| BASE_CASE1_DFN_R85_L1BC_fws.dat | Cell ECPM flow-wetted surface area (i.e. intersectional sum of fracture area in computational cells). |
| Hard coded values | Description |
| ID numbers for selected "pumping cells" in all <Well> | Id numbers taken from Table 4-1 and Table 4-3. Used to prescribe sink term (Section 3.3.3). |
| Output files | Description |
| Assembled_Cross-List.dat | Interaction table (e.g. Table 4-8). In each particle execution, the table is continuously updated by appending new output at the end of the table. |
| <Well>__Cross-paths.plt | Output for 3D visualisation of interacting particle trajectories. Tecplot format. |
| <Well>__All_<Layout>_D__<File type>.dat | Output for 2D visualisation of recharge/discharge areas (i.e. Figure 4-5 to Figure 4-16). Tecplot format. |
| <Well>__All_<Layout>_D__Exit_loc.dat | Performance measures for interacting particle trajectories, according to the so-called "Exit location format", specified in [2)] |

[1)] Variable parameters are <Well> = Well 1 to 28, <Layout> = particle release point, SFR 1 or SFR 2 (referring to SFR 3), <Type> = discharge or recharge, depending on particle-tracking direction. Constant parameters are <Bedrock case> = BASE_CASE1_DFN_R85, <time slice> = 5000 AD. Note that particularly for Subtask B, specifications were also made to well abstraction rate.

[2)] Td12_Exit_locations_2013-04-15__READ_ME_____.txt

# Appendix B

## Task Description – SR-PSU TD-12

| | | | |
|---|---|---|---|
| **Date** | 130212 | 131022 | 140227 |
| **Version** | 0.1 | 0.2 | 1.0 |
| **Approved** | | | Magnus Odén |

| | |
|---|---|
| **Name of task** | Simulations of water-supply wells in support of the SR-PSU safety assessment |
| **Code** | DarcyTools v. 3.4 |
| **Modellers** | Johan Öhman |

### B.1 Scope of work

This modelling task concerns future water-supply wells in rock and is carried out in support of the SR-PSU safety assessment. Specifically, the task is performed to study (1) the influence on groundwater flow through SFR 1/SFR 3 and (2) groundwater flow paths between SFR 1/SFR 3 and wells drilled in rock.

The output from the task is expected to provide a general understanding of the effects of wells in rock in the SFR area and data for dose assessments. Specifically, the underlying model setup to be used is the same as in TD-11 (see model domain in Figure B-1). TD-11 (and TD-08) are used as inputs to the biosphere assessment and concern future groundwater flow paths for undisturbed conditions, i.e. groundwater flow driven by natural gradients in the absence of well discharge. Hence, combining the TD-11 and TD-12 outputs facilitates dose assessments related to contaminated well water.

The task is to be performed in three steps (A–C, see below), each focusing on a specific aspect related to future wells drilled in rock.

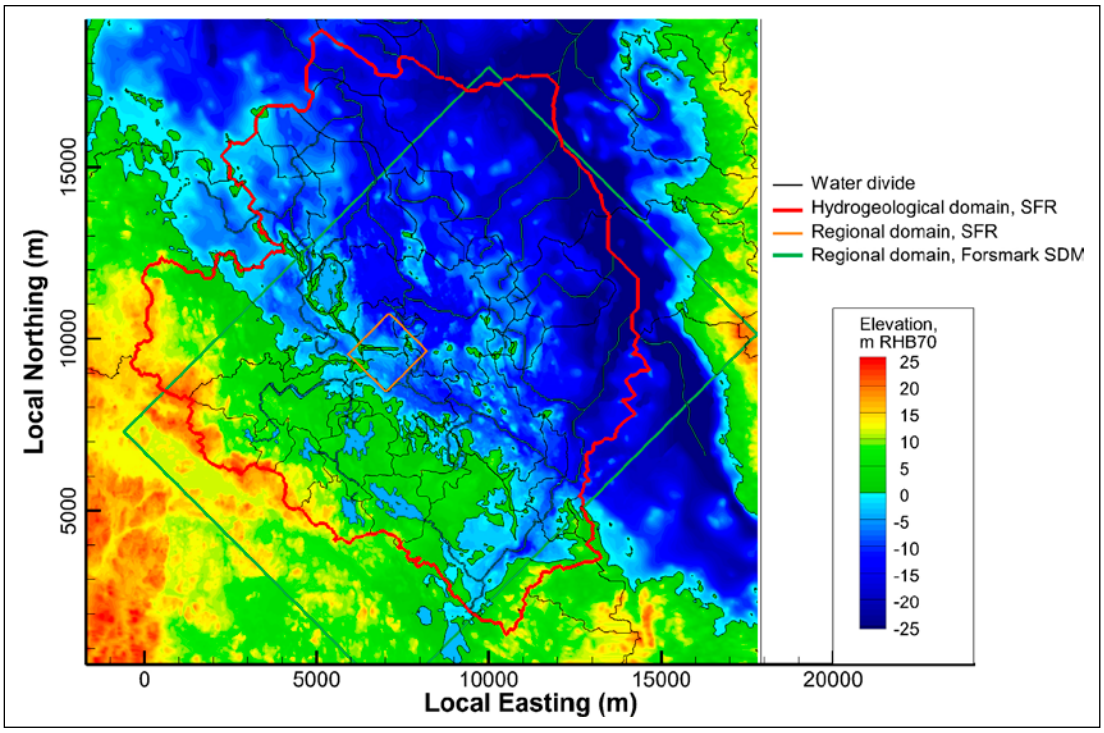


***Figure B-1.*** *DarcyTools model domain (red line).*

## B.2 Setup of models

The underlying DarcyTools model setup to be used in this task is the same as the setup used in TD-11 (see Figure B-1). The 5000 AD model setup is to be used, including the TD-11 model area and grid, SFR 1/SFR 3 layout, material properties, boundary conditions and intrinsic state conditions, with the following specifications:

- BASE_CASE1_DFN_R85, i.e. HCD: Base case 1 and HRD: DFN R85.
- HSD and DEM: RLDM and DEM (produced by SR-PSU/Biosphere) for 5000 AD.
- Surface hydrology: Geometry of lakes and streams (produced by SR-PSU/Biosphere) for 5000 AD.
- Shoreline: 5000 AD.

The coordinate system to be used is RT 90 2.5 gon V/0:15, rotated and with a local origo at (1626000, 6692000); see e.g. Öhman et al. (2013).

## B.3 Modelling sequence, Step A – C

### B.3.1 Step A – Wells associated to potential arable land (11 wells) and the potential well interaction area (1 well)

In step A, using the 5000 AD DarcyTools model setup steady-state flow simulations are carried out for totally 12 wells in rock (see map in Figure B-2), one well per flow simulation, with a depth of 60 m in rock. The wells are screened across the regolith (i.e. between the ground surface and the regolith/rock interface) and ≈ 4 m (depending on the local vertical model discretisation) into the rock. The screen and the well bottom are represented by assigning a small vertical hydraulic conductivity at the screen and well bottom ($K_v \approx 10^{-11}$ m/s), whereas the well discharge is assigned in the "pumped cell", i.e. the DarcyTools model cell along the well with the highest horizontal hydraulic conductivity.

The RT 90 coordinates (X, Y) of the 12 wells to be simulated are shown in Table B-1. 11 of these wells are associated to potential arable land and are located at the centres of potential future agricultural settlements. One well (157_2, no. 2) is included only to test a "worst-case scenario", as it is located in the potential well interaction area (this is further investigated in step C) and not associated to potential arable land. The well discharge ($Q_{well}$) is set to 700 L/d, corresponding to the total water demand for a self-sustaining community of modern farmers used in SR-PSU.

As a prior step, well capacities are to be tested at the locations shown in Figure B-2 and Table B-1, as these locations primarily are chosen based on potential future land use and associated settlements (11 wells), and not on the hydrogeological properties of the rock. Hence, prior to production simulations, some or all wells may be slightly relocated (< 100 m) to locations with sufficient well capacities and/or with potentially larger capture of particles released at SFR 1 and/or SFR 3. Moreover, prior to production simulations, tests are to be carried to find a proper modelling sequence (recharge phase, steady-state phase) for representation of water-supply wells in DarcyTools.

For each well, particle tracking is to be performed as follows:

- Forward tracking of totally $10^6$ particles released within SFR 1 waste-storage facilities (1BTF, 2BTF, 1BLA, 1BMA and Silo, proportionally to facility volume).
- Forward tracking of totally $10^6$ particles released within SFR 3 waste-storage facilities (2BLA, 3BLA, 4BLA, 5BLA, 2BMA and 1BRT, proportionally to facility volume).
- Backward tracking of totally $10^6$ particles released within the "pumped cell".

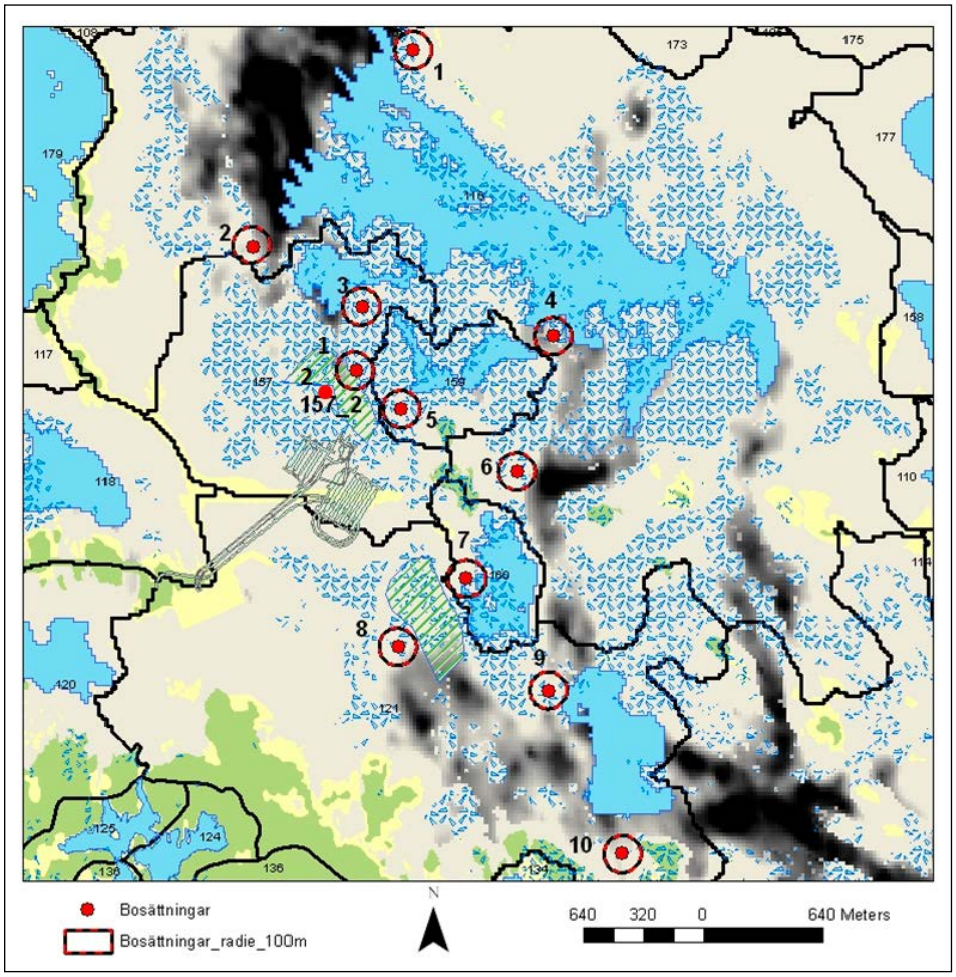


***Figure B-2.*** *Locations of the 12 wells to be simulated in step A. Based on tests of well capacities, wells may be slightly relocated (< 100 m) prior to production simulations. Well 157_2, no. 2 is in the potential well interaction area, and not associated to potential arable land.*

**Table B-1. Coordinates of wells.**

| Well id | Easting (RT 90) | Northing (RT 90) |
|---|---|---|
| 1 | 1633455 | 6704141 |
| 2 | 1632597 | 6703081 |
| 3 | 1633182 | 6702751 |
| 4 | 1634204 | 6702592 |
| 5 | 1633386 | 6702198 |
| 6 | 1634009 | 6701862 |
| 7 | 1633736 | 6701284 |
| 8 | 1633373 | 6700918 |
| 9 | 1634174 | 6700681 |
| 10 | 1634574 | 6699798 |
| 157_2, no. 1 | 1633149 | 6702405 |
| 157_2, no. 2 | 1632994 | 6702298 |

### B.3.2 Step B – Influence of well discharge

In step B, the same types of flow and particle-tracking simulations as in step A are to be performed to investigate the influence of well discharge. Specifically, step B is performed by assigning the following well discharges for well 157_2, no. 2 (i.e. the well in the potential well interaction area, not associated to potential arable land):

- $Q_{well}$ = 1,000 L/d, which approximately corresponds to the present-day water demand for 5 individuals.
- $Q_{well}$ = 1,400 L/d, i.e. twice the well discharge in step A (700 L/d).
- $Q_{well}$ = 2,800 L/d, i.e. four times the well discharge in step A.

### B.3.3 Step C – Wells drilled in the well interaction area downstream from SFR

In step C, 8 wells are to be simulated in the well interaction area, i.e. the area (or rather, volume) in which water-supply wells in rock may have the highest concentration of radionuclides originating from SFR. As shown in Figure B-3, the well interaction area is delineated based on TD-11 particle trajectories in the elevation interval from –80 to –10 m in the rock. The locations of the 8 wells to be simulated are shown in Figure B-4. In step C, well depths, screening and discharge are the same as in step A.

## B.4 Output and reporting

The output to be produced from the task involve the following:

- DarcyTools input/output files for each simulation in steps A–C.
- Well capacties and simulated drawdown.
- Tunnel cross flow (SFR 1 and SFR 3).
- Results of forward and backward particle tracking.

The model setup, execution and modelling results are to be presented in a P-report.

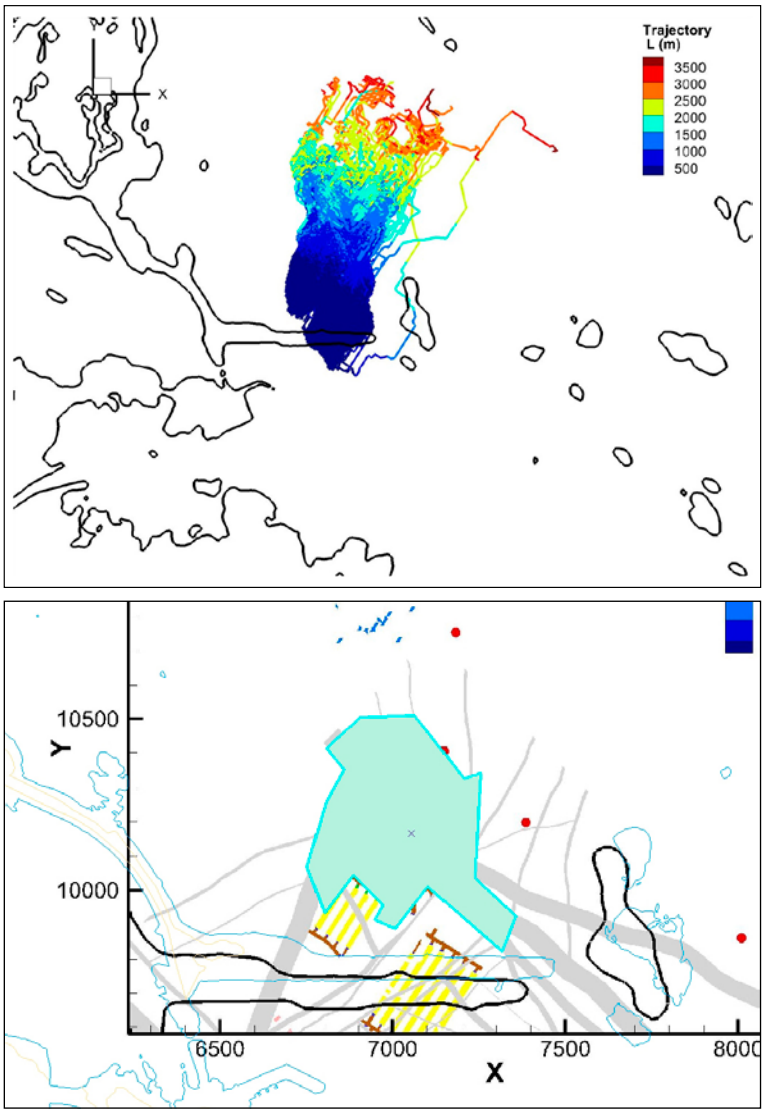


***Figure B-3.*** *TD-11 particle trajectories (upper figure) and delineated well interaction area (lower figure).*

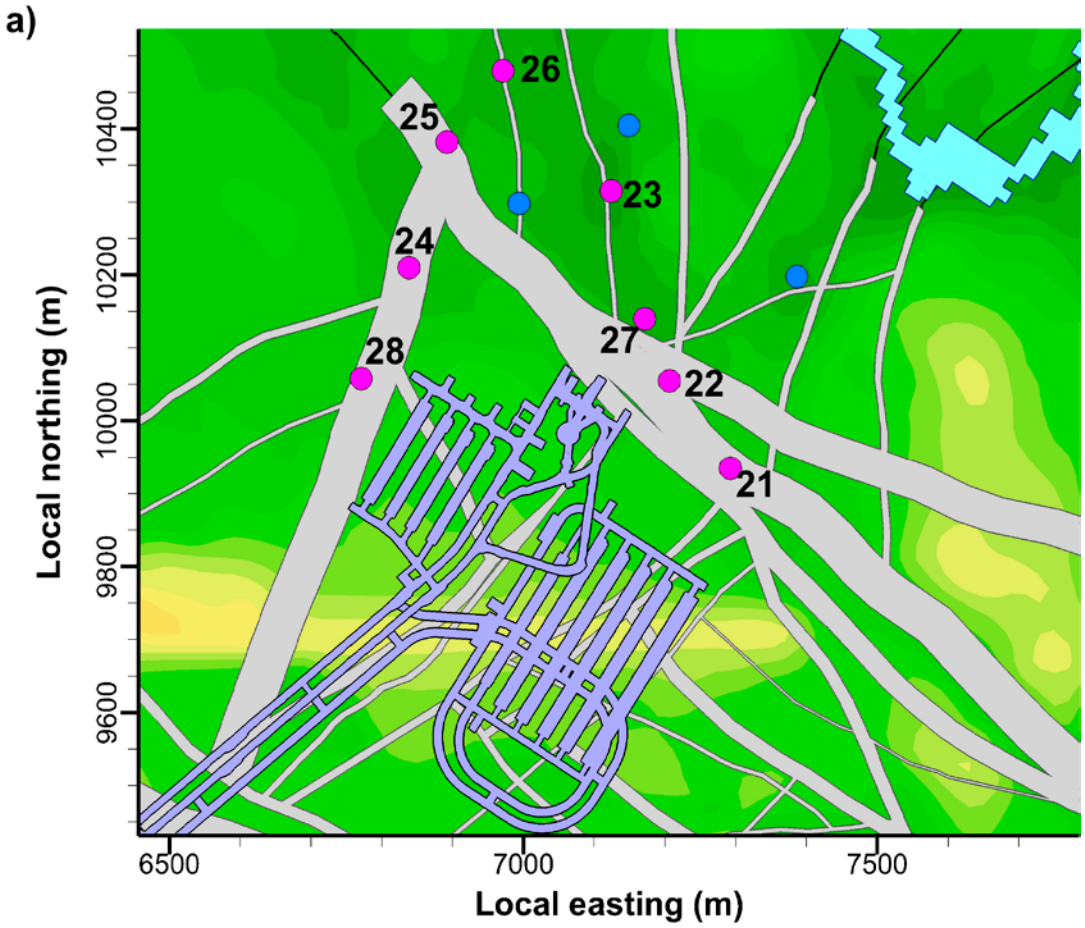


***Figure B-4.*** *Locations of the 8 wells (lilac dots, 21–28) to be simulated in step C. The blue dots are wells simulated in steps A and B (e.g. well 157_2, no. 2 in the potential well interaction area, tested in step A, is located between wells 23 and 24).*